INFORMATION TO USERS

This manuscript has been reproduced from the microfilm master. UMI films the text directly from the original or copy submitted. Thus, some thesis and dissertation copies are in typewriter face, while others may be from any type of computer printer.

The quality of this reproduction is dependent upon the quality of the copy submitted. Broken or indistinct print, colored or poor quality illustrations and photographs, print bleedthrough, substandard margins, and improper alignment can adversely affect reproduction.

In the unlikely event that the author did not send UMI a complete manuscript and there are missing pages, these will be noted. Also, if unauthorized copyright material had to be removed, a note will indicate the deletion.

Oversize materials (e.g., maps, drawings, charts) are reproduced by sectioning the original, beginning at the upper left-hand corner and continuing from left to right in equal sections with small overlaps.

ProQuest Information and Learning
300 North Zeeb Road, Ann Arbor, MI 48106-1346 USA
800-521-0600

POLYMER ADSORPTION

IN

LAMINAR TUBE FLOW OF DRAG REDUCING FLUIDS

BY

JAE EK SON

A thesis submitted in partial fulfillment

of the requirement for the degree of

Doctor of Philosophy

in the

Department of chemical engineering

University of Ottawa

Ottawa, Canada

June, 1978

ABSTRACT

The results of an experimental investigation concerned with the characterization of polymer adsorption and flow behaviour in the vicinity of the tube wall during steady uniform laminar flow are reported.

Two Polyox homologues (Coagulant and WSR 301) have been tested at various concentrations (10 to 100 ppm) and flow rates. Measurements were conducted using five different tube diameters to study the effect of the tube size on the polymer adsorption onto the wall.

0.3M K_2SO_4 aqueous solution was employed as a poor solvent to investigate the effect of polymer coiling (in solution) on the polymer adsorption. The degree of coiling was inferred by the measurement of intrinsic viscosity.

Polymer degradation was also measured with duration of time. A considerable decrease in viscosity and in polymer adsorption (anomalous zone thickness) in tube was observed with an increase in the duration of a dilute polymer solution.

The thickness of the anomalous zone associated with polymer adsorption in laminar flow of a dilute polymer solution in a tube was correlated with the drag reduction manifested in turbulent flow by a mathematical equation with macromolecular size and tube diameter as parameters. The data suggested that the polymer adsorption could be a fundamental basis for the turbulent drag reduction phenomenon.

ACKNOWLEDGEMENT

Financial support through Postgraduate Scholarship and Research Assistantship from the National Research Council of Canada is greatfully acknowledged.

The author would like to express his gratitude to Dr. William Kozicki, the supervisor of this project, for his most valuable help, guidance and suggestions throughout the project. Thanks are also due to Mr. G. Gasperetti and his assistants for the construction of the apparatus.

Appreciation is also expressed to Union Carbide for their donation of the Polyox resins.

The author wishes to thank to those who are especially important to him - his family: his father, now gone, his mother, and his wife, Myong-Suk. The author remembers their sacrifices and encouragements.

TABLE OF CONTENTS

LIST OF FIGURES

LIST OF TABLES

NOMENCLATURE

a	Constant in Eq. (2.4); subscript k refers to non-solvent; subscript w refers to distilled water
a_1, b_1, c_1	Constants defined by Eq. (5.5-5)
a', b', c'	Constants defined by Eq. (5.8-1)
a_2, a_3	Constants defined by Eqs. (5.9-7) and (5.9-10), respectively
A_i, B_i	Functions defined by Eq. (3.4-5)
b	Constant defined by (a-0.5)
c	Polymer concentration in the mainstream
c_a	Polymer concentration in the adsorption zone
c_c	Polymer concentration in the concentrated layer; asterisk * refers to the maximum concentration at the interface with the adsorption zone
D	Tube diameter
D_e	Effective diameter of a macromolecule; $\tilde{D}_e=D_e/\Delta$
DR	Drag reduction defined by Eq. (5.8-2)
f	Friction factor; subscript s refers to pure solvent; subscript a refers to solution
$f(\tau)$	Function of shear stress, denoting velocity gradient

g	Gravitational constant
$g(\tau,y)$	Correction term defined by Eq. (3.2-1)
k	Permeability; $\bar{K} = k/R^2$
K	Constant in Eq. (2.4)
k_{ad}, k_{de}	Rate constants defined by Eqs. (5.5-2) and (5.5-3), respectively
k_i	Geometric factor characterizing porous medium
K_1, K_2, K_3	Constants defined by Eqs. (5.6-2), (5.6-4) and (5.9-7), respectively
K_H	Huggins constant
L	Tube length
M, $\bar{M}_w$	Molecular weight of polymer, weight averaged molecular weight
m_i	Coefficients in the velocity polynomial in Eq. (3.2-5); prime ' refers to dimensionless coefficients
n	Adsorption level index
n'	Constant defined by Eq. (5.5-1)
n_o	Number of macromolecules
$\tilde{N}$	Avogadro number
Q	Flow rate
r	Radial distance from the centre axis of the tube; $\bar{r} = r/R$
R	Tube radius

Re	Reynolds number
r_{ad}, r_{de}	Rate of adsorption of polymer molecules defined by Eq.(5.5-2), rate of desorption of polymer molecules defined by Eq. (5.5-3)
$\sqrt{\overline{r^2}}$, $\sqrt{\overline{r_o^2}}$	Root-mean-square end-to-end distance of a polymer macromolecule, the same for unperturbed macromolecule
s	Shape factor
s_o	Specific surface of a molecule
u, $u^<$, $u^>$	Local velocity, the same in the anomalous zone, the same in the mainstream, respectively; $\bar{u} = \frac{u\,\eta}{R\,\tau_w}$; $\bar{u}^< = \frac{u^<\eta}{R\,\tau_w}$; $\bar{u}^> = \frac{u^>\eta}{R\,\tau_w}$
U	Velocity vector in Eq. (3.4-1)
u_R	Effective velocity at the wall defined by Eq. (3.2-18); $\bar{u}_R = \frac{u_R\,\eta}{R\,\tau_w}$
u_w	Average velocity deficiency; $\bar{u}_w = \frac{u_w\,\eta}{R\,\tau_w}$
$\langle u \rangle$	Average velocity; $\langle\bar{u}\rangle = \frac{\langle u\rangle\eta}{R\,\tau_w}$
w	Mass flow rate
y	Distance from the wall; $\bar{y} = y/R$; $\tilde{y} = y/\Delta$; $\overset{o}{y} = y/D_e$
α	Constant defined by Eq. (5.5-1)
$\alpha(\varepsilon)$	Function of porosity defined by Eq. (3.4-8)

δ^*	Laminar sublayer thickness
δ^+	A dimensionless group defined by Eq. (A.9-1)
δ_a	Adsorption zone thickness; $\tilde{\delta}_a = \delta_a/\Delta$
δ_c	Concentrated layer thickness; $\tilde{\delta}_c = \delta_c/\Delta$
Δ	Anomalous zone thickness; $\bar{\Delta} = \Delta/R$
Δ_∞	Limiting anomalous zone thickness; $\bar{\Delta}_\infty = \Delta_\infty/R$
Δh	Head loss of fluid in the test section
ΔP	Pressure loss of fluid in the test section
ε	Porosity in the adsorption zone
η	Viscosity of solution in the mainstream
η_s	Viscosity of pure solvent
$[\eta]$	Intrinsic viscosity
η_r	Relative viscosity, η/η_s
η_{sp}	Specific viscosity, $\eta_r - 1$
η_a	Viscosity coefficient defined by Eq. (3.3-6); $\eta_{ar} = \eta_a/\eta_s$
η_c	Viscosity of solution in the concentrated layer
ρ	Density of solution or solvent
τ	Shear stress defined by $r(P_o-P_L)/2L$
τ_w	Shear stress at the wall defined by $R(P_o-P_L)/2L$
Φ, Φ_o	Universal constant defined by Eq. (2.5), the same for the unperturbed molecules

1. INTRODUCTION

Recent interest in the mechanics of flow of dilute polymer solution has been motivated by a phenomenon referred to as Toms effect - the reduction in pressure drop required to maintain the flow achieved under turbulent flow condition by the addition of a minute amount of a high molecular weight polymer to the fluid.

Research activity received a stimulus when Fabula (3) revealed the existence of effective water soluble additives in his pipe flow studies. The work in dilute polymer solutions was subsequently extended to other systems such as flow along flat plates, around spheres, immersed objects, through porous media etc. with possible applications in petroleum oil well flooding and fracturing operations, in irrigation processes, fire fighting, hydrodynamic vehicles of various kinds and in industrial flow systems. Considerable interest has been generated by the possibility of increasing flow capacity of given systems or reducing pumping power requirement for the same capacity because of the obvious associated cost benefits.

Various possible mechanisms have been proposed to explain the Toms effect, but these can usually explain one or more but not all of the manifestations of the phenomenon. There is evidence suggesting that adsorption mechanism may explain the observed characteristics of the Toms phenomenon.

It has long been suspected that an adsorbed zone may have a role to play in turbulent drag reduction. Most recently, extensive experimental measurements were carried out for the strong support of the polymer adsorption effect on the drag reduction phenomenon in turbulent flow. The measurement conducted in turbulent flow studied the effects of different chemical structures, varying molecular weights, and using different solvents. However, experimental difficulties associated with the fluid behaviour in the turbulent flow regime have greatly complicated the analysis of the data.

While extensive work has been carried out in the turbulent flow regime, relatively little attention has been focused on laminar flow. The systematic deviations between measurements of simple laminar viscometric flow of dilute polymer solutions have usually been overlooked or attributed simply to variations of the solution viscosity, whereas an in-depth analysis ascribes the anomalous flow behaviour to the polymer adsorption onto the tube wall.

The objective of the present work is to investigate the anomalous flow behaviour of polymer solutions in laminar flow using dilute solutions of a drag reducing polymer, the so called Polyox series, and to study the effect of polymer coiling (in solution) on the polymer adsorption by the addition of small amount of a salt, here K_2SO_4, which causes the polymer to become more coiled and even precipitate at

higher salt concentration. The degree of the coiling was established from the intrinsic viscosity measurements.

Polymer degradation effects also were studied since polymer degradation has been found to cause an appreciable change of drag reduction in the turbulent flow and of molecular weight with duration of time.

An investigation of the flow in laminar flow regime was conducted with different molecular weights of the same homologue series, with varying polymer concentrations and using test sections with different tube diameters.

In addition, it was of interest to determine whether the surface effect associated with polymer adsorption from dilute polymer solution onto the tube wall in laminar flow could be correlated with the drag reduction in turbulent flow.

Finally, an attempt was made to account for turbulent drag reduction in terms of the parameters characterizing polymer adsorption in laminar flow regime of the dilute polymer solutions.

2. LITERATURE SURVEY

2.1 Introduction

The drag reduction phenomenon evoked by the addition of high molecular weight additive to a liquid was first studied by Toms(1) in 1948. There are indications that the effect was actually known much earlier (2) during World War II. However no intensive research was undertaken to study this phenomenon until 1963 when Fabula (3) reported the existence of more efficient additives such as polyethylene oxide, polyacrylamide, etc., which are effective in very low concentrations, of the order of a few part per million.

Subsequently this area has been investigated extensively, as evidenced by the fact that Lumley (4), Hoyt (5) and Virk (6) have published review papers dealing with drag reduction.

The ultimate goal of a fundamental study of friction reducing polymer solutions is the understanding of the interaction of the macromolecules on the flow process whose study requires the coordinated use of results and techniques from different fields such as fluid mechanics, rheology, polymer physics, and surface chemistry. Since many aspects of the turbulent flow of Newtonian fluids are still poorly understood, the insights gained through study of a flow which has been profoundly altered by polymer molecules may eventually

aid in the understanding of the entire realm of fluid flow behaviour.

A number of theoretical explanations have been offered for the drag reduction effect, however as yet no mechanism consistent with all the experimental observations of the effect has appeared. Explanations have ranged from slip theory to several theories based on viscoelastic characteristics of the solution (7-14). Among them, some of the most relevant work to the present subject of the polymer adsorption onto the wall are reviewed and discussed below from the literature.

2.2 Wall effect

Oldroyd (15) was the first to attempt to explain the mechanism behind the Toms effect. He suggested that tube wall may introduce a preferred direction locally in a normally isotropic material. If the liquid is a solution of a linear high polymer, an external constraint may be imposed by the wall on the ways in which long chain molecules near the wall can rotate and therefore it is possible that an abnormally mobile laminar sublayer of a thickness comparable with molecular dimensions can exist at the tube wall.

An effective velocity of slip associated with an increased laminar sublayer thickness has no effect on the velocity distribution in the turbulent region except to

superpose upon it a uniform velocity equal to the effective slip velocity in direction of the flow. Kozicki et al. (16) have employed this principle to explain some aspects of the enhancement in flow. Physically an actual slip at the wall does not occur, however the effective velocity of slip is a convenient means of representing quantitatively the enhancement in flow manifested by the thickening of the laminar sublayer which is produced by the presence of the polymer molecules.

In the case of the above turbulent flow studies, the wall effects characterized by an effective slip velocity may also be considered to be manifestations of polymer adsorption onto the wall.

2.3 Adsorption of polymer

One other aspect of the wall effect relates to polymer adsorption in which it is postulated an adsorbed zone of polymer molecules on the inner wall of the pipe, or other flow surface, is produced during the flow of polymer solution. Although experimental evidence for the adsorption of certain high molecular weight polymers from solutions in laminar flow through capillary viscometers (17-22) and porous disk (23) has long been available, El'perin et al. (24) seem to have been the first to propose an adsorption mechanism for the Toms effect in turbulent flow. But they do not appear to have carried out detailed adsorption measurement of any

kind, although Kowalski (25), David and Ponter (26) described tests in which a small pipe, initially conveying a polymer solution, was then switched to the pure solvent. The drag reduction effect persisted for about 15 minutes, lending credence to a wall adsorbed zone which was slowly washed off.

Wells and Spangler (27) injected a polymer solution into a pipe in which water was flowing turbulently at both near the wall and the axis of the pipe; in the former case, the wall shear stress was reduced almost directly downstream from the injection point, whereas in the latter case the drag reduction was observed relatively much further downstream, presumably only after the macromolecules had diffused to the region.

Finally, Arunachalam and Fulford (28) obtained direct experimental evidence in the form of adsorption measurements which showed increased additive concentration at the pipe wall. More recently Hand and Williams (29) have studied what they referred to as an adsorbed-entangled layer and concluded that the Toms effect is due to the formation of such layer from the bulk solution. They observed the kinetics of a wall layer depletion for different polymer in a measurement of the time dependent solvent rate and monitored the build-up of a wall layer in a flow by infrared absorption measurement.

McComb (30) reported that the addition of Polyethylene oxide to water in a capillary U-tube produced quite a large

reduction in the degree of damping of oscillation: in terms of the increase in amplitude and in total number of oscillation of the polymer solution to that of the solvent alone. It was established that this form of drag reduction was due to a coating of the additive onto the tube wall.

2.4 Analysis of polymer adsorption

On the theoretical side, much work has been reported on the physical chemistry and thermodynamics of polymer adsorption from solutions and on the conformation of the adsorbed macromolecules (31-36). Most of the published work appear to be studies on kinetics and equilibrium in the static systems, however little attention appears to have been given to a detailed analysis describing polymer adsorption in a flowing systems.

Schofield and Blair (37,38) and Oldroyd (39) attempted to develop a method of detecting anomalous flow behaviour near the tube wall in laminar flow through straight tubes. They succeeded in demonstrating the existence of such a wall effect in laminar flow of some non-Newtonian liquids through tubes (40).

By an extension of Oldroyd's analysis, Kozicki et al. (41,42) further showed that polymer adsorption or gel formation leads to a negative effective velocity at the wall and have demonstrated the applicability of the analysis to their data.

They also proposed a model which explains polymer adsorption and the transition to the separation phenomenon observed in tubes of different diameters under varying shear stresses (43). It was postulated that polymer molecules adsorbed onto the tube wall give rise to a less mobile, more viscous layer in the vicinity of the solid surface which results in decreased flow rate. As the shear stress is increased over critical value, the polymer molecules tend to uncoil and hence the molecules are distorted to elongate and align in the direction of flow near the tube wall, which manifests an effective velocity of slip at the wall.

Hand et al. (29) have postulated that the adsorbed polymer adopts a conformation of runs of segments which are attached to the surface, interspaced with loops entered into solution. In a flow situation, these loops can act as entanglement sites for subsequent polymer chains in flowing solution. Thus, an adsorbed entangled "mat" can be formed at the wall.

Recently Kozicki et al. (44) have proposed a scheme of detailed analysis for characterizing polymer adsorption and flow in the proximity of a conduit wall in the steady laminar flow of dilute polymer solutions of linear random coiled macromolecules. The analysis assumes a region of anomalous flow adjacent to the wall wherein effects associated with inhomogeneities of the fluid are confined.

Since turbulent flow includes a laminar sublayer,

investigation of polymer adsorption and flow under laminar flow condition may also give an insight into the behaviour near the wall in turbulent flow and the mechanism responsible for turbulent drag reduction.

2.5 Polymer degradation

Determination of polymer degradation on flow of solutions of high molecular weight materials is essential for appropriate interpretation of drag reduction measurements, for the determination of the true dependence of drag reduction on polymer concentration and molecular weight, and for selection of the most suitable drag reducing polymer for a given application.

The phenomenon of polymer degradation has been under investigation for more than three decades and numerous excellent papers have been published. The lack of an understanding may be attributed to the multiplicity of factors which can contribute to the molecular breakdown.

Polymer molecules can be degraded by both mechanical and chemical means. Degradation during flow may result from a combination of the two, depending on the polymer-solvent system. Some of the more important and significant factors contributing to polymer degradation, presented in the literature, are discussed briefly in the following.

Polymeric hydrocarbons are subject to oxidation by

atmospheric oxygen and it is generally agreed that the oxidation reaction proceeds by a free radical, chain mechanism (45-47). These radicals can be formed by absorption of heat, ultraviolet light, high energy radiation, mechanical stress, and reaction with radicals from foreign sources.

Metal ions may also catalyze the formation of oxygen free radicals capable of initiating degradation. Arunachalam (48) indicated that considerable degradation had occurred in his polymer solutions after few days of storage of the diluted solutions, which introduced uncertainties in the results of drag reduction. This phenomenon may be one example of the chemical degradation of polymer during storage.

Shear degradation has been studied under various high speed mixing conditions (49-54), in laminar flow (55,56), and in turbulent flow systems (57-59). Nakano and Minoura (49,50) have studied the degradation of Polyethylene oxide and Polymethylmethacrylate in benzene by high speed stirring. The effects of polymer concentration, solvent, stirring speed, and initial degree of polymerization on the rate of scission were investigated. Their studies show that the polymer degradation was not caused by the interaction of polymer chains by observing a similar decrease in the intrinsic viscosity, regardless of change in solution concentration.

Buche (60) and Bestal (61) have presented theories postulating that the entanglement along the polymer chains plays a major role in the rupture process for the shear

degradation of high polymers. Since shear degradation occurs also in the limit of infinite dilution (57-59,62), the interaction between solvent and polymer chains may also bring about scission, and entanglement of polymer chains are not necessary.

Patterson et al. (56) carried out a study on the degradation and drag reduction for Polyisobutylene in toluene and cyclohexane. They found that Polyisobutylene degraded faster in toluene (a better solvent) than in cyclohexane (a poorer solvent) even though the drag reduction effect is greater in toluene than in cyclohexane. However, Ramakrishnan and Rodriguez (63) suggest contrary to Patterson that degradation of Polyethylene oxide seems to be more rapid in a poor solvent (benzene) than in a good solvent (trichloroethylene).

Ram and Kadim (55) studied the shear degradation of Polyisobutylene in laminar flow through capillaries. The effect of initial molecular weight, concentration, temperature, and wall shear stress on degradation were investigated. They found that the apparent viscosity of a given polymer solution (measured under low shear condition) decreased with time of shear at high stresses and approached an asymptotic value and that the magnitude of the value decreased as the shear stress increased.

Thus, polymer degradation (chain breakage) may impose severe limitations on uses whose effectiveness

is controlled by the very high molecular weight molecules which have been shown to be more sensitive to high shear. This problem has been encountered in such practical applications as viscosity index improvement of lubricating oils (64-66) and drag reduction. It also impaires the reliability of rheological characterization at high shear and the molecular weight determination by Gel Permeation Chromatography (58).

Arunachalam (48) and Patterson et al (56) discussed the shear degradation associated with pump and recirculation. Pruitt and Crawford (67) suggested that the high speed gear pump normally employed destroys the drag reducing properties of the additives. The slippage in the gear pump, at the 400 psi. operating pressure, evidently degraded the polymers since no drag reduction was observed with a 10 ppm Polyethylene oxide solution in the 100 ft section when the gear pump was used in place of the hydraulic cylinder drive.

It is therefore clear that in the flow process of drag reducing polymer solution, molecular degradation caused by both chemical and mechanical factors does occur.

2.6 Non-solvent effect

It is well known that the most efficient additives have been soluble high molecular weight polymers. Solvent power was also shown to be an important factor in the observed

drag reduction in earlier studies of Hershey and Zakin (68) who observed 40% less drag reduction for Polyisobutylene in a poor solvent (benzene) than in a good solvent (cyclohexane).

Peyser and Little (69) also observed percent drag reduction of polystyrene in a variety of non-aqueous liquids of varing solvent power, where it was again found that drag reduction was better in good solvent.

The effect of salt concentration on drag reduction of aqueous solutions of non-ionic polymers such as Polyethylene oxide has been briefly discussed in the literature (70,71). It has been generally concluded that the presence of salt has little effect on the observed drag reduction. While this may be true for salt concentration such as those occurring in sea water, it cannot be true for higher salt concentration or for such as Potassium carbonate or sulfate, which have strongly depressant effects on the intrinsic viscosity and the precipitation temperature of polyethylene oxide (72).

The first extensive work done on the effect of a salt upon the drag reduction of high molecular weight polymers appears to be that of Pruitt, Rosen and Crawford (67). These authors attempted to analyze their drag reduction data by devising a correlation in terms of the exponent a in the Mark-Houwink equation, $[\eta] = KM^a$. That is:

$$\frac{DR_k}{DR_w} = \frac{a_k - 0.5}{a_w - 0.5} \quad ,$$

where subscriptw refers to the values in distilled water while k refers to the values in non-solvent.

The drag reduction of the three Polyethylene oxide polymers was examined in water and five Potassium sulfate solutions ranging from 0.1 to 0.8 Molar concentration.

Recently Little and Patterson (73) suggested that these solvent properties which bring about decided conformational changes in the molecules (as indicated by intrinsic viscosity) also affect, in apparently analogous fashion, the turbulent friction reduction efficiencies of these molecules. The decrease in turbulent friction reduction resulting from the increasingly collapsed state of the polymer coil suggests a possibility of correlating the friction reduction with the changes in expansion factor of the polymer molecule. In general, increasing concentration of salt produced progressive decrease in the drag reducing efficiency of polymer.

2.7 Polymer characterization

Bailey and Callard (72) have given a comprehensive discussion of the properties of Polyethylene oxide in aqueous solution with and without non-solvent. This polymer, which is highly crystalline, is soluble in water due to the hydration of the ether oxygen in a manner which is apparently unique to the Polyethylene oxide structure. This hydration,

which must be a hydrogen bond interaction, is disrupted by thermal and salting out influences. Thus Polyethylene oxide resins are unique in linearity of structure, non-ionic character, and water solubility. This linear relatively non-polar structure displays a high degree of polymer-solvent interaction in water which is observed in the development of structual viscosity to an unusual degree.

The intrinsic viscosity or the limiting viscosity number of a polymer in a solution is defined by

$$[\eta] = \lim_{c \to o} \left[(\eta - \eta_s)/\eta_s \, c \right]$$

when η is the viscosity of the solution at concentration c and η_s is the viscosity of the pure solvent.

Many equations have been put forward to enable the determination of $[\eta]$ graphically or by calculation. The best known equations today are those of Kramer (74), Huggins (75), and Schultz and Blaschke (76), respectively:

$$\ln \eta_r/c = [\eta] + (K_H - 0.5) [\eta]^2 \, c \qquad (2.1)$$

$$\eta_{sp}/c = [\eta] + K_H [\eta]^2 \, c \qquad (2.2)$$

$$\eta_{sp}/c = [\eta] + K_H [\eta] \, \eta_{sp} \qquad (2.3)$$

where η_r is the relative viscosity,

η_{sp} is the specific viscosity,

η_{sp}/c is the reduced viscosity,

and K_H is Huggins constant.

Ibrahim (77) discussed the above equations and suggested that Eq. (2.3) is the only one which should be used on the basis that Eq. (2.1) is an insufficient approximation of Eq. (2.2) which, moreover, is an inadequate approximation of Eq. (2.3). However, it seems that none of the relationships can describe all polymer systems.

In recent work, Hanna (78) observed experimentally that the Schultz and Blaschke equation is an adequate representation for his Polyox-distilled water system.

For a given combination of polymer and solvent, at a fixed temperature, the intrinsic viscosity appears to be a unique function of the molecular weight, represented by the Mark-Houwink equation. This function is expressed as a simple power function:

$$[\eta] = K M^{a}, \qquad (2.4)$$

containing two empirical constants, K and a.

In practice, the molecular weight is always a distributed quantity. The constants, K and a, are therefore based on measurements of polymer fractions with a narrow molecular weight distribution. An empirical method for predicting the $[\eta]$ - M relationship which has been widely used is based on the correlation of experimental points by means of straight line on a log-log scale.

The large deviations in the values for the constants, K and a, can be found in the literature, even in measurement

with the same combination of polymer and solvent but performed by different investigators (71,72,78,79). This is to be expected, if Eq. (2.4) is an approximation of a curved line. If in the approximation, a low value of a is chosen, a higher value of K is found in correlation of the experimental data.

In general, a is dependent on the degree of coiling or extension of the polymer chain and will vary with the solvent used while K is a function of the temperature of the solution (67,80,81). In the literature a number of theoretical studies about intrinsic viscosity can be found. However, a wide discussion of hydrodynamic interaction is given by Kirkwood and Riseman (82,83), using the Oseen formula (84) which arises as a solution of the Navier-Stokes equation of hydrodynamics.

In all the latter developments, the formulation of the hydrodynamic interaction is based on the K-R method. An analysis physically equivalent to the K-R theory was developed independently by Debye and Buche (85) who solved Navier-Stokes equation with boundary conditions appropriate for the uniform density sphere model.

They suggested the theoretical relationship,

$$[\eta] = \Phi_o \sqrt{\overline{r_o^2}}^3 / M, \qquad (2.5)$$

where Φ_o is a function of the draining parameter. Theory also predict that $[\eta]$ is proportional to M^{ν}; ν is a constant. It was the intent of Kirkwood and Riseman, and also Debye

and Buche to interpret a value of ν between 0.5 and 1.0 as arising from the draining effect.

While most of the above theories are necessarily restricted to the study of unperturbed chains, in fact, the intrinsic viscosity of perturbed chains is most important since it is used, along with the molecular dimension and the second virial coefficient, to characterize the polymer. If the draining effect is assumed to be negligible for ordinary flexible high molecular weight polymer molecules (81), it is predicted that the intrinsic viscosity is proportional to the square root of the molecular weight, and that a value of "a"greater than 0.5 in Eq. (2.4) is interpreted as arising from the excluded volume effect.

Indeed it was from this point of view that Flory (81,86) introduced the discussion of the excluded-volume effect in a polymer chain. Replacing $\sqrt{\bar{r}_o^2}$ by $\sqrt{\bar{r}^2}$ in Eq. (2.5), Flory and Fox (81, 87) proposed the following empirical equation for the flexible polymer,

$$[\eta] = \Phi\sqrt{\bar{r}^2}^3/M, \qquad (2.6)$$

where they originally regarded Φ as equal to Φ_o. Φ depends on the excluded volume effect, although not on the draining parameter. The theoretical value of Φ_o lies between 1.81×10^{21} to 3.62×10^{21}(81,82,88-93).

In general, the numerical value of Φ is regarded to be $0.8(\Phi_o)$, with $\Phi_o = 2.66 \times 10^{21}$ (93) and the factor 0.8

used to account for the use of a good (rather than theta) solvent in most drag reduction studies (6,84).

3. THEORETICAL BACKGROUND

3.1 Introduction

Since the original work by Oldroyd (39) who proposed the method of detecting anomalous behaviour near the tube wall, numerous theoretical treatments of the physical status of polymer adsorption have been studied mainly in static flow systems. However there was no detailed analysis available to describe the polymer adsorption phenomenon in a dynamic flow system.

Recently, Kozicki et al. (44) have proposed a scheme of analysis for characterization of polymer adsorption in the vicinity of tube wall occurring in steady laminar flow of dilute polymer solutions. This approach will be adopted in the present analysis as a basis for the characterization of the anomalous flow behaviour of dilute polymer solutions in laminar flow.

3.2 Velocity profile

The problem considered is the steady uniform laminar flow of a dilute polymer solution in a tube where there is polymer adsorption onto the wall.

The velocity gradient for this flow can be represented generally by

$$\frac{du}{dy} = f(\tau) + g(\tau, y), \qquad (3.2\text{-}1)$$

where the function $f(\tau)=\tau/\eta$ represents the velocity gradient in the mainstream of flow, determined by the constitutive equation of state for the fluid. In the polymer concentration range of drag reducing fluids, η is the Newtonian viscosity in the mainstream. The function $g(\tau, y)$ given by

$$\begin{aligned} g(\tau, y) &\neq 0 \qquad \text{for } 0 \leq y < \Delta \\ &= 0 \qquad \text{for } \Delta \leq y \leq R \quad , \end{aligned} \qquad (3.2\text{-}2)$$

is a correction term in the wall region, where the flow characteristics are altered in consequence of the polymer adsorption onto the tube wall. The thickness of the anomalous zone is Δ. The schematic of flow near the tube wall is depicted in Fig. (3.1).

Integration of Eq. (3.2-1) with respect to y gives the velocity expression,

$$u = \int_0^y f(\tau)\ dy + \int_0^y g(\tau,y)\ dy. \qquad (3.2\text{-}3)$$

For $y \geq \Delta$, the second term on the right becomes a constant,

$$u_R = \int_0^{\Delta} g(\tau,y)\ dy, \qquad (3.2\text{-}4)$$

defined as the effective velocity at the wall. It is the displacement of the velocity profile in the mainstream due to the wall effect. Since the function $g(\tau,y)$ characterizing

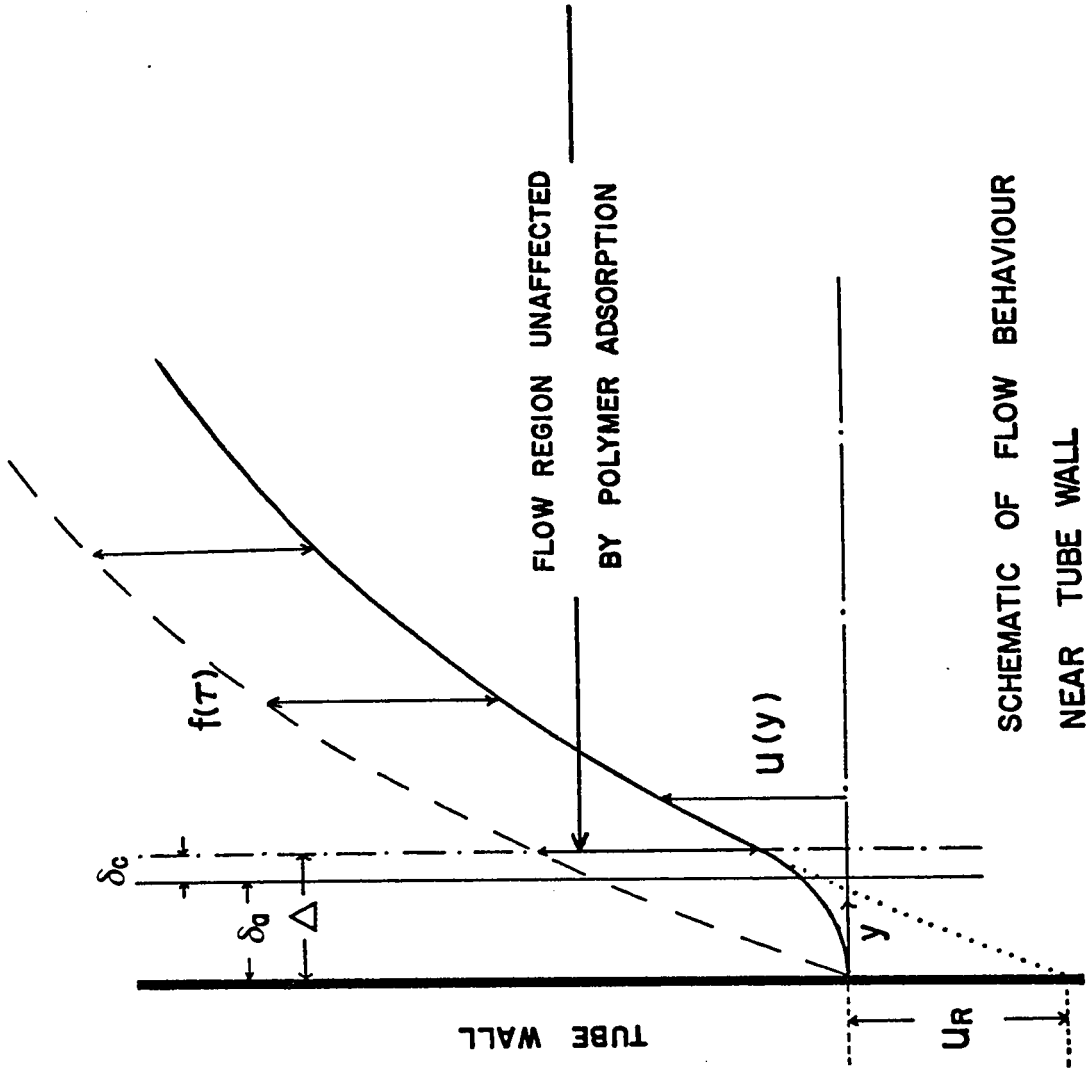
SCHEMATIC OF FLOW BEHAVIOUR
NEAR TUBE WALL
FLOW REGION UNAFFECTED
BY POLYMER ADSORPTION
TUBE WALL
U(y)
f(τ)
y
δc
δa
Δ
UR

Figure 3.1

the distinct behaviour in the anomalous zone is not readily amenable to evaluation, a direct approach is used in the development of the velocity distribution.

We assume the following polynomial for the velocity distribution in the anomalous zone ($o \leq y \leq \Delta$):

$$u^{<} = m_o + m_1 y + m_2 y^2 + - - - + m_{n+2} y^{n+2} \qquad (3.2\text{-}5)$$

To evaluate the coefficients m_i, (n+3) boundary conditions are imposed as follows:

B.C. (1):

$$\frac{du^{<}}{dy} = \frac{\tau}{\eta} = (1 - \frac{y}{R}) \frac{\tau_w}{\eta} \qquad \text{at } y = \Delta \qquad (3.2\text{-}6)$$

B.C. (2):

$$\frac{\eta}{R-y} \frac{d}{dy} \left[(R - y) \frac{du^{<}}{dy} \right] = \frac{dP}{dz} \qquad \text{at } y = \Delta \qquad (3.2\text{-}7)$$

B.C. (3):

$$u^{<} = 0 \qquad \text{at } y = 0 \qquad (3.2\text{-}8)$$

B.C.'s (4) to (n+3):

$$\frac{du^{<}}{dy} = \frac{d^2u^{<}}{dy^2} = - - - = \frac{d^nu^{<}}{dy^n} = 0 \qquad \text{at } y = 0 \qquad (3.2\text{-}9)$$

Boundary conditions (1) and (2) assume the continuity of the first and second velocity derivatives across the anomalous zone - mainstream interface, and take advantage of the constitutive equation of state and the equation of motion, applicable to the mainstream, respectively. Boundary condition (3) specifies the no-slip condition at the wall.

The remaining boundary conditions comprise the adsorption conditions at the wall. These determine the bluntness of the profile near the wall in a way that the bluntness increases progressively with increase in the number of conditions, n. Since blunter profiles are associated with higher polymer adsorption levels, the exponent n serves as an index of the level of polymer adsorption. It is seen that whereas B.C.'s (1) to (3) apply uniformly, the number of adsorption conditions is variable and depends upon the polymer adsorption level, n.

By first applying B.C.'s (3) to (n+3), Eq. (3.2-5) is reduced to 2 terms as follows, in dimensionless form,

$$\overline{u}^{<} = m'_{n+1}\,\overline{y}^{n+1} + m'_{n+2}\,\overline{y}^{n+2} \qquad (3.2\text{-}10)$$

Recasting boundary conditions (1) and (2) into dimensionless form, we obtain

B.C. (1):

$$\frac{d\overline{u}^{<}}{d\overline{y}} = 1 - \overline{\Delta} \qquad \text{at } \overline{y} = \overline{\Delta} \qquad (3.2\text{-}11)$$

B.C. (2):

$$\frac{1}{1-\overline{y}}\,\frac{d}{d\overline{y}}\left[(1-\overline{y})\,\frac{d\overline{u}^{<}}{d\overline{y}}\right] = -2, \qquad \text{at } \overline{y} = \overline{\Delta} \qquad (3.2\text{-}12)$$

which may be used to evaluate the coefficients m'_{n+1} and m'_{n+2} in Eq. (3.2-10):

$$m'_{n+1} = \frac{(n+1) - n\overline{\Delta}}{(n+1)\overline{\Delta}^{n}} \qquad (3.2\text{-}13)$$

and

$$m'_{n+2} = \frac{(n-1)\bar{\Delta} - n}{(n+2)\bar{\Delta}^{n+1}} \qquad (3.2\text{-}14)$$

The velocity distribution is therefore given by the following function of the position variable for the anomalous zone, $\tilde{y} = y/\Delta$:

$$\bar{u}^{<} = \bar{\Delta} \left\{ \left[\frac{(n+1)-n\bar{\Delta}}{n+1} \right] \tilde{y}^{n+1} + \left[\frac{(n-1)\bar{\Delta}-n}{n+2} \right] \tilde{y}^{n+2} \right\} \qquad (3.2\text{-}15)$$

$$\text{for } 0 \leq \tilde{y} \leq 1$$

The parameters influencing the velocity distribution are the polymer adsorption level and anomalous zone thickness.

Although the development of Eq. (3.2-15) is based on the use of a polynomial expression, the equation is not limited in its application to integer values of n, but is amenable to continuous variation of the index. For noninteger values of the adsorption index, it can be shown that the conditions at the wall, Eq. (3.2-9), are still satisfied with n rounded off to the nearest lower integer.

Substitution of n=0 in Eq. (3.2-15) results in

$$\bar{u}^{<} = \bar{y} - \frac{1}{2}\bar{y}^2, \qquad (3.2\text{-}16)$$

the familiar parabolic profile for a Newtonian fluid without a surface effect. Setting $n = \infty$, one obtains $\bar{u}^{<} = 0$, i.e. a complete immobile anomalous zone at the maximum adsorption level.

Eq. (3.2-3) evaluated at the edge of the anomalous zone can be used to determine U_R explicitly,

$$u_R = u^{<}(\Delta) - \int_o^{\Delta} f(\tau)\, dy \qquad (3.2\text{-}17)$$

Introduction of the velocity distribution given by Eq. (3.2-15) gives

$$\bar{u}_R = - \frac{n\bar{\Delta}}{n+2} \left[1 - \frac{(n-1)\bar{\Delta}}{2(n+1)} \right] . \qquad (3.2\text{-}18)$$

A negative effective velocity at the wall is manifested by the polymer adsorption. $\bar{u}_R$ vanishes when either the anomalous zone thickness or adsorption level is zero.

With $\bar{u}_R$ known, the velocity distribution in the mainstream can also be evaluated in accordance with Eqs. (3.2-3) and (3.2-4) by

$$\bar{u}^{>} = \frac{1}{2} (1 - \bar{r}^2) + \bar{u}_R \qquad (3.2\text{-}19)$$

3.3 Average velocity

The average velocity for the flow with polymer adsorption obtained by integration of the velocity distribution, Eqs. (3.2-15) and (3.2-19), across the tube cross section,

$$\langle \bar{u} \rangle = 2 \int_o^{\bar{\Delta}} \bar{u}^{<} (1 - \bar{y})\, d\bar{y} + 2 \int_{\bar{\Delta}}^{1} \bar{u}^{>} (1 - \bar{y})\, d\bar{y}, \qquad (3.3\text{-}1)$$

is given by

$$\langle \bar{u} \rangle = \frac{1}{4} + \bar{u}_w, \qquad (3.3\text{-}2)$$

where $\bar{u}_w$ is the negative displacement in average velocity (average velocity deficiency), associated with polymer adsorption:

$$\bar{u}_w = -\frac{n\bar{\Delta}}{n+2}\left[1 - \frac{3n^2+6n-1}{2(n+1)(n+3)}\bar{\Delta} + \frac{n^2+3n-2}{(n+3)(n+4)}\bar{\Delta}^2 - \frac{(n-1)(n+2)}{4(n+3)(n+4)}\bar{\Delta}^3\right] \quad (3.3\text{-}3)$$

In Eq. (3.3-3), the diminution of flow is related to the two parameters characterizing the polymer adsorption.

Since Eq. (3.3-2) is the experimental basis for the evaluation of $\bar{u}_w$, the latter equation is expressed with variables which are experimentally measurable, by the following equation:

$$\frac{8(\langle u\rangle - u_w)}{D} = \frac{\tau_w}{\eta} , \quad (3.3\text{-}4)$$

where η is the viscosity of bulk solution. In the limiting case of no wall effect, Eq. (3.3-4) reduces to

$$\frac{8\langle u\rangle}{D} = \frac{\tau_w}{\eta} . \quad (3.3\text{-}5)$$

Eq. (3.3-4) can also be expressed as follow:

$$\tau_w = \eta_a \frac{8\langle u\rangle}{D}, \quad (3.3\text{-}6)$$

where $\eta_a = (1 - u_w/\langle u\rangle)$, referred to as viscosity coefficient, which is a combined value resulted from the effects of bulk solution viscosity and polymer adsorption onto the tube wall. Eq. (3.3-6) can be rewritten as a dimensionless form,

$$\langle\bar{u}\rangle = \frac{\eta}{4\eta_a} \tag{3.3-7}$$

Substituting Eq. (3.3-7) into Eq. (3.3-2),

$$\bar{u}_w = \frac{1}{4}\left(\frac{\eta}{\eta_a} - 1\right) \tag{3.3-8}$$

Eq. (3.3-8) provides a simple method for evaluating $\bar{u}_w$ from the experimental values of η and η_a.

The variation in the thickness of anomalous zone with n, at a given value of $\bar{u}_w$, can be seen in Eqs. (3.3-2) and (3.3-3). Assuming $\bar{\Delta} << 1$, Eq. (3.3-2) can be approximated by:

$$\langle\bar{u}\rangle = \frac{1}{4} - \frac{n}{n+2}\,\bar{\Delta} \tag{3.3-9}$$

At the maximum adsorption level, this becomes

$$\langle\bar{u}\rangle = \frac{1}{4} - \bar{\Delta}_{n=\infty} \tag{3.3-10}$$

Combining the latter gives

$$\bar{\Delta} = \frac{n+2}{n}\,\bar{\Delta}_{n=\infty} \tag{3.3-11}$$

The computed dimensionless anomalous zone thickness, therefore, decreases with increasing n, and $\bar{\Delta}_{n=\infty}$ represents the minimum thickness producing the observed diminution in the average velocity. Consideration of the flow occurring in the anomalous zone will result in a larger thickness of the latter than $\bar{\Delta}_{n=\infty}$.

It should be noted that Eq. (3.3-11) does not

apply when n approach zero. The large values predicted for $\overline{\Delta}$ would contradict the premise that $\overline{\Delta}$ is very small.

As the basis for further analysis, it is envisaged that the polymer adsorption produces a zone adsorbed polymer of thickness δ_a, within the anomalous zone, and that only solvent micromolecules flow in the porous network so formed (valid where the effective pore diameter is less than the diameter of a polymer molecule). The polymer molecules in the flowing fluid which are diverted away from the adsorption zone results in the production of a concentrated layer of the polymer with thickness δ_c, such that $\Delta=\delta_a+\delta_c$. The velocity distribution for the anomalous zone enables one to characterize the adsorption zone and concentrated layer.

3.4 Porosity distribution in the adsorption zone

It is assumed that the flow in the adsorption zone follows Brinkman's law for flow through a porous medium with a free surface (94),

$$\nabla P = - \frac{\eta_s}{k} U + \eta_s \nabla^2 U, \qquad (3.4\text{-}1)$$

where k is the permeability; η_s is the effective viscosity of the fluid. The validity of using the same viscosity in both terms on the right side of Eq. (3.4-1) has been discussed by Neale et al. (95). As indicated, η_s becomes the viscosity of the solvent.

For the case of no adsorption, $k=\infty$, $\eta_s=\eta$, and Eq. (3.4-1) reduces to the expected form describing flow in an unobstructed pipe. Appropriately, the velocity distribution, Eq. (3.2-15), is also the superficial velocity distribution in the context of flow through the adsorption zone.

Eq. (3.4-1) in cylindrical coordinates can be solved for the permeability,

$$\bar{k} = \frac{k}{R^2} = \frac{\bar{u}^{<}}{\frac{1}{(1-\bar{y})}\frac{d}{d\bar{y}}\left[(1-\bar{y})\frac{d\bar{u}^{<}}{d\bar{y}}\right] + 2\eta_r}, \qquad (3.4\text{-}2)$$

where the relative viscosity, η_r, is the polymer solution viscosity in the mainstream divided by the viscosity of the solvent. The Schultz and Blaschke equation relates the relative viscosity to the intrinsic viscosity and solution concentration by

$$\eta_r = 1 + \frac{c\,[\eta]}{1 - K_H\, c\,[\eta]}, \qquad (3.4\text{-}3)$$

where K_H is Huggins' constant.

Substitution for $\bar{u}^{<}$ given by Eq. (3.2-15), in Eq. (3.4-2), gives the radial variation in permeability of the adsorption zone:

$$\bar{k} = \frac{\bar{\Delta}^2\,(1-\tilde{y}\bar{\Delta})(A_2\tilde{y}^2 - A_3\tilde{y}^3)}{B_o - B_1\tilde{y} + B_2\tilde{y}^2 + 2\,\bar{\Delta}\eta_r(1-\tilde{y}\bar{\Delta})\tilde{y}^{1-n}}, \qquad (3.4\text{-}4)$$

where the A_i and B_i are given by

$$A_2 = \frac{(n+1) - n\bar{\Delta}}{n+1}$$

$$A_3 = \frac{n - (n-1)\bar{\Delta}}{n+2}$$

$$B_o = n\left[(n+1) - n\bar{\Delta}\right] \qquad (3.4\text{-}5)$$

$$B_1 = (n+1)\left[n + (2-n\bar{\Delta})\bar{\Delta}\right]$$

$$B_2 = \bar{\Delta}\,(n+2)\left[n - (n-1)\bar{\Delta}\right] .$$

The relationship of the permeability to the porosity is given by the Blake-Kozeny equation:

$$\bar{k} = \frac{\bar{\Delta}^2\,\tilde{D}_e^2\,\varepsilon^3}{s^2 k_i\,(1-\varepsilon)^2} \quad , \qquad (3.4\text{-}6)$$

where the geometric parameter k_i is a function of porosity, and s is a particle shape factor related to the specific surface s_o of the particles comprising the porous medium by $s_o = s/D_e$. The shape factor is 6 for a sphere and 4 for an infinite cylinder.

However, high molecular weight linear macromolecules are thought to form random coils which are approximately spherical in shape. Henceforth, the adsorbed macromolecules are assumed to retain the spherical conformation with effective diameter D_e, and that the flow of solvent occurs around the peripheral region in the random coiled conformation, i.e. there is no flow of solvent through the polymer coils.

Lumping all of the parameters involving ε including the k_i together, Eq. (3.4-6) can be expressed in the form analogous to Neale and Nader (96):

$$\bar{k} = \left[\frac{\tilde{D}_e \bar{\Delta}}{2\,\alpha(\varepsilon)}\right]^2 . \qquad (3.4\text{-}7)$$

The values of $\alpha(\varepsilon)$ for homogeneous swarms of monosized spheres have been tabulated by the latter.

For the determination of the porosity distribution curves, the latter tabulation was used directly in the numerical evaluation of Eq. (3.4-7) by the following empirically fitted equation:

$$\alpha(\varepsilon) = \frac{4.0\ (1-\varepsilon)^{0.6}}{\varepsilon^{1.92}} , \qquad (3.4\text{-}8)$$

which gives a reasonably good representation not only for the theoretical results of Neale and Nader but also for the experimental data of Martin et al. (97).

Combination of Eqs. (3.4-4) and (3.4-7) gives the following equation to be solved numerically for the porosity distribution in the adsorption zone, with $\bar{\Delta}$, n, $\tilde{D}_e$ and η_r (or c and $[\eta]$) as parameters:

$$\frac{(1 - \tilde{y}\bar{\Delta})(A_2\tilde{y}^2 - A_3\tilde{y}^3)}{B_o - B_1\tilde{y} + B_2\tilde{y}^2 + 2\eta_r \bar{\Delta}(1-\tilde{y}\bar{\Delta})\tilde{y}^{1-n}} - \left[\frac{\tilde{D}_e}{2\,\alpha(\varepsilon)}\right]^2 = 0 \qquad (3.4\text{-}9)$$

3.5 Relationship of porosity ε to concentration c in the adsorption zone

The adsorbed macromolecules in the adsorption zone are assumed to be spherical with effective diameter D_e and the flow of solvent is around the peripheral zone of the random conformation, i.e. there is no flow of solvent through the polymer coils.

In a given volume of the adsorption zone, the concentration of macromolecules can be expressed as follow:

$$c = \frac{n_o 100\ M}{\tilde{N}\ V}\ , \qquad (3.5\text{-}1)$$

where c = concentration, g/dl

V = volume of adsorption zone, cm^3

n_o = number of macromolecules in V

M = molecular weight

$\tilde{N}$ = Avogadro number.

Since the volume occcupied by spheres can be expressed as

$$n_o \times \frac{\pi}{6} D_e^3,$$

the void space will be $V - n_o \frac{\pi}{6} D_e^3$.

Therefore porosity becomes

$$\varepsilon = 1 - \frac{n_o \frac{\pi}{6} D_e^3}{V}\ . \qquad (3.5\text{-}2)$$

Rearranging Eq. (3.5-1),

$$\frac{n_o}{V} = \frac{c\,\tilde{N}}{100\,M} \cdot \qquad (3.5\text{-}3)$$

Substituting Eq. (3.5-3) into Eq. (3.5-2), one can obtain porosity as a function of concentration:

$$\varepsilon = 1 - \frac{c\,\tilde{N}}{100\,M}\,\frac{\pi}{6}\,D_e^3 \cdot \qquad (3.5\text{-}4)$$

Solving for c, we obtain

$$c = \frac{600\,M}{\pi\tilde{N}\,D_e^3}\,(1 - \varepsilon). \qquad (3.5\text{-}5)$$

Utilizing Flory-Fox equation, Eq. (2.6), with the assumption of $\sqrt{\overline{r^2}} = D_e$,

$$[\eta] = \Phi\,\frac{D_e^3}{M},$$

Eq. (3.5-4) can be written as

$$\varepsilon = 1 - \frac{\pi\,\tilde{N}\,c_a\,[\eta]}{600\,\Phi} \cdot \qquad (3.5\text{-}6)$$

Substituting $\tilde{N} = 6.023 \times 10^{23}$,

$$\Phi = 2.1 \times 10^{21},$$

finally $$\varepsilon = 1 - 1.5\,c_a\,[\eta] \qquad (3.5\text{-}7)$$

which indicates a simple relationship between porosity and concentration of the macromolecules in the adsorption zone for a given intrinsic viscosity.

3.6 Polymer concentration distribution in the concentrated layer

Referring to Eq. (3.4-3), the polymer concentration in the concentrated layer can be expressed as

$$c_c = \frac{\eta_c/\eta_s - 1}{[\eta]\left[1 + K_H(\eta_c/\eta_s - 1)\right]} \quad . \tag{3.6-1}$$

The viscosity in the concentrated layer may be expressed as

$$\eta_c = \frac{\tau}{du/dy} \tag{3.6-2}$$

or in dimensionless form,

$$\frac{\eta_c}{\eta} = \frac{\bar{\Delta}\ (1 - \tilde{y}\ \bar{\Delta})}{d\bar{u}^{<}/d\tilde{y}} \quad . \tag{3.6-3}$$

Introduction of the velocity distribution, Eq. (3.2-15), gives

$$\frac{\eta_c}{\eta} = \frac{1 - \tilde{y}\ \bar{\Delta}}{\left[(n+1) - n\bar{\Delta}\right]\tilde{y}^n - \left[n - (n-1)\bar{\Delta}\right]\tilde{y}^{n+1}} \quad , \tag{3.6-4}$$

which is valid for $\delta_a/\Delta \leq \tilde{y} \leq 1.0$.

Multiplication of Eq. (3.6-4) by Eq. (3.4-3) gives the viscosity ratio η_c/η_s, which may be substituted in Eq. (3.6-1) to obtain the polymer concentration distribution in the concentrated layer. The polymer concentration distribution is a function of the parameters n, $\bar{\Delta}$, c and $[\eta]$.

At the edge of the anomalous zone, $\tilde{y} = 1.0$, Eq. (3.6-4) gives $\eta_c/\eta = 1.0$, for which Eq. (3.6-1) also

gives $c_c = c$, i.e. the concentration of polymer at the edge of the anomalous zone is that in the mainstream.

3.7 Determination of the adsorption zone thickness

The location within the anomalous zone of the interface between the adsorption zone and the concentrated layer is established with the aid of a material balance. Due to the assumed impermeability of the adsorption zone to passage of polymer, all of the convective transport of polymer in the anomalous zone occurs in the concentrated layer and a polymer balance in the anomalous zone leads to

$$2\,\P\,c \int_o^{\Delta} u^{<}(R-y)\ dy = 2\,\P \int_{\delta_a}^{\Delta} c_c\, u^{<}(R-y)\ dy, \qquad (3.7\text{-}1)$$

or, in dimensionless form,

$$\int_o^1 \bar{u}^{<}(1-\tilde{y}\bar{\Delta})\ d\tilde{y} = \int_{\tilde{\delta}_a}^1 \left(\frac{c_c}{c}\right) \bar{u}^{<}(1-\tilde{y}\bar{\Delta})\ d\tilde{y}. \qquad (3.7\text{-}2)$$

The location of the interface $\tilde{\delta}_a$ is found numerically so as to satisfy Eq. (3.7-2). It is a function of the parameters appearing in the velocity and concentration distribution.

4. EXPERIMENTAL

4.1 Description of equipment

A simple, once through gravity flow system was employed for the pressure drop - flow measurement. Fig. (4.1) is a schematic diagram of the apparatus comprised of a supply tank, constant head device, and five test sections of tubing with different tube diameters.

Cathetometers were used in the measurement of the pressure drop across each test section of tubing.

The flow rate measurements were carried out by the bucket and stop watch method employing the GRAM-ATIC electrical balance with the sensitivity of 0.0001 g supplied by Fisher Scientific Co. for the measurement of the mass collected in the bucket. A stop watch with 0.1 second subdivisions was used to time the flow rate.

The Cannon Fenske Routine viscometer was used for supplementing the tube flow data measurements.

4.1-1 Test section

Five annealed and seamless, type 304, stainless steel tubes were used as the test sections, ranging from 1.26718 to 0.30521 cm in inside tube diameter. These were supported horizontally on a board. The inside surfaces of the tubes were smooth.

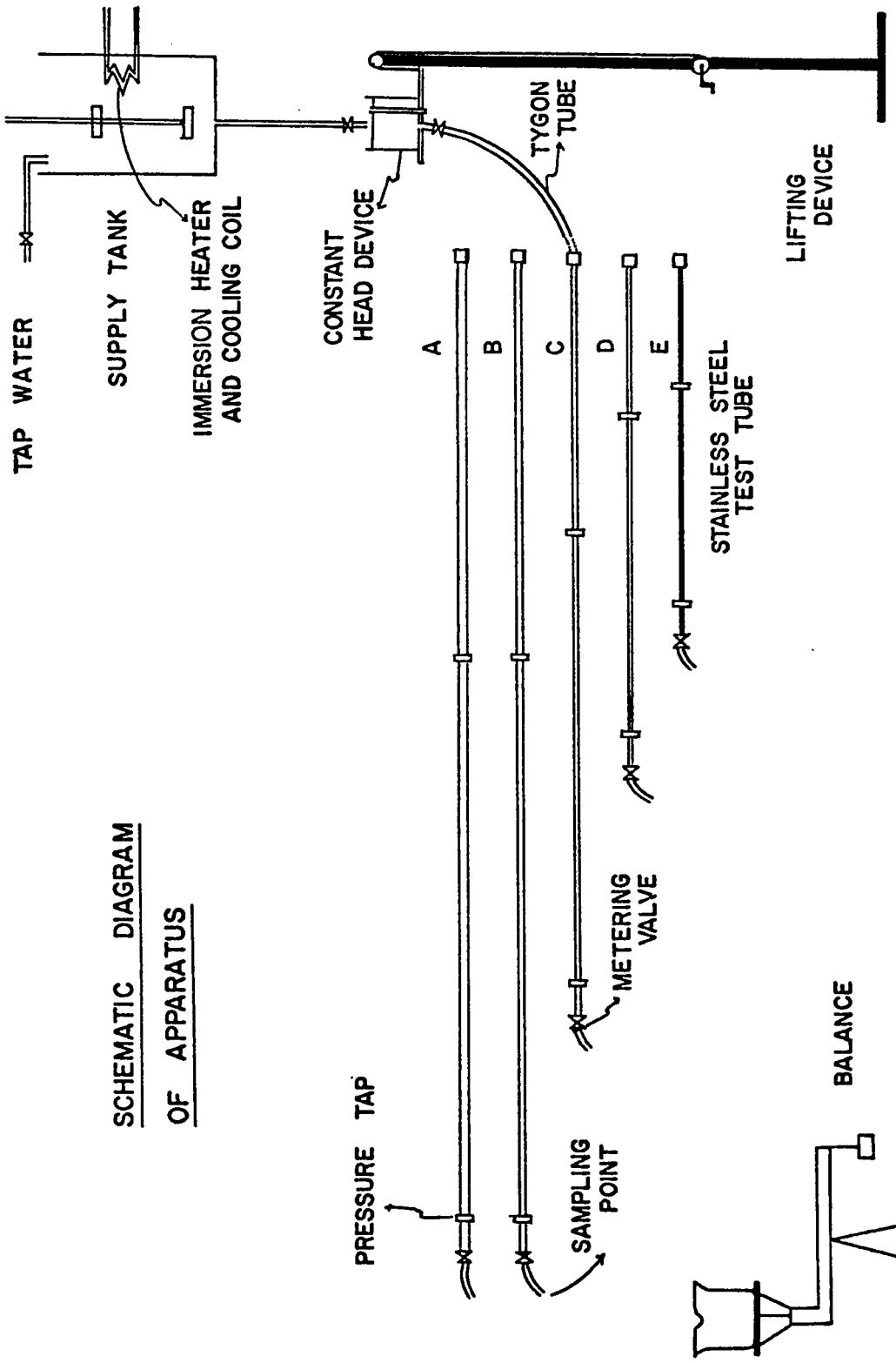

SCHEMATIC DIAGRAM OF APPARATUS

Figure 4.1

Each tube was rigidly supported at multiple points along its length to ensure stability and straightness. Each tube was equipped with a pressure tap near the tube inlet and a second near the tube outlet. The dimensions of the tubes are given in Table (4.1).

An entrance length of over 300 tube diameters considered to be long enough for attainment of fully developed flow was provided for each test section. The downstream pressure tap was situated at a distance of over 30 tube diameters from the discharge end of each tube.

The tube length was decreased with decreasing tube diameter to permit the achievement of an Re up to 1000 at the available maximum level of head in the constant head device. The pressure drop increases rapidly as tube diameter decreases for a given tube length. Each tube was connected to the constant head device through a flexible Tygon tube for a smooth entrance of the solution and easy connection of the Tygon tube to the different test sections. A suitable valve was situated on the Tygon tube for a quick operation of the solution influx to the test section.

The flow was controlled by a valve situated at the downstream end of test section and finally exited into a bucket used to obtain the flow rate.

Table 4.1

Dimensions of test tubes

	Tube diameter	Total length	Entrance region	Test section	End region
A	1.26718	1007	360.3(284)	608.7(480)	38(30)
B	0.94311	1008	359.6(381)	610.4(647)	38(40)
C	0.62711	760	271.2(432)	450.8(719)	38(60)
D	0.43887	530	171.9(392)	320.1(730)	38(87)
E	0.30521	380	121.7(399)	220.3(722)	38(125)

( ): ratio to tube diameter

unit: cm

Table 4.2

Dimensions of pressure taps

	Diameter of manometer hole	Ratio to tube diameter	Diameter of glass manometer
A	0.185	0.146	0.179
B	0.140	0.148	0.150
C	0.094	0.150	0.099
D	0.064	0.146	0.099
E	0.064	0.200	0.099

unit: cm

4.1-2 Pressure tap and glass manometer

The holes for the pressure taps on test sections were drilled with a slowly rotating drill taking extreme care so as not to leave any burrs around the holes on the inside of the tubes. The holes were drilled perpendicular to the tangent plane (horizontal) at the highest point on the tube surface with the tube in the horizontal position.

The ratio of the hole diameter to the inside tube diameter of test section, d/D, was about 0.15 in order to minimize flow disturbances by the presence of the hole. In the case of the smallest tube, the tube wall could not be penetrated by the drill pin and the next layer drill pin was used. The details of the manometer connection are shown in Fig. (4.2).

The diameter of glass manometer was chosen to match as closely as possible to the diameter of pressure tap hole in test section. In the case of the two tubes with the smallest tube diameters, the oscillation of the liquid levels in glass manometers was significant. This phenomenon might result from the capillarity of the glass manometers when the glass manometers have the same order of inside diameters with the pressure tap holes in the test sections. It was found that the degree of oscillation could be reduced by employing one step larger size of the glass manometer.

The dimensions of the pressure tap unit for all

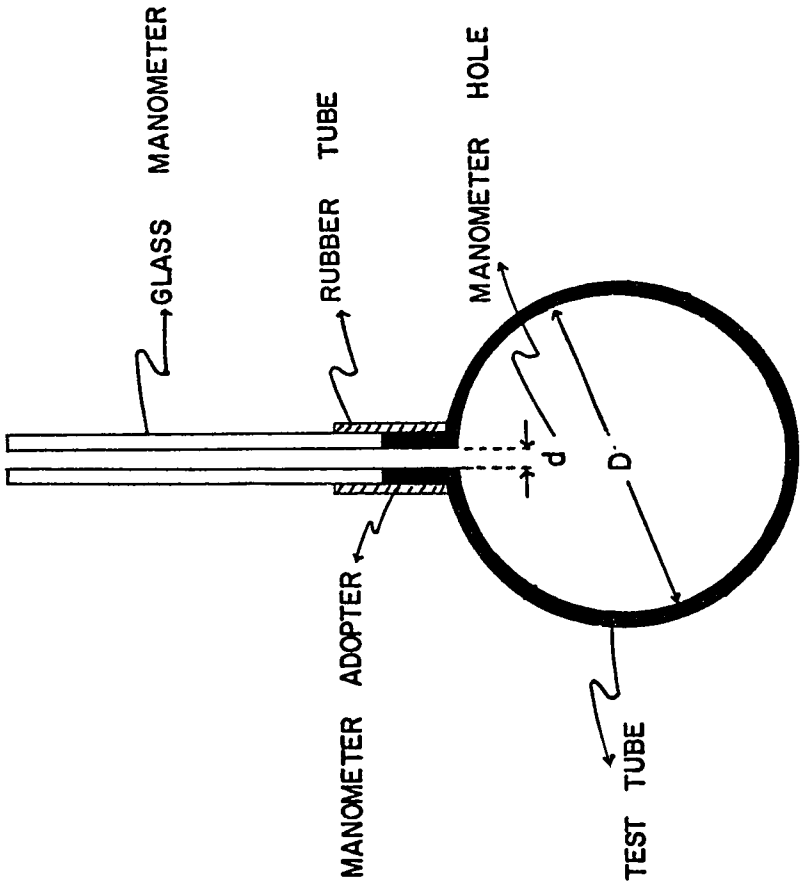

PRESSURE TAP

Figure 4.2

test sections are listed in Table (4.2). In order to ensure that there would be no protuberances at the tap holes in the inner surface of test sections, tubes were cut 60 cm from the upstream pressure tap holes so that a suitable stainless steel rod with a fine file at the end could reach easily to the tap hole to remove the burrs. A small special scraping tool made of a stainless steel wire was also used to remove the burrs attached to the pressure tap hole wall.

After the removal of the burrs, the segment test sections were then supported along its length and tensioned to make it straight to be rejoined by a standard tube-tube union made of stainless steel.

The length of the glass manometer was chosen to give an appropriate level of manometer fluid for the entire flow region. There was no problem of the visibility of the liquid interface in the glass manometer. Glass manometer was joined to the manometer adapter with the help of a flexible rubber tube as shown in Fig. (4.2).

4.1-3 Supply tank and constant head device

Polymer master solution was diluted in a stainless steel container with a capacity of 100 liters. This polymer solution reservoir was equipped with a tap water inlet for the cleaning of the tank after experiment, a level indicator to show the solution level, immersion heater and cooling coil

with a stirrer located inside of tank for the temperature control at the room temperature, 25°C, and a solution outlet. A suitable valve was situated at the outlet of the supply tank to regulate the flow of polymer solution, avoiding an excess overflowing in the constant head device.

The constant head device employing the overflow system was constructed so that the fluid was gravity-fed into the test section at a constant pressure head as shown in Fig. (4.3).

4.1-4 Cathetometer

Fluid levels shown in the glass manometers were measured by cathetometers with the accuracy of 0.001 cm supplied by the Precision Tool Instrument Co. Two cathetometers were used for both upstream and downstream of each test section. The difference of scales between two cathetometers can be corrected by measuring the liquid levels of the glass manometers when the valve at the end of the test section was closed on the ground that the both liquid levels of the glass manometers should be in a horizon in such a static state.

To ensure the completeness of the liquid levels in glass manometers, a reference tube was employed: two glass tubes at the end connected directly to each other with a flexible tygon tube having half inch in inside diameter, located vertically at upstream and downstream as closely as possible to the respective glass manometers. If the glass manometers

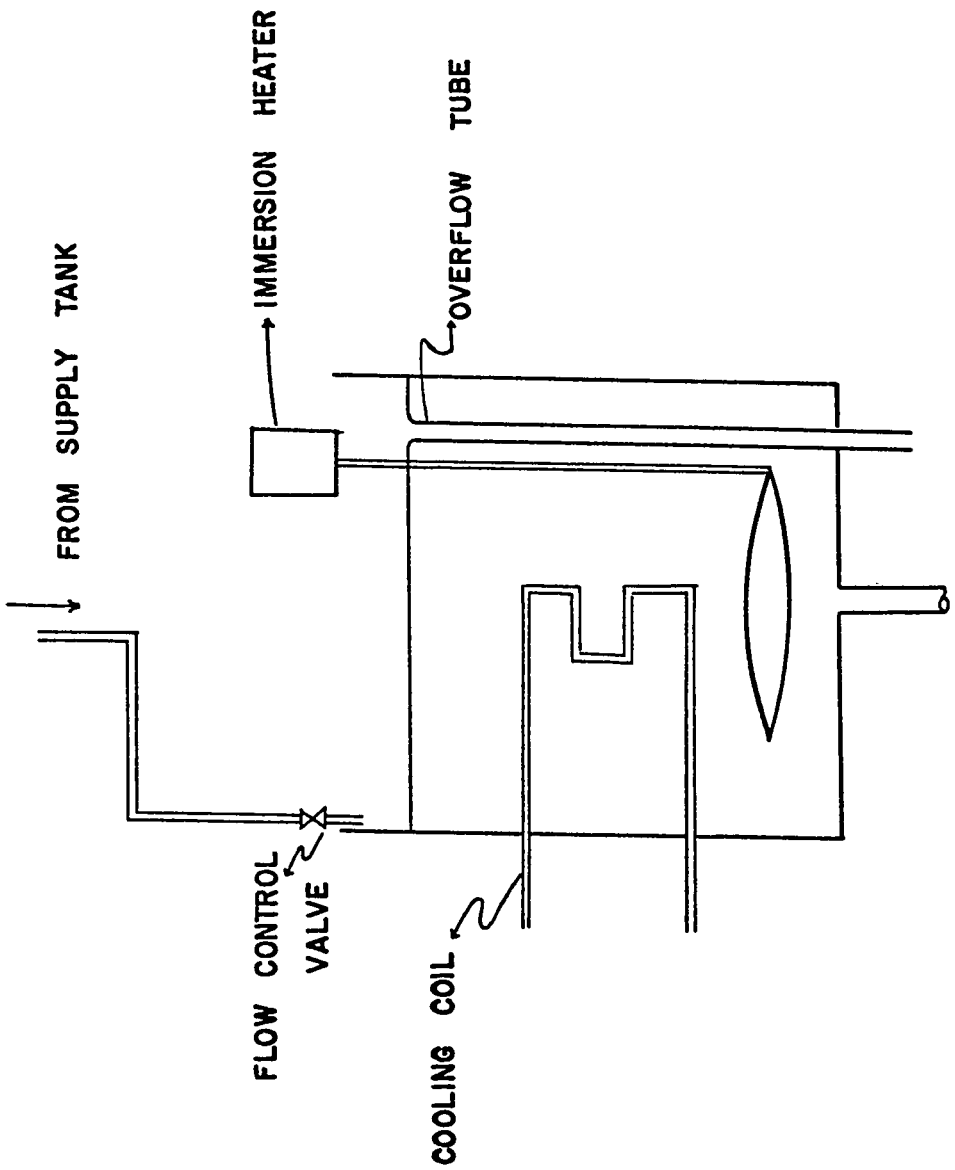
FROM SUPPLY TANK
IMMERSION HEATER
OVERFLOW TUBE
FLOW CONTROL VALVE
COOLING COIL
CONSTANT HEAD DEVICE

Figure 4.3

are completely cleaned and installed on test section, the difference of the fluid levels between glass manometer and reference tube should be same for both upstream and downstream in a test section at the static flow condition.

4.1-5 Cannon Fenske viscometer and pycnometer

Flow measurements were made in Cannon Fenske viscometer No. 50, having a constant, 0.004132 at 25°C, immersed in a constant temperature bath supplied by Precision Scientific Co. as shown in Fig. (4.4). The temperature in the bath was controlled by a stainless steel coil with cold water, and by an immersible electric heating rod which was regulated by a thermoregulator with a sensitivity of ± 0.1°C.

Liquid movement for the homogeneous temperature in the bath was accomplished by a submersible pump and an electric stirrer. Measurements of the flow time were taken with an electric timer with a graduation of 0.1 second.

The solution density was measured in pycnometer bottle having a double wall for insulation.

4.2 Experimental procedure

4.2-1 Preparation of equipment

Distilled water was used for all processes through

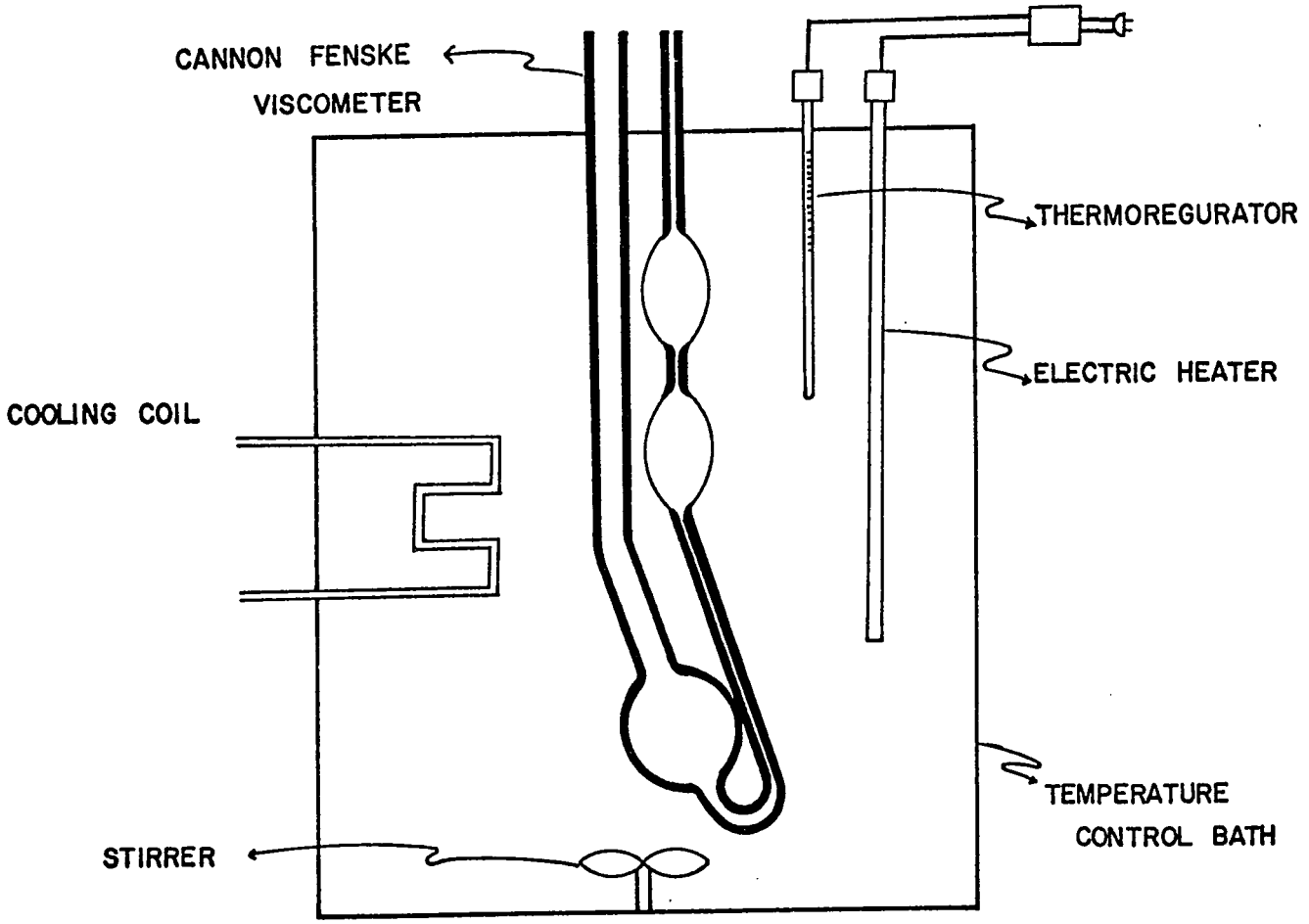

Cannon Fenske viscometer in a constant temperature bath

Figure 4.4

experiment: cleaning, calibration and preparation of solution. Tap water was used only for the preliminary cleaning of supply tank and test sections after each measurement, and then followed by the cleaning with distilled water. Traces of organic materials were removed by using acetone.

After cleaning of test section, the glass manometer was installed vertically on the pressure tap hole with the help of a rubber tube.

The position of each cathetometer was corrected to be completely balanced for both frame and telescope.

Glass manometers were cleaned carefully before installation with chromic acid which has been proved to be the most effective solvent for the removal of organic material in the inner surface of glass manometer.

4.2-2 Preparation of polymer solution

Special samples of Polyox Coagulant and Polyox WSR 301 were used for the present study, provided by Union Carbide Corp. The characteristics of the polymers which are relevant to this work are listed in Table (4.3).

It is well known that the pressure drop - flow rate measurements depend significantly on the way in which the drag reducing polymer solution were prepared. In the present investigation, it was clearly demonstrated that it was necessary to develop a standard procedure to obtain

Table 4.3

Characteristics of the polymers in solutions used in the present work

	$[\eta]$, dl/g	$\bar{M}_w \times 10^{-6}$	$\sqrt{\bar{r}^2}$
Polyox Coagulant in distilled water	14.2	3.94	2986.2
Polyox Coagulant in 0.3M K_2SO_4	7.3		2392.2
Polyox WSR 301 in distilled water	8.9	2.18	2098.3
Polyox WSR 301 in 0.3M K_2SO_4	4.7		1696.1

$\sqrt{\bar{r}^2}$: root-mean-square end-to-end distance of polymer macromolecule, Å.

$[\eta] = 0.875 \times 10^{-4} \bar{M}_w^{0.79}$ for Polyox at 25°C in distilled water

$[\eta] = 2.1 \times 10^{21} \frac{\sqrt{\bar{r}^2}^3}{\bar{M}_w}$ Flory-Fox Equation

reproducible results (see RESULTS AND DISCUSSION).

The method used in preparation of the polymer solutions in this work was based on information provided by Union Carbide Corp. (101) and by Arunachalam (48), with some modification.

For the Polyox group additives, cold mixing was known to be the most suitable. First, a required amount of polymer for a given concentration was weighed in a dry pad. Then a corresponding quantity of solvent (distilled water) to make a master solution of 1% by weight concentration was measured in a container.

The weighed polymer was sprinkled at regular intervals uniformly over the surface of the solvent in a thin layer to avoid lumping of the polymer particles. Occasional gentle stirring was applied using a glass rod to ensure an adequate dispersion of the solute. Any agglomerate formation of polymer particles would result in a considerably longer time to dissolve the particles. The process of dispersing the polymer took about 20-30 minutes per batch depending on the amount of polymer required.

After the completion of the polymer dispersion, the entire container with glass rod was closed air tight and stored in a dark room. After 24 hours, the polymer was dissolved completely with no visible traces of undissolved lumps. It was found that any mechanical stirring during the polymer dispersion was not helpful for the polymer dispersion,

but rather caused polymer agglomeration by the presence of the liquid vortex in the container.

The resultant 1% by weight master solution was diluted later as required in subsequent test runs. It was found that the 1% solution could be stored in an air tight container for several days with no apparent effect on the properties of the diluted solutions.

4.2-3 Pressure drop measurement

A well prepared 1% solution was added slowly to the supply tank containing the required amount of distilled water for a predetermined concentration of polymer in the diluted solution.

The diluted solution was allowed to stand for an hour with gentle mixing by an overhead electric stirrer equipped with two blades attached to the upper and lower parts of the stirrer axis for homogeneous mixing. The preparation of the diluted polymer solutions in poor solvent involved the addition to the aqueous polymer solution of K_2SO_4 powder in the amount required to produce a solution 0.3 molar in K_2SO_4. The K_2SO_4 was found to dissolve rapidly in the dilute polymer solutions.

A freshly prepared solution was then transferred into the constant head device made of transparent acrylic material. Mechanical stirring was not provided to avoid disturbances affecting the constant level surface. The

location of the level in the constant head device could be altered as required to give a desired flow rate in the test section.

When a steady flow in the constant head device was achieved, the valve was opened permitting the solution to flow into the test section. After a few minutes, the outlet valve of the test section was closed, stopping the flow, and the liquid levels in the upstream and downstream glass manometers were measured and compared with the level in the reference tube. Differences between the values for the upstream and downstream manometer levels were interpreted as indicating that the glass manometers were not thoroughly clean or attributed to foulty installation of the glass manometers. The glass manometers were then removed to be cleaned again with chromic acid and reinstalled carefully.

The above procedure was repeated as required. It was found that there was no problem with the manometer reading if the glass manometers were cleaned well with chromic acid. Air bubbles entrapped in the manometer were removed using a suction rubber tube.

When the equipment was in operating order, the outlet valve of the test section was set for a desired flow rate and the flow was allowed to proceed for a minute to attain steady flow. Steady flow was indicated by constant levels in the glass manometers. Pressure drop was measured by reading the liquid levels in the glass manometers with cathetometers

provided for both the upstream and downstream test sections. The fluid was collected for a known interval of time determined by a stop watch in a suitable size container. The efflux was weighed and recorded. The procedure was repeated at progressively increasing flow rates.

When the flow rate was changed, the outlet valve of supply tank was also checked to ensure an overflow in the constant head device. The flow rates in the test section were varied but did not exceed Reynolds number of 1000 to ensure the flow was laminar.

Readings were taken at seven different flow rates which were adjusted in approxemately equal increments for each tankful of dilute solution. The solution was not recirculated in order to avoid complications arising from shear degradation. A separate freshly prepared batch of dilute solution was used with each tube to avoid problems associated with aging of the polymer. After the completion of the measurements, the equipment was flushed and cleaned with distilled water.

4.2-4 Measurement by Cannon Fenske viscometer

Determinations of the viscosity of samples taken from the efflux collected were carried out with a Cannon Fenske viscometer. This data was used as a supplement to the data collected in the tube flow measurements.

The viscometer was carefully cleaned with acetone as solvent. Air was flushed through the instrument to remove the final traces of solvent. Periodically, it was necessary to remove traces of organic deposits with chromic acid.

The presence of a trace of contaminants in a capillary tube introduces considerable errors in the measurements. Great care was taken to obtain an exact loading when charging the sample solution into the viscometer. Significant loading errors may be attributed to the fact that the driving fluid head is dependent upon the amount of liquid in the instrument. Thus, if too much liquid is charged into the instrument, the level in the lower reservoir is too high and the driving head is correspondingly reduced.

Several measurements of effluent time were carried out on the same solution to obtain an average value. The variation in the time measurements was within ±0.1 second. The bath temperature was controlled by a thermoregulator to within ±0.1^{o}C.

The pycnometer was calibrated using distilled water. Its volume was determined to be 49.2126 ml at 25^{o}C.

5. RESULTS AND DISCUSSION

5.1 Calibration

The tube diameters were calibrated by carrying out pressure drop - flow rate measurements using distilled water. A straight line was fitted by the method of least squares to the data. The inside tube diameter was calculated from the slope of the line. The detailed calculation procedure is shown in Appendix 1.

Figs. (5.1) and (5.2) show the plot of pressure drop vs. flow rate obtained by the water run, yielding the calibrated tube diameters of 1.26718, 0.94311, 0.62711, 0.43887 and 0.30521 centimeters for the tubes with the designations of A, B, C, D and E respectively.

Fig. (5.3) shows the water data plotted as shear stress vs. shear rate using the calibrated tube diameters. The experimental data points for all five tube diameters fall on the same straight line. The slope is given by the viscosity of distilled water at $25^{o}C$, i.e. 0.89372 centipoise.

This figure gives an indication of the reliable equipments and the reproducible data.

5.2 Degradation of polymer

One of the difficulties involved in the study of dilute polymer solution is the degradation of the polymer

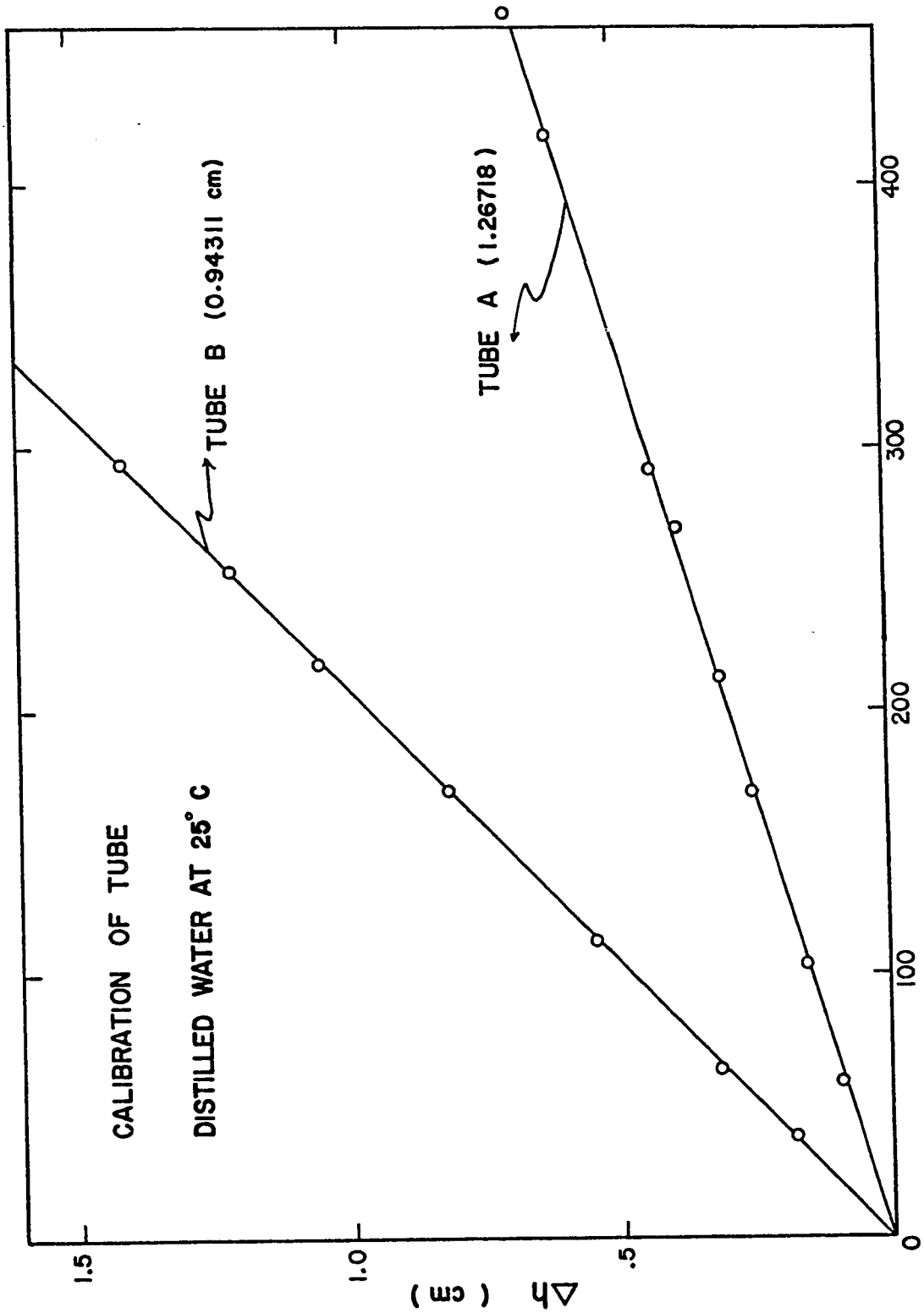

Figure 5.1 : Plot of Δh vs. w for the calibration of tube diameter with distilled water at $25^{o}C$ for tube A and B

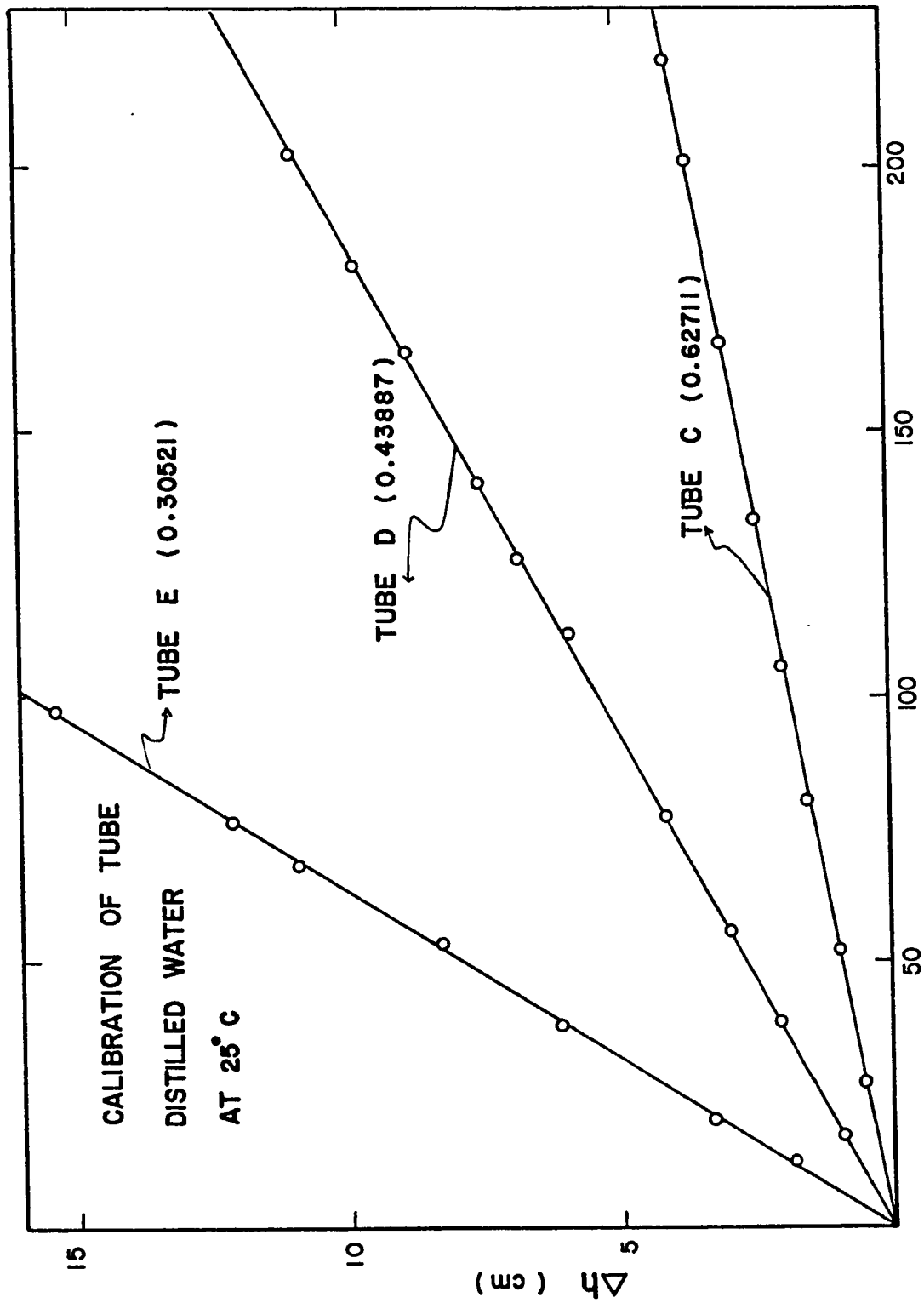

Figure 5.2 : Plot of Δh vs. w for the calibration of tube diameter with distilled water at $25^{o}C$ for tube C, D and E

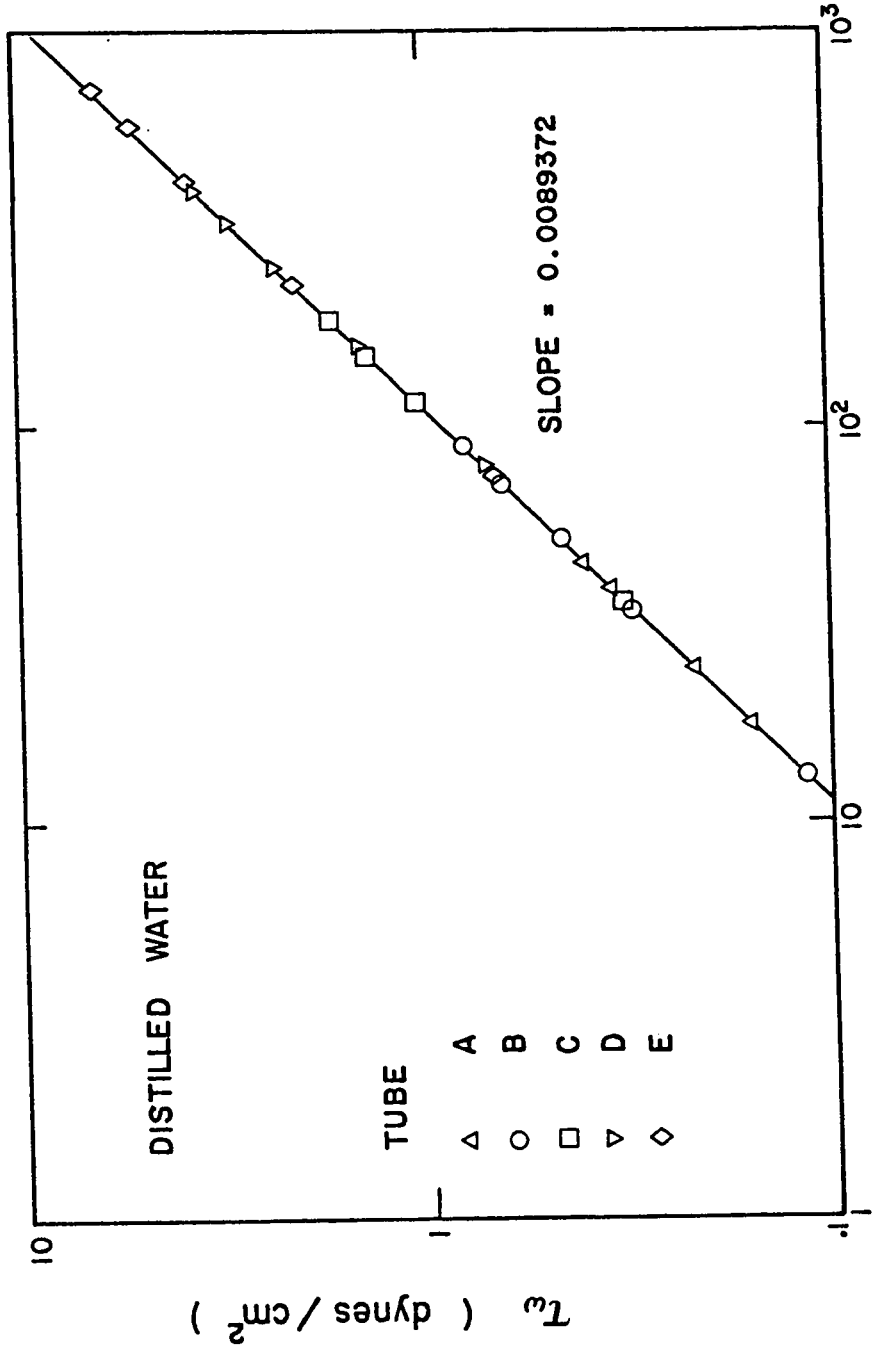

Figure 5.3 : Plot of τ vs. $8\langle u\rangle/D$ for distilled water with five different tube diameters

additives due to many factors.

Fig. (5.4) shows one of these effects indicating the polymer degradation by aging which was inferred by the viscosity measurements of the polymer solution in Cannon Fenske viscometer. It is indicated that the viscosity of the polymer solution of Polyox Coagulant is significantly decreased with duration of time, for the solution at rest in a container.

This degradation was found to be more severe for the polymer in a poor solvent (0.3M K_2SO_4) than in a good solvent (distilled water), which might be attributed to the increased coiling of macromolecules or the acceleration of the degradation by the existence of metal Potassium ion in the solution.

The above degraded polymer solutions were used to obtain pressure drop - flow rate data in tube flow measurement. As shown in Fig. (5.5), the significant changes in flow curves were detected with duration of time for 100 ppm solution of Polyox Coagulant in tube B. The deviation of the flow curves due to the aging may introduce uncertainties in the analysis of the results. For this reason, the diluted polymer solution was used as soon as it was made for the present measurement.

One other major source of the polymer degradation is the shear developed by the molecules at various stages of the process. Pruitt (67) encountered severe mechanical

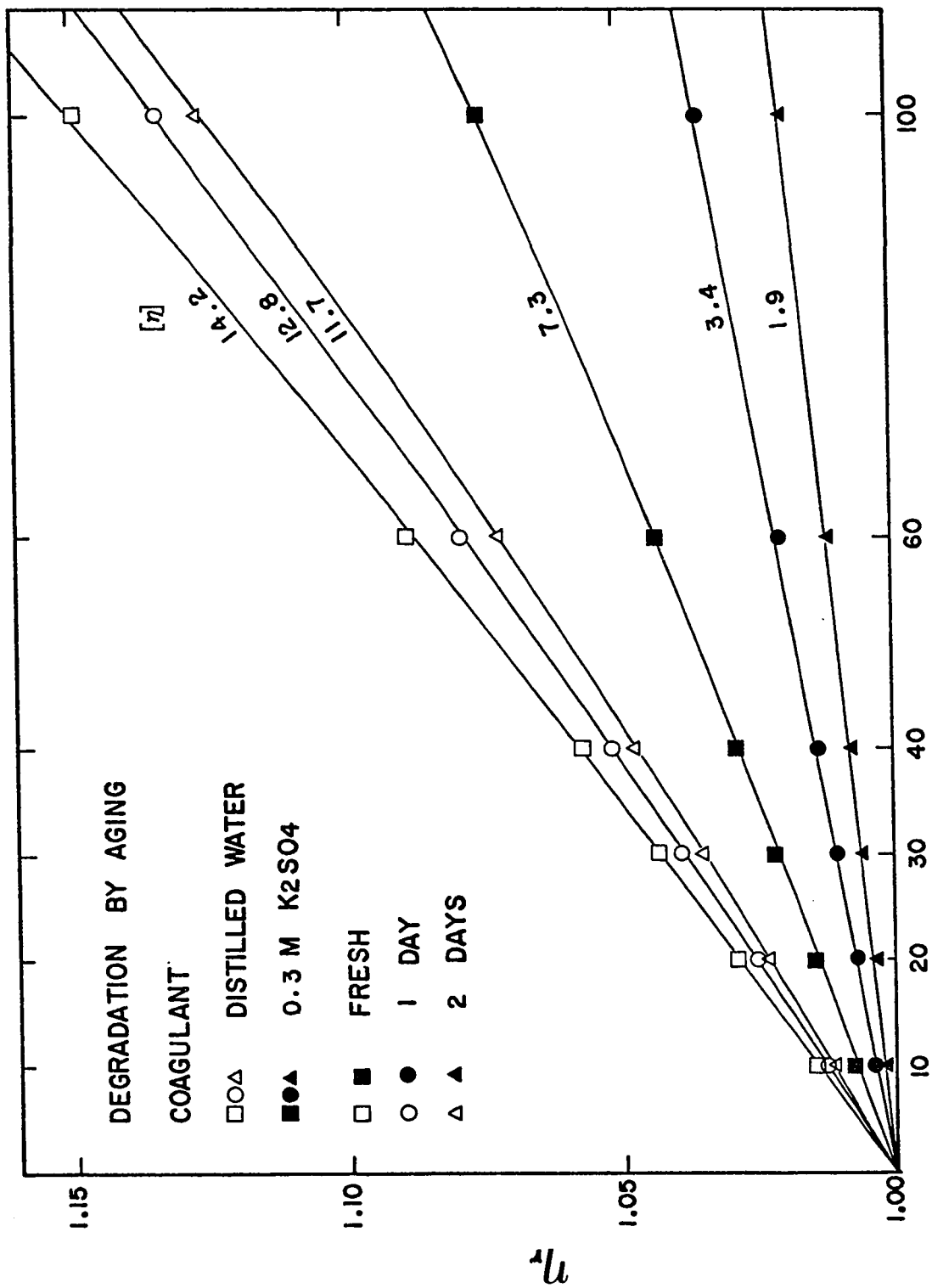

Figure 5.4 : Plot of η_r vs. c from Cannon Fenske viscometer measurements for Polyox coagulant

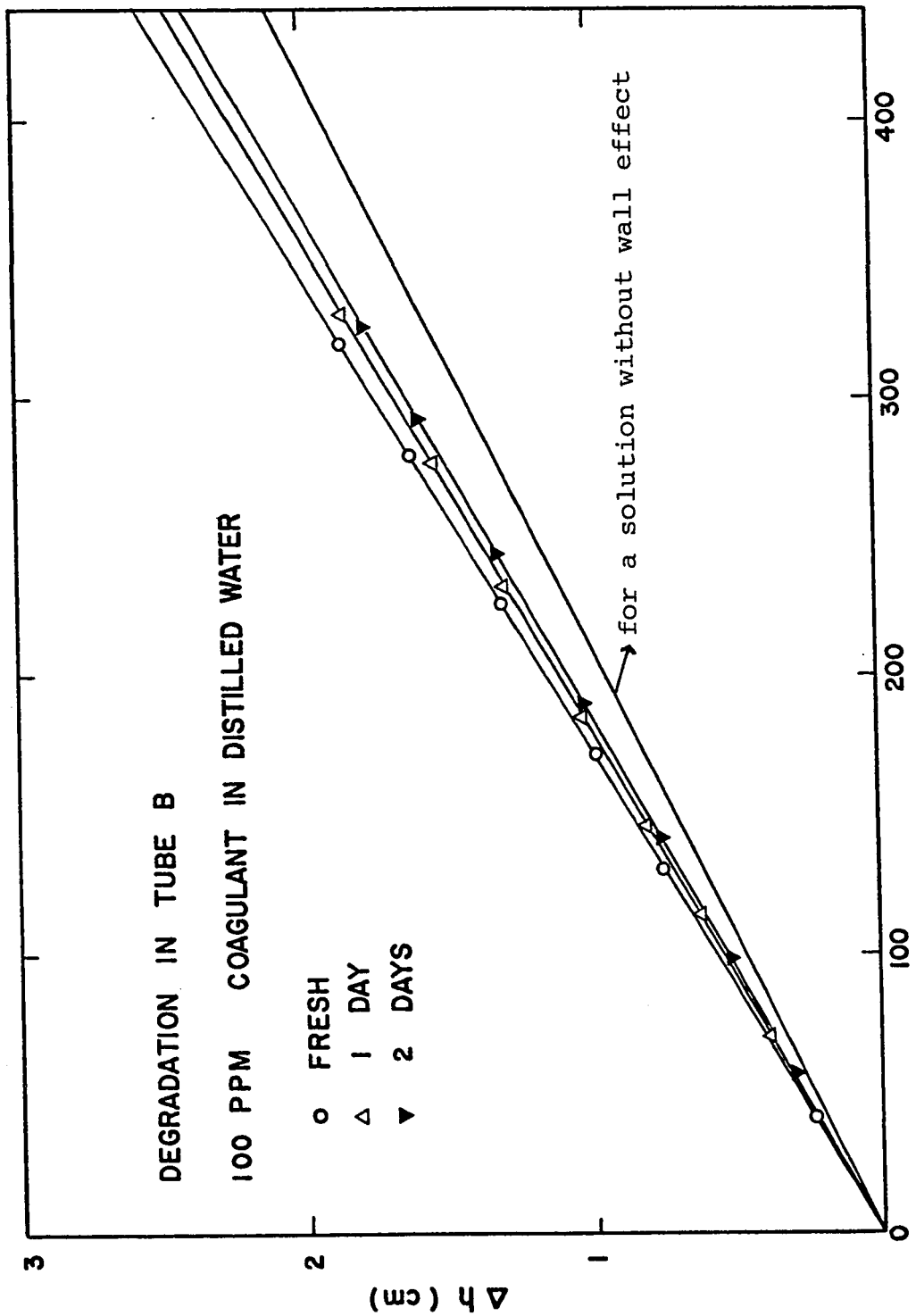

Figure 5.5 : Plot of Δh vs. w for Polyox coagulant in tube B

shear degradation in the use of a high speed gear pump in which the shear at the 400 psi. operating pressure evidently tended to degrade polymers. For this reason, recourse was made in the present study to a constant head device to eliminate a major source of polymer degradation.

Arunachalam (48) also detected shear degradation during recirculation of a dilute polymer solution according to the following pattern: the degradation due to shear was considerable in the early stage of recirculation, decreasing on further recirculation, and tending toward a final degraded value. This makes it necessary to collect data in a simple pass of a freshly prepared polymer solution to ensure reproducibility of the results, as was carried out in the present work.

5.3 Pressure drop - flow measurement

The pressure drop measurements were collected as a function of flow rate for dilute solutions of Polyox Coagulant and Polyox WSR 301 with five different tube diameters and at various solution concentrations: 10, 20, 30, 40, 60 and 100 ppm. The experimental data are presented in Appendix 11.

As indicated in Figs. (5.6) and (5.7) showing the flow data for aqueous solutions of Polyox Coagulant and Polyox WSR 301, respectively, in tube B, the plots of the

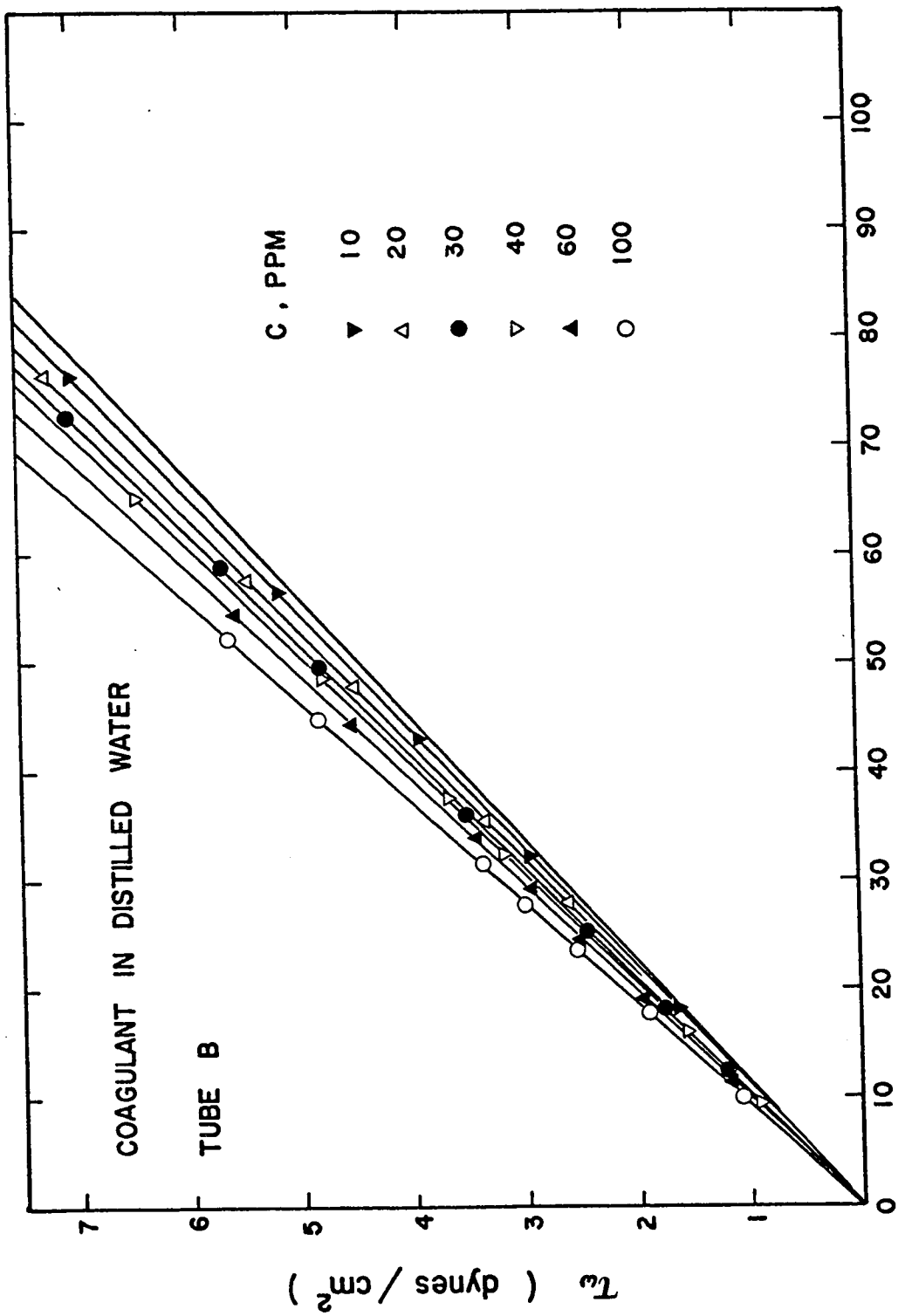

Figure 5.6 : Plot of τ_w vs. $8\langle u\rangle/D$ for Polyox coagulant in distilled water

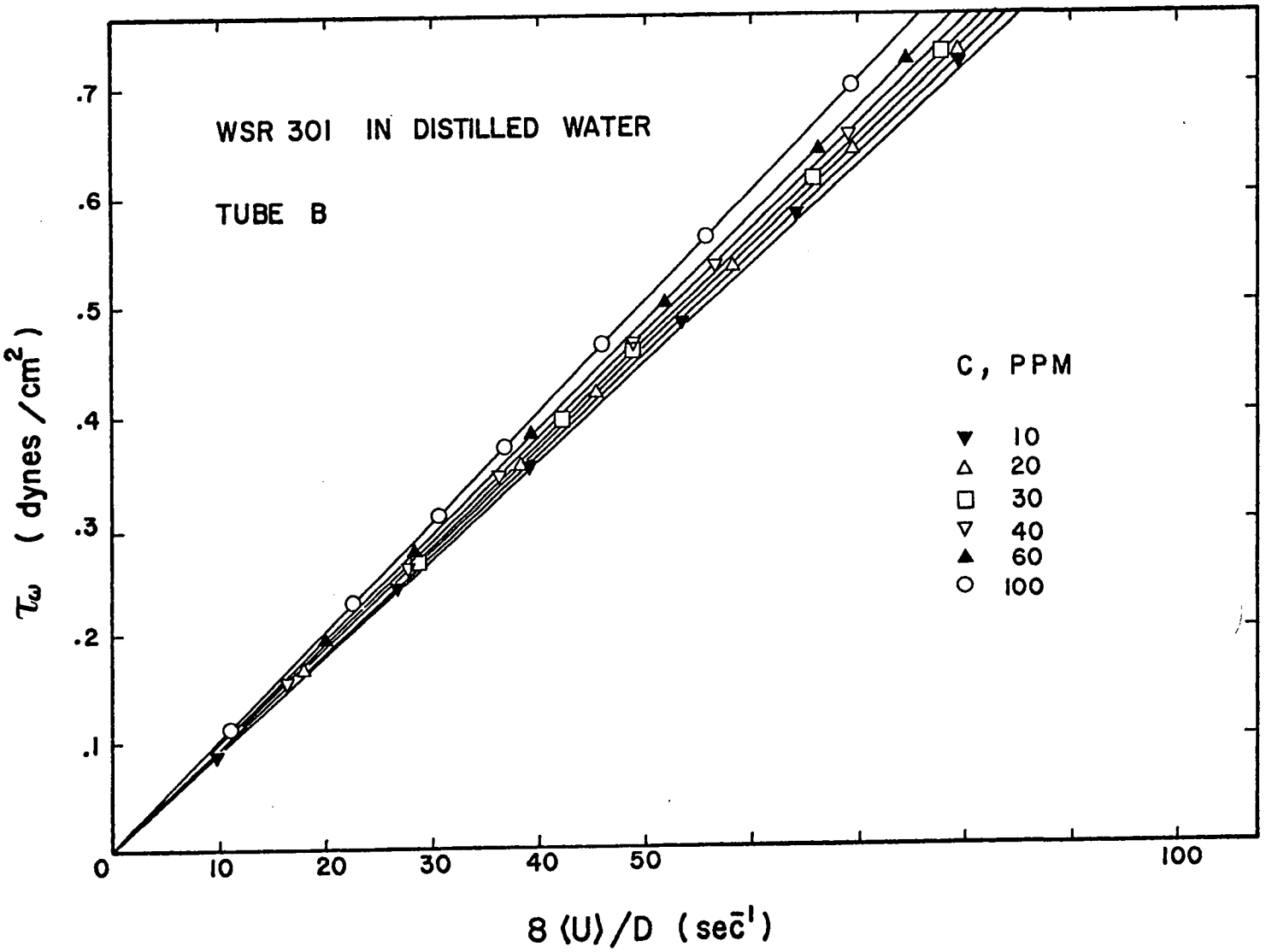

Figure 5.7 : Plot of τ_w vs. 8<u>/D for Polyox WSR 301 in distilled water

data in the form of shear stress at the wall τ_w vs. $8\langle u\rangle/D$ could be represented by straight lines and a simple linear relationship over the range of measurement.

Solution densities required in converting the measured solution flow rates to velocities were determined to be essentially the same as that of the solvent at the concentration used and hence the density of the solvent was used in all calculations. On the other hand, the evaluations of the viscosities of the dilute solutions which were found to be 10% greater than for the pure solvent, in the case of the maximum solution concentration, were employed in the further analysis of the data.

It is noteworthy to point out that the preliminary tests carried out to determine the normal stresses in the Weissenberg rheogoniometer of the dilute Polyox solutions used in this work showed no normal stress components though solutions at much higher concentrations (i.e. > 0.25%) did possess measurable normal stresses. Therefore it can be said that the drag reducing polymer solutions based on Polyox are inelastic in the polymer concentration range involved.

5.4 Average velocity deficiency u_w

The linearity of the τ_w vs. $8\langle u\rangle/D$ which was shown in the previous section indicates that the viscosity coefficient η_a defined in Eq. (3.3-6) is independent of the

wall shear stress for a given polymer solution concentration and tube diameter. Therefore Eq. (3.3-8) provides a simple and convenient means for evaluation of $\bar{u}_w$ experimentally in terms of this quantity and the solution viscosity.

Figs. (5.8) and (5.9) show the dependence of η_a on the polymer concentration and on the tube diameter for aqueous solutions of Polyox Coagulant and Polyox WSR 301, evaluated from the measurements collected using five different tube diameters and supplemented by the data collected with the Cannon Fenske viscometer. The variation of the viscosity coefficient plotted as η_{ar} ($=\eta_a/\eta_s$) with tube diameter is attributed to the adsorption of the polymer onto the tube wall.

The determination of the solution viscosity unobscured by polymer adsorption is based on the assumption that the polymer adsorption effect is zero in the limit as the tube diameter at the particular polymer concentration approaches zero, i.e. $\lim_{D\to 0} \eta_{ar} = \eta/\eta_s$. As seen from Figs. (5.8) and (5.9), solution viscosities evaluated by this method are consistent with values provided by the Cannon Fenske viscometer which is the basis of the evaluations by previous workers, leading as well to intrinsic viscosities in agreement with those universally evaluated by the capillary viscometer method. It is seen from Eq. (3.3-8) that the evaluation of the solution viscosity by extrapolation of η_{ar} to the limit at D = 0 leads to the expected results that

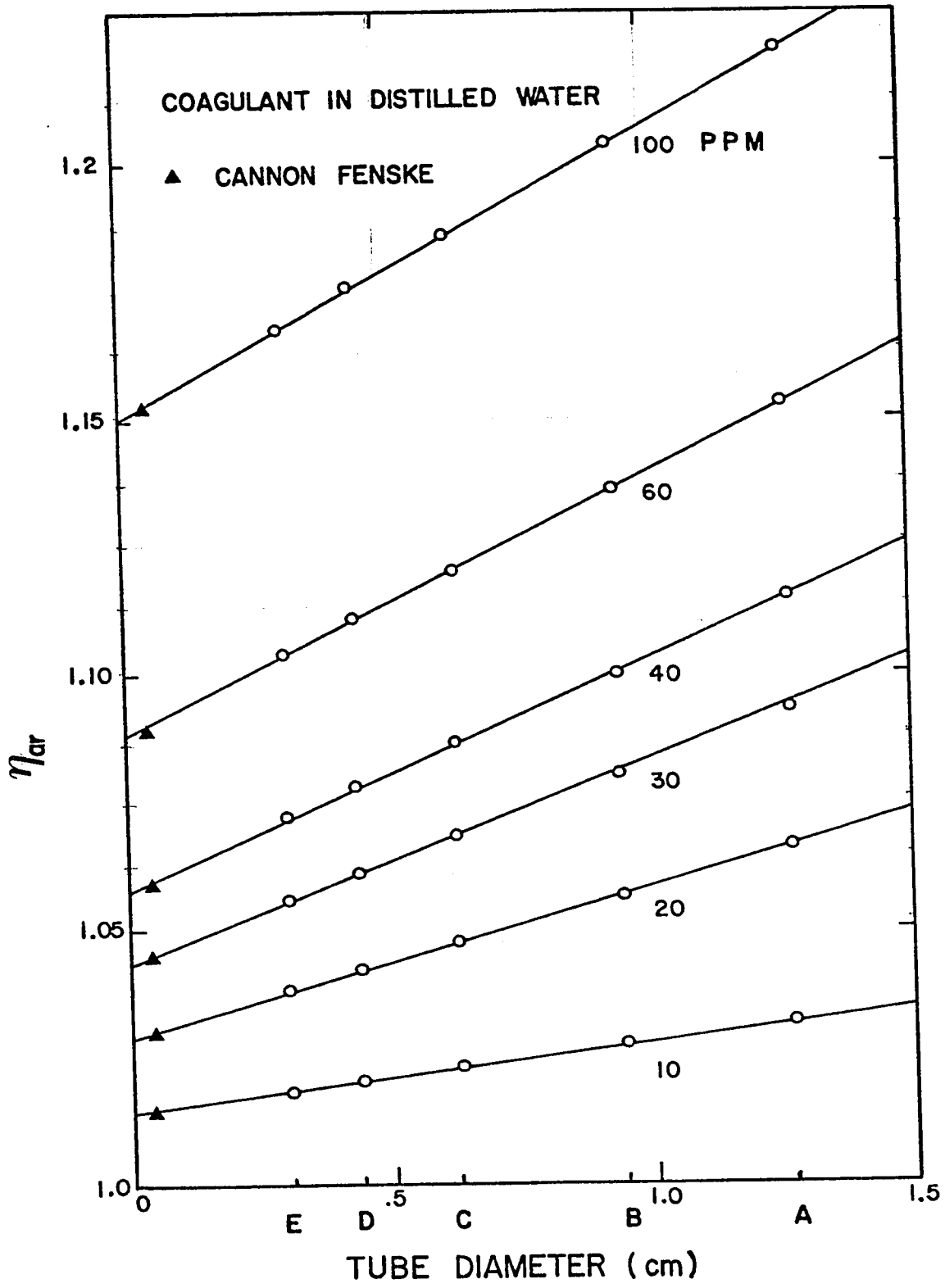

Figure 5.8 : Plot of η_{ar} vs. D for Polyox coagulant in distilled water

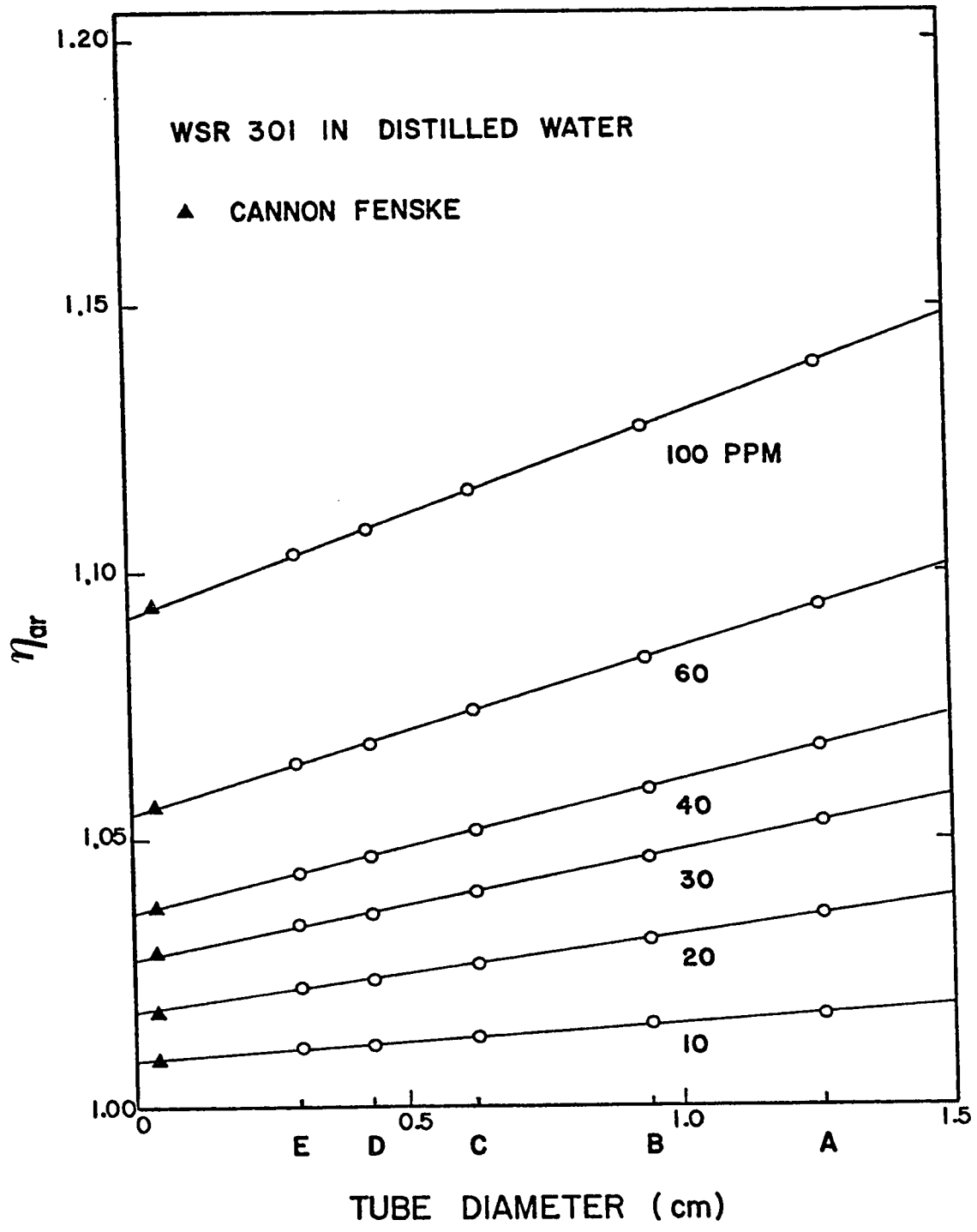

Figure 5.9 : Plot of η_{ar} vs. D for Polyox WSR 301 in distilled water

the quantity $\bar{u}_w$ characterizing polymer adsorption is zero when the tube diameter is zero.

Figs. (5.10) and (5.11) show the typical graphs depicting the average velocity deficiency $\bar{u}_w$, evaluated in this case from the data for the two polymers in distilled water, as a function of the polymer concentration with tube diameter as parameter. The observation that $\bar{u}_w$ is independent of the flow rate, which follows from the previous observation and discussion, is noteworthy.

5.5 Anomalous zone thickness

The details of the procedure used to calculate the anomalous zone thickness are presented in the Appendix 4 along with the complete computer program. The algorithm employed in the calculation of $\bar{\Delta}$ from $\bar{u}_w$ discussed in the latter Appendix, embodies the assumption that the polymer concentration is continuous across the interface between the adsorption zone and the concentrated layer which comprise the anomalous zone. Since $\bar{\Delta}$ is calculated from $\bar{u}_w$, it is a function of the same variables affecting $\bar{u}_w$, viz. polymer concentration in the bulk solution and tube diameter.

The evaluations of the anomalous zone thickness are shown in Figs. (5.12) through (5.15) for the four polymer systems investigated as a function of the polymer concentration with tube diameter as parameter.

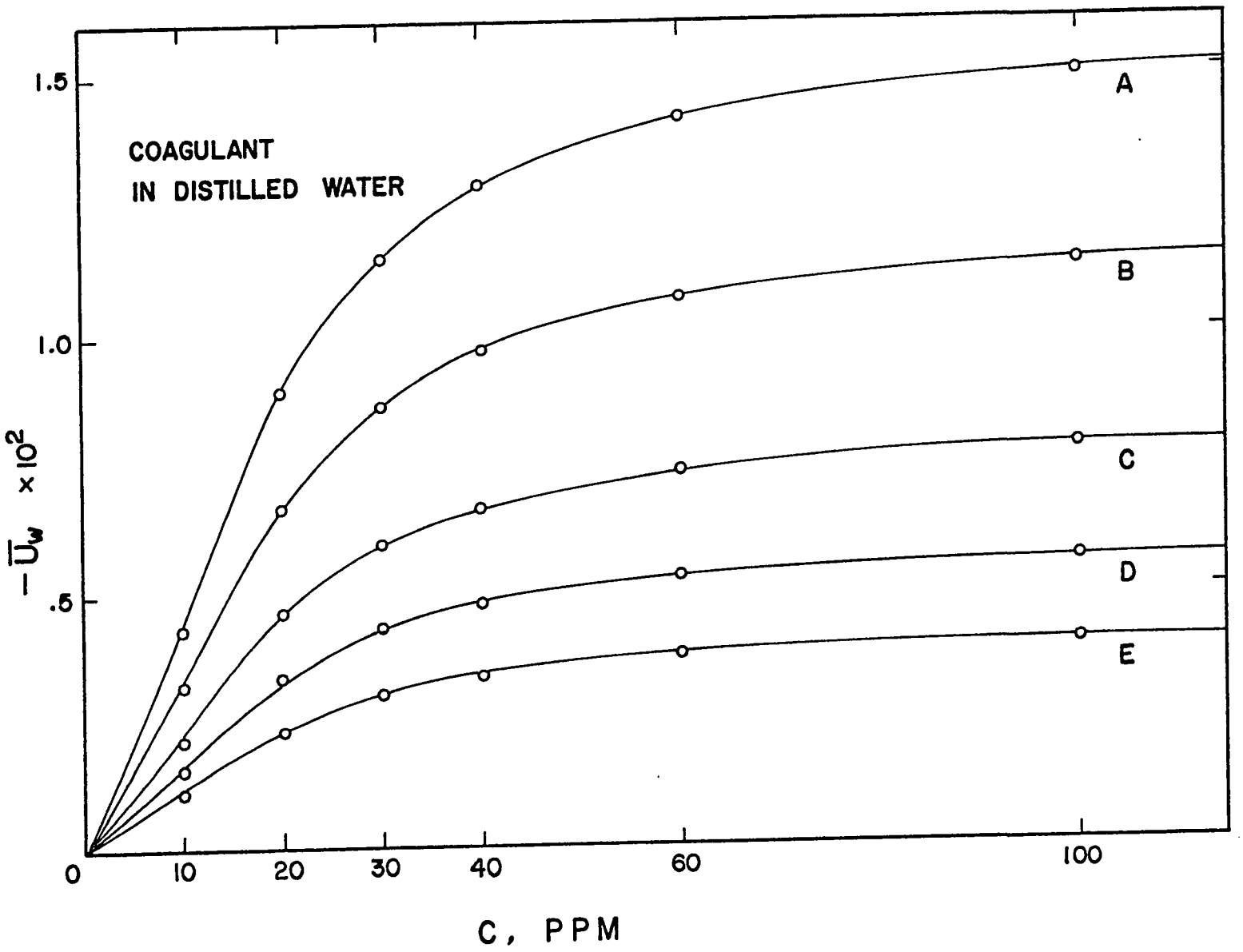

Figure 5.10 : Plot of $-\bar{u}_w$ vs. c for Polyox coagulant in distilled water

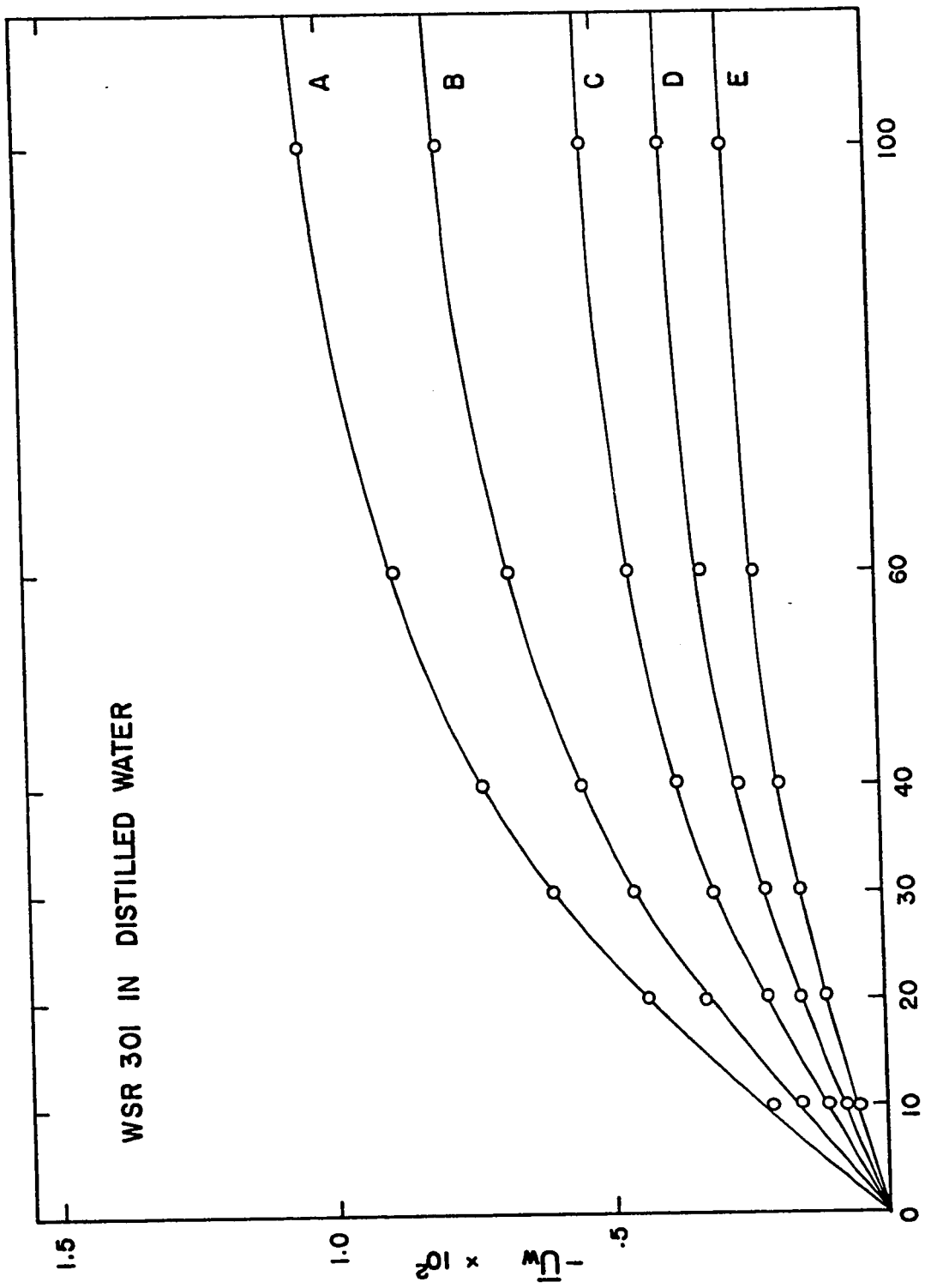

Figure 5.11 : Plot of $-\bar{u}_w$ vs. c for Polyox WSR 301 in distilled water

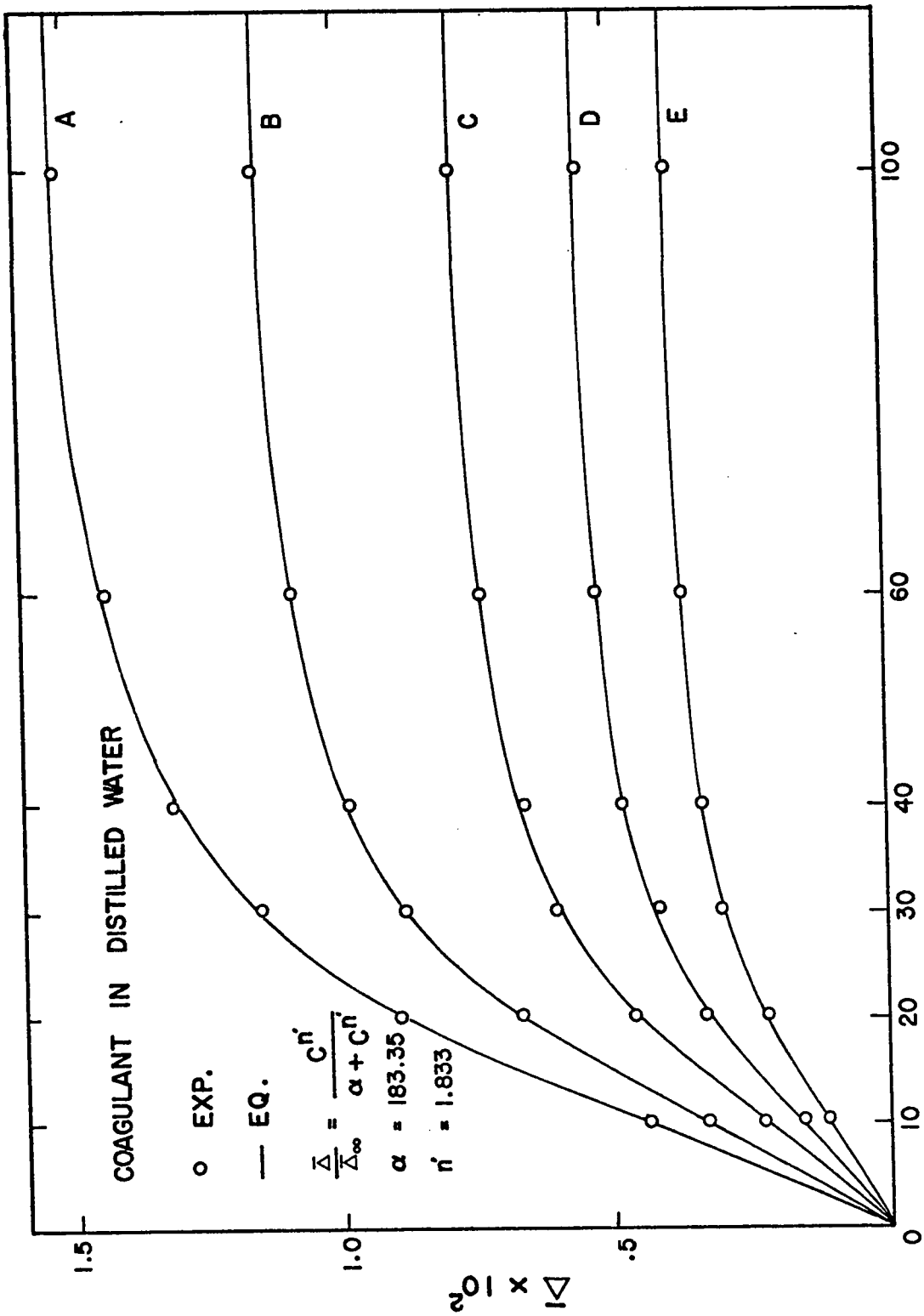

Figure 5.12 : Plot of $\bar{\Delta}$ vs. c for Polyox coagulant in distilled water

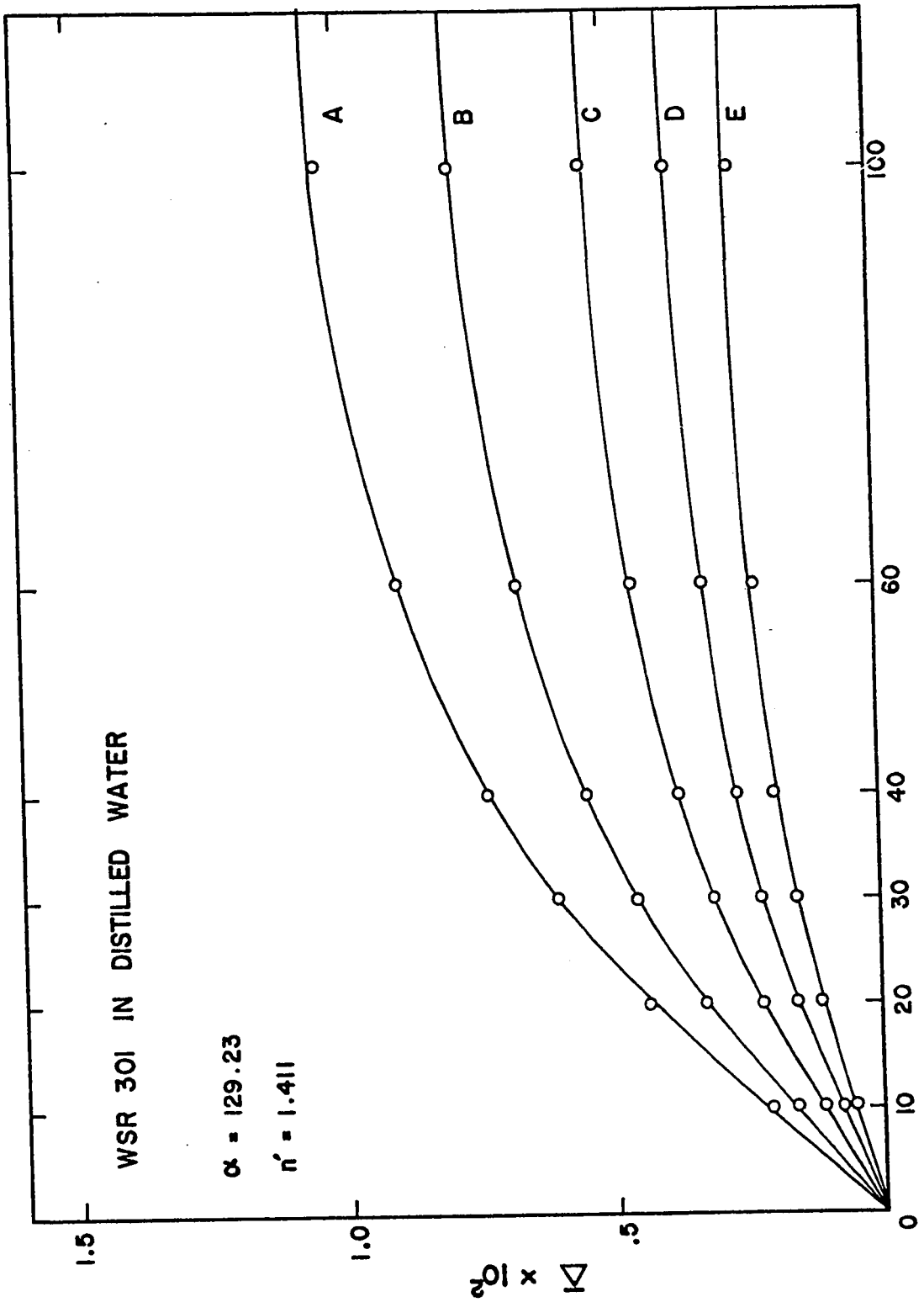

Figure 5.13 : Plot of $\bar{\Delta}$ vs. c for Polyox WSR 301 in distilled water

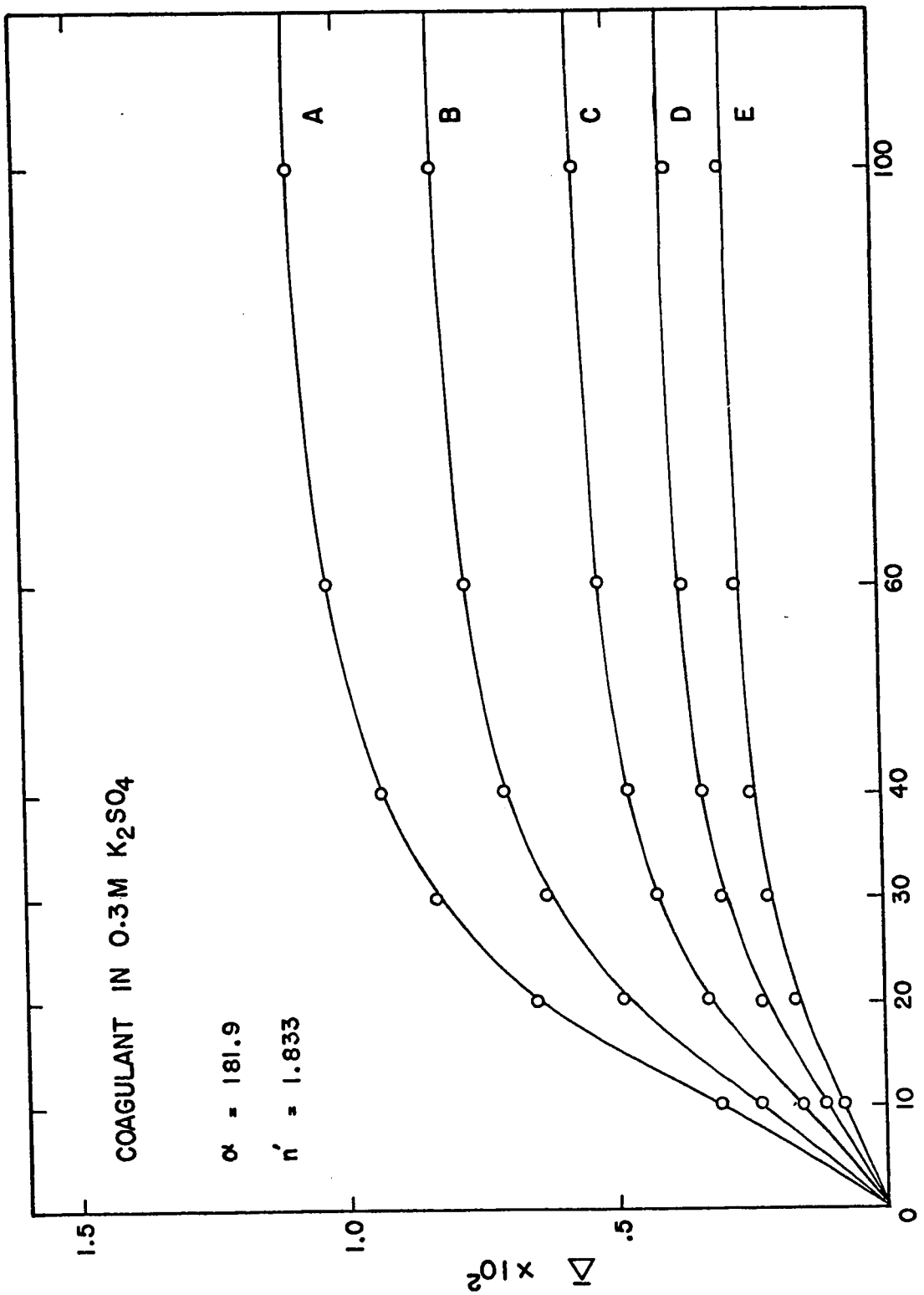

Figure 5.14 : Plot of $\bar{\Delta}$ vs. c for Polyox coagulant in 0.3M K_2SO_4

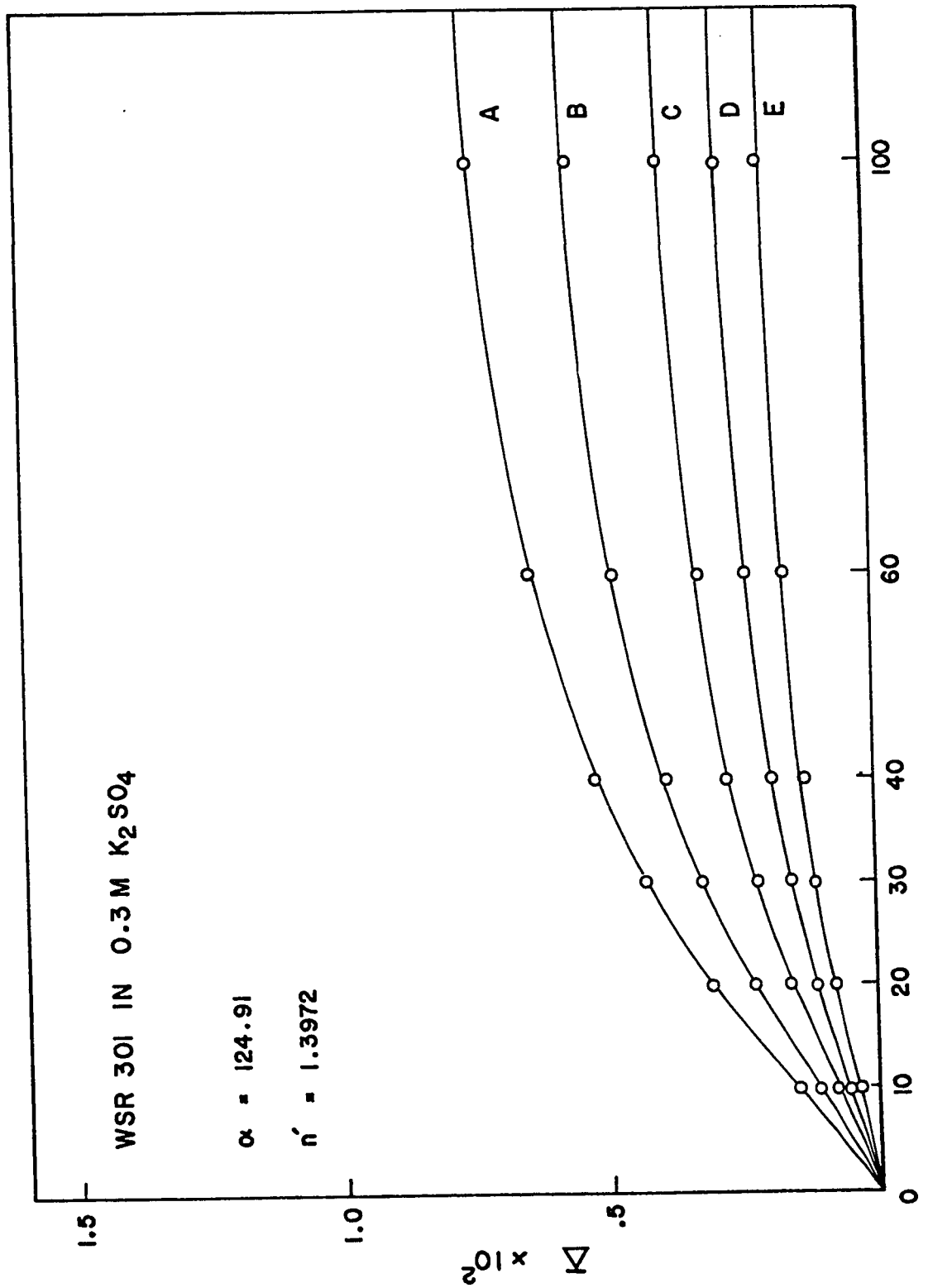

Figure 5.15 : Plot of $\bar{\Delta}$ vs. c for Polyox WSR 301 in 0.3M K_2SO_4

As observed in the latter figures, the anomalous zone thickness increases with increasing polymer concentration and tube diameter. Furthermore, it is found in Figs. (5.12) and (5.13) that the anomalous zone thickness of the Polyox Coagulant is greater than that of the Polyox WSR 301, implying the increased polymer adsorption in the higher molecular weight polymer. The effect is also indicated in Figs. (5.14) and (5.15) for the polymers in the 0.3M K_2SO_4 aqueous solution.

The effect of solvent can be found in Figs. (5.12) through (5.15) in which the adsorption of polymer is markedly dependent on the solvent used in a way that a good solvent (distilled water) produces a higher anomalous zone thickness than a poor solvent (0.3M K_2SO_4). In the context, high and low intrinsic viscosities of the respective solutions are taken as indications of good and poor solvent power.

In the present work, the following modified Langmuir type equation was used to represent the adsorption data:

$$\frac{\bar{\Delta}}{\bar{\Delta}_\infty} = \frac{c^{n'}}{\alpha + c^{n'}}, \qquad (5.5\text{-}1)$$

where $\bar{\Delta}$ is the anomalous zone thickness at the bulk solution concentration c, $\bar{\Delta}_\infty$ is the upper limiting anomalous zone thickness, and n' and α are empirical constants.

$\bar{\Delta}_\infty$ was chosen as a value which has a minimum standard deviation when data was correlated to Eq. (5.5-1) by least squares fitting with the varying $\bar{\Delta}_\infty$ for polymer systems

investigated with tube diameter as parameter. The details are described in the Appendix 5.

The employment of the Langmuir type equation resulted from the similarity of shape between the type of adsorption under discussion and the type of the original Langmuir equation. As seen in the Figs. (5.12) through (5.15), the above correlation gives a good representation of the isotherms for the adsorption of polymer from the Polyox solutions at the relatively low concentrations involved in this work.

The values determined by the method of least squares fitting for the parameters α and n' in aqueous solvent were, respectively, 183.25 and 1.83 for the Polyox Coagulant, and 129.23 and 1.41 for the Polyox WSR 301. Polymer solutions prepared with the poor solvent were found to have nearly the same values as found with the aqueous solvent.

The values reflect the more rapid increase of the adsorption ratio $\frac{\bar{\Delta}}{\bar{\Delta}_\infty}$ in the low concentration range of the Polyox Coagulant compared to the Polyox WSR 301. In other words, the solution with the higher molecular weight polymer approaches the upper adsorption limit more rapidly at the lower concentrations, although the limiting adsorption level may vary markedly as the solvent changed.

In view of the satisfactory fitting by Eq. (5.5-1), a preliminary attempt at a development of this equation might be appropriate. The general behaviour suggests the

three dimensional approach extended from the two dimensional approach used in the development of the original Langmuir equation.

In this model, the adsorption of the polymer macromolecules takes place until all of the adsorption sites in an imaginary three dimensional lattice are filled. The rate of adsorption of polymer molecules, which is proportional to the number of lattice sites available for adsorption, is thus given by

$$r_{ad} = k_{ad}\, c^{n'}\, (1 - \frac{\bar{\Delta}}{\bar{\Delta}_\infty}), \qquad (5.5\text{-}2)$$

where $\bar{\Delta}_\infty$ is the limiting thickness of the adsorption zone. The use of the power index n' in anticipation of the result may be justified on the basis of the fact that the polymer concentration adjacent to the adsorption zone differs from the concentration in the bulk solution.

The rate of desorption is given by

$$r_{de} = k_{de} \frac{\bar{\Delta}}{\bar{\Delta}_\infty}. \qquad (5.5\text{-}3)$$

The use of the anomalous zone thickness Δ , in place of the adsorption zone thickness δ_a in the foregoing, is permissible due to the small difference in the two quantities (less than 2%).

By equating the polymer adsorption and desorption rates at steady state,

$$k_{ad}\, c^{n'}\, (1 - \frac{\bar{\Delta}}{\bar{\Delta}_\infty}) = k_{de}\, \frac{\bar{\Delta}}{\bar{\Delta}_\infty} \qquad (5.5\text{-}4)$$

and rearranging, we obtain the desired result:

$$\frac{\bar{\Delta}}{\bar{\Delta}_\infty} = \frac{c^{n'}}{\alpha + c^{n'}} ,$$

where $\alpha = k_{de}/k_{ad}$.

The above kinetic treatment is applied to adsorption and desorption of the solute alone. Thus it is implied that the adsorption equilibrium is governed essentially by the way in which the solute is adsorbed, rather than by competition between solute and solvent for the interface.

It was found that the dependence of the limiting thickness of the anomalous zone on polymer type and tube diameter could be represented well by the following correlation involving intrinsic viscosity:

$$\bar{\Delta}_\infty = a_1 [\eta]^{b_1} D^{c_1}, \qquad (5.5\text{-}5)$$

with the empirical constants given a_1=0.003919, b_1=0.5179, and c_1=0.946.

Anomalous zone thicknesses as expressed in multiples of the macromolecular diameter, Δ/D_e, are shown in Figs. (5.16) through (5.19) as a function of polymer concentration. It is noteworthy that for the same solvent, the limiting value of Δ/D_e is substantially the same for Polyox Coagulant and Polyox WSR 301 in the case for tube A in distilled

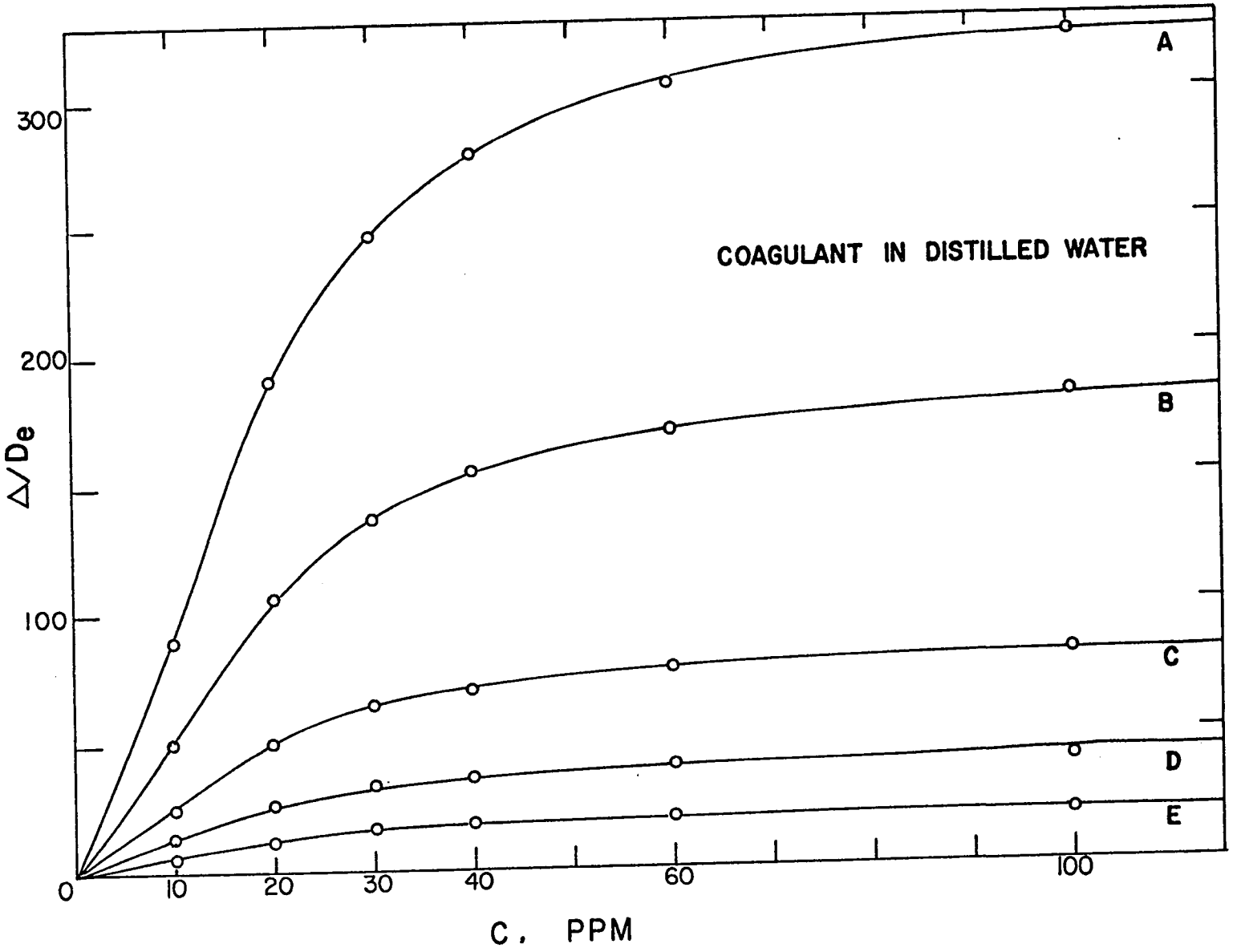

Figure 5.16 : Plot of Δ/D_e for Polyox coagulant in distilled water

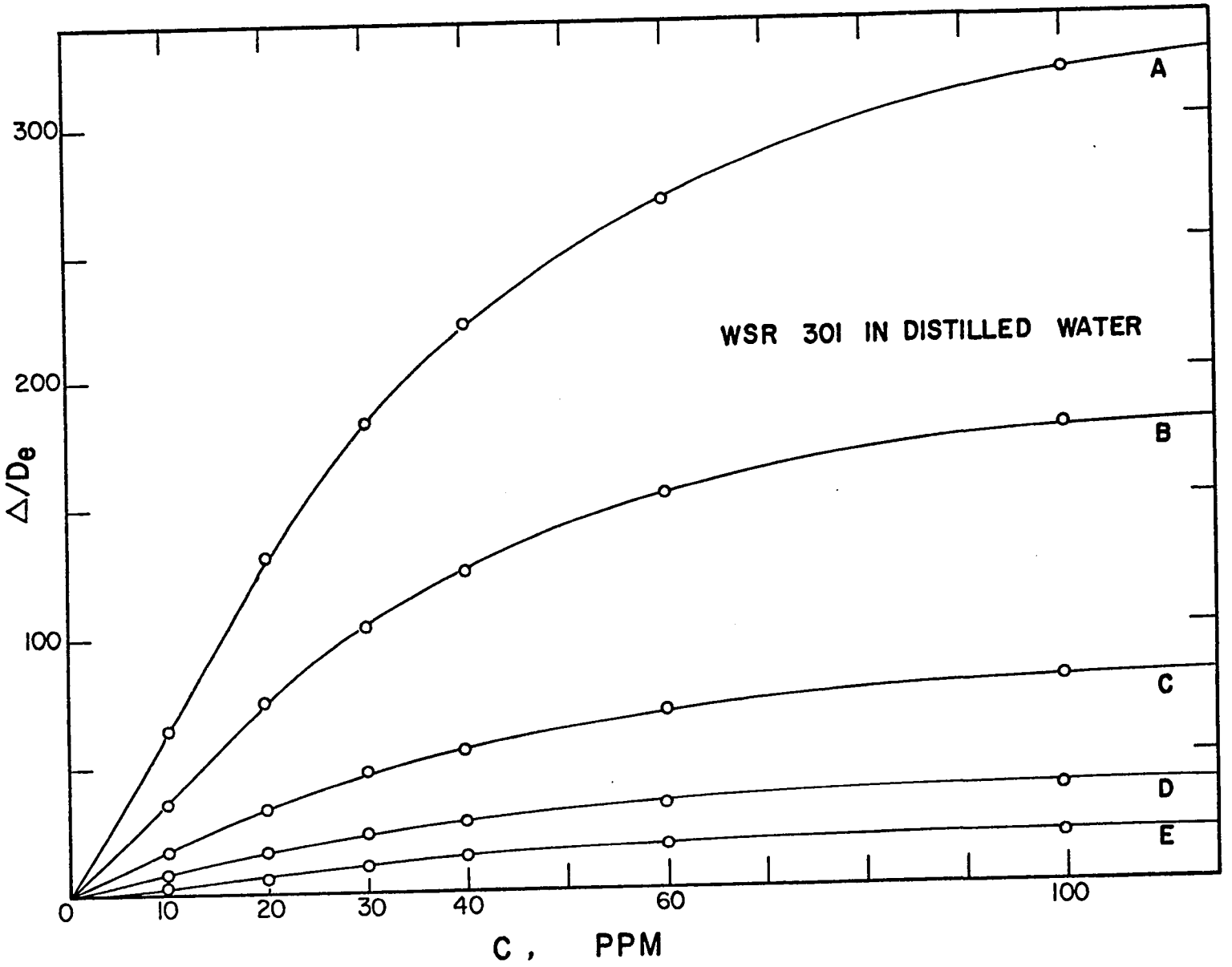

Figure 5.17 : Plot of Δ/D_e for Polyox WSR 301 in distilled water

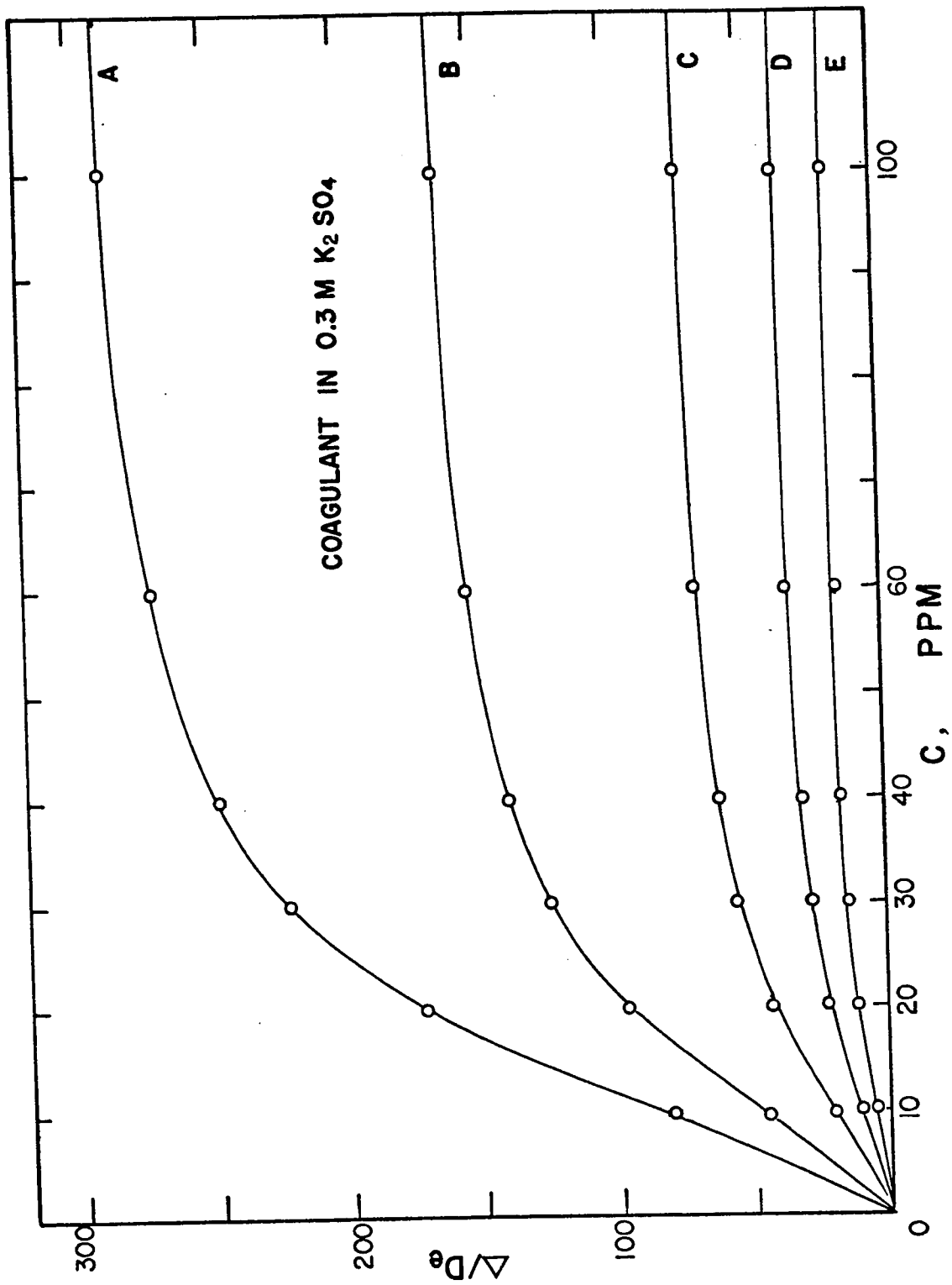

Figure 5.18 : Plot of Δ/D_e for Polyox coagulant in 0.3M K_2SO_4

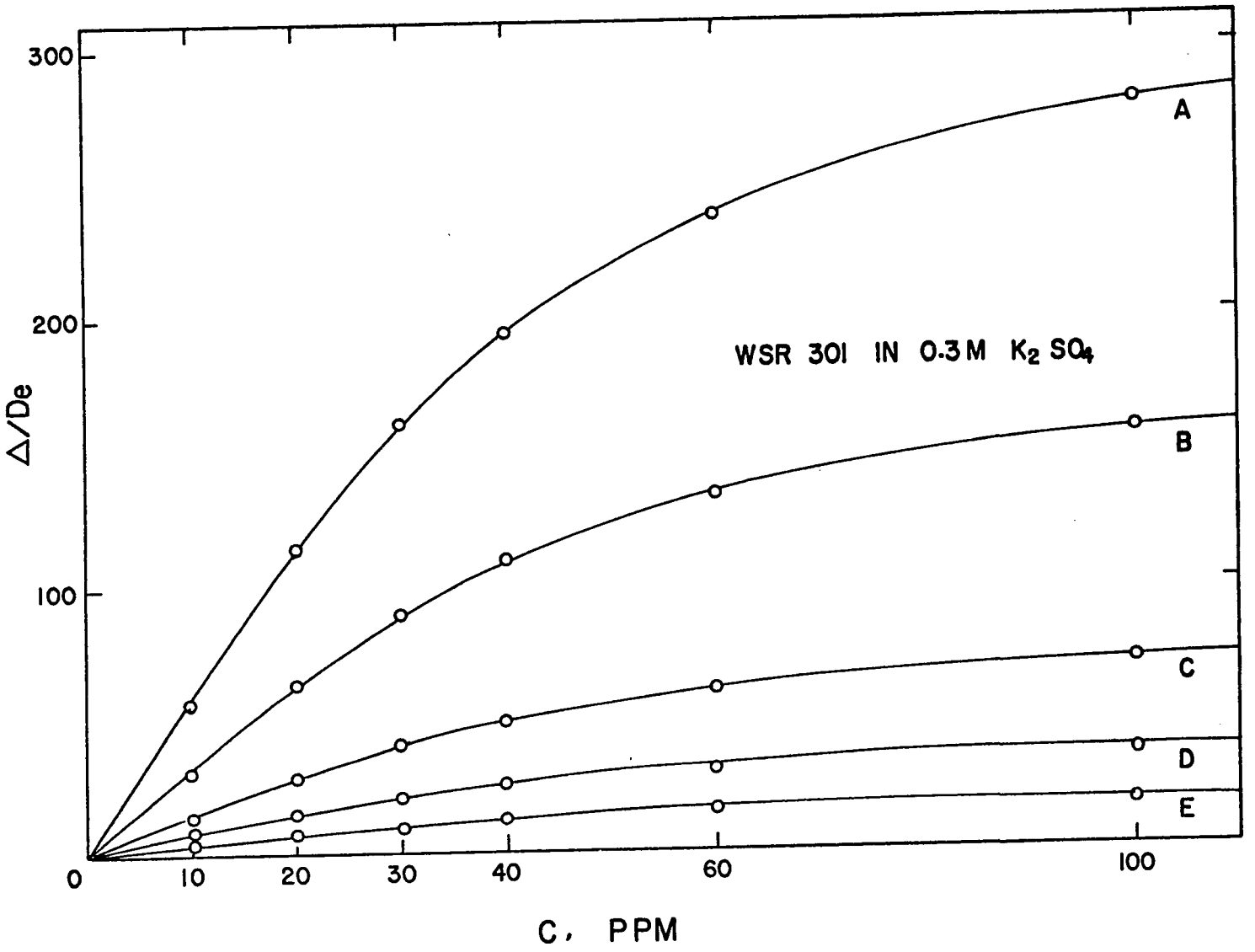

Figure 5.19 : Plot of Δ/D_e for Polyox WSR 301 in 0.3M K_2SO_4

water and 0.3M K_2SO_4 solution as shown in Figs. (5.20) and (5.21), respectively.

The maximum limiting thickness for the Polyox Coagulant aqueous solution in tube A corresponds to three times the length of the macromolecule when extended to its maximum length, which may imply the possibility of multimolecular layer formation of the polymers onto the tube wall. The evaluation of the maximum length of polymer molecule at its fully extended configuration is given in Appendix 9.

5.6 Diameter effect

The dependence of polymer adsorption on tube diameter is illustrated in Figs. (5.12) through (5.15) in which anomalous zone thickness is plotted as a function of polymer concentration with tube diameter as parameter.

It is found that the anomalous zone thickness increases with increasing tube diameter, represented by Eqs. (5.5-1) and (5.5-5) as discussed in the previous section. Combining the latter equations, we obtain

$$\bar{\Delta} = a_1 [\eta]^{b_1} D^{c_1} \frac{c^{n'}}{\alpha + c^{n'}} . \qquad (5.6\text{-}1)$$

For a fixed polymer concentration in a given polymer-solvent system, Eq. (5.6-1) can be reduced to

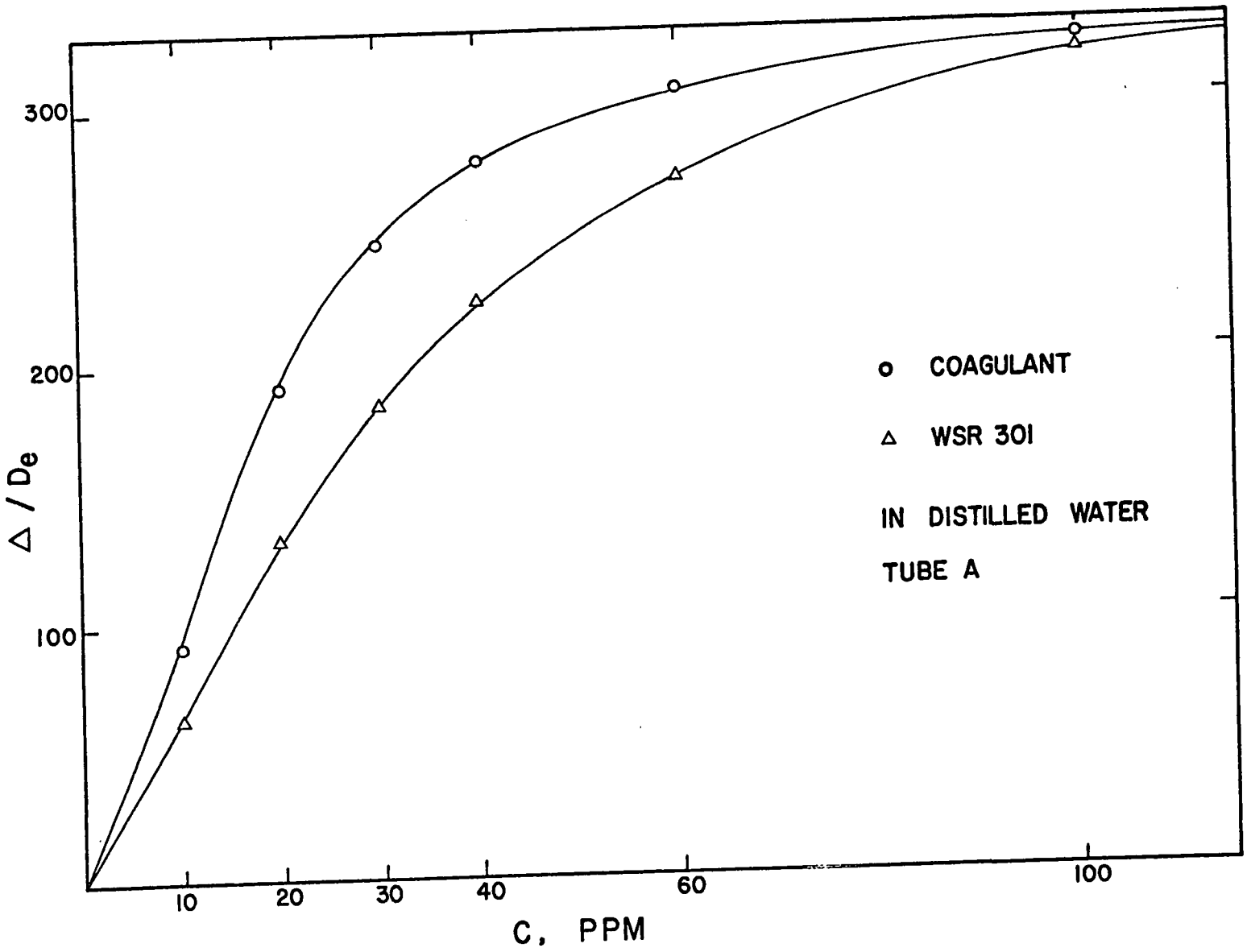

Figure 5.20 : Plot of Δ/D_e for Polyox coagulant and Polyox WSR 301 in distilled water with tube A

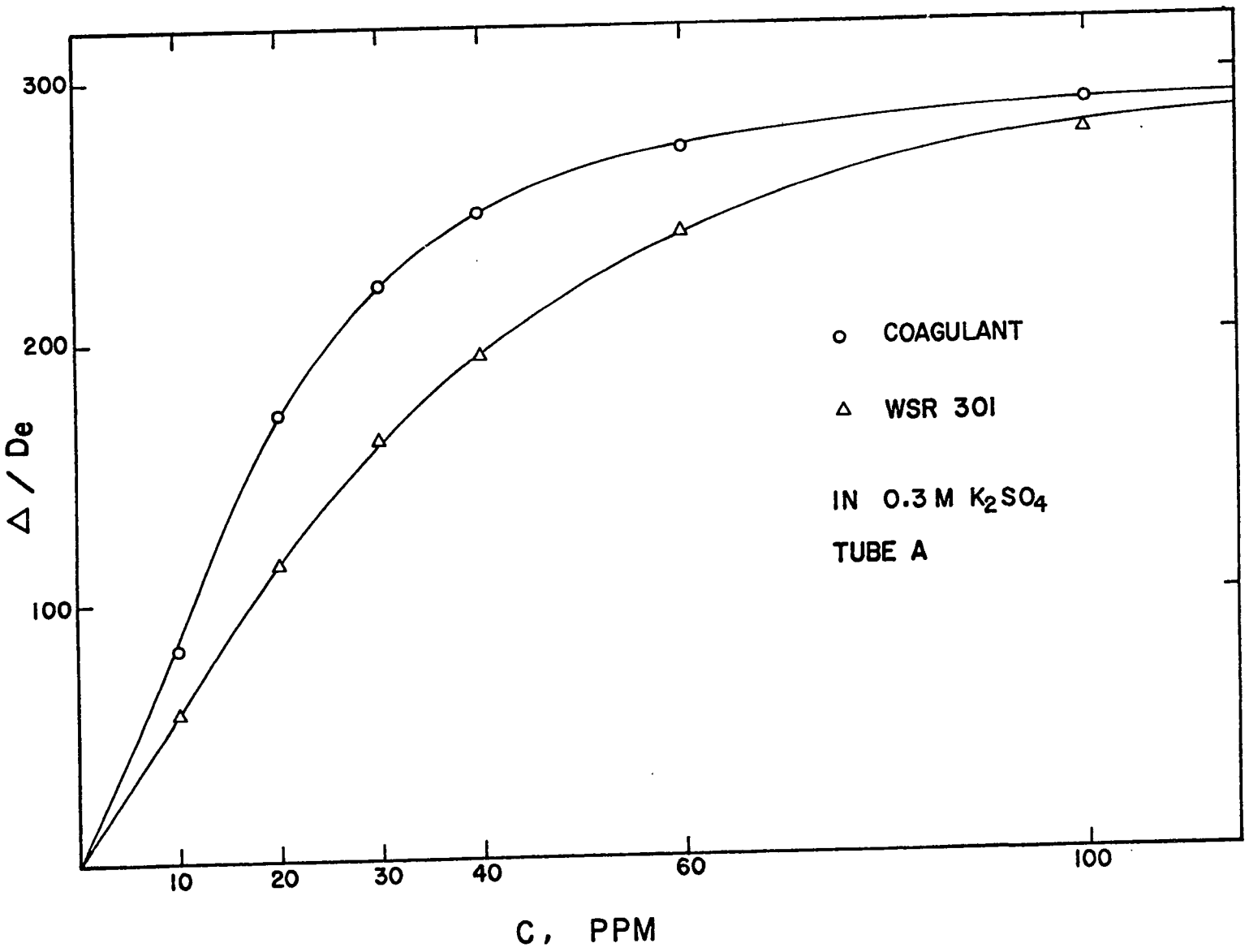

Figure 5.21 : Plot of Δ/D_e for Polyox coagulant and Polyox WSR 301 in 0.3M K_2SO_4 with tube A

$$\overline{\Delta} = K_1 R^{c1}$$

or $$\Delta = K_1 R^{c1+1}, \qquad (5.6\text{-}2)$$

where R is tube radius, and the constant K_1 is given by

$$K_1 = a_1 [\eta]^{b_1} 2^{c_1} \frac{c^{n'}}{\alpha + c^{n'}}$$

The constant c_1 has the experimentally determined value of 0.946, enabling Eq. (5.6-2) to be approximated by

$$\Delta = K_1 R^2, \qquad (5.6\text{-}3)$$

which indicates that the thickness of the anomalous zone varies approximately as the square of the radius in the range of tube radii investigated.

In Fig. (5.22), Δ/R^2 is plotted as a function of polymer concentration for various tube diameters. It is found that there are no significant variations of Δ/R^2 with tube diameter, which is consistent with the above behaviour indicated in Eq. (5.6-3).

5.7 The nature of the anomalous zone

The analysis assumes that the anomalous zone is comprised of an adsorption zone and a concentrated fluid layer in juxtaposition. Only the solvent micromolecules flow in the pore space between the adsorbed macromolecules of the adsorption zone, which is responsible for the polymer build-up

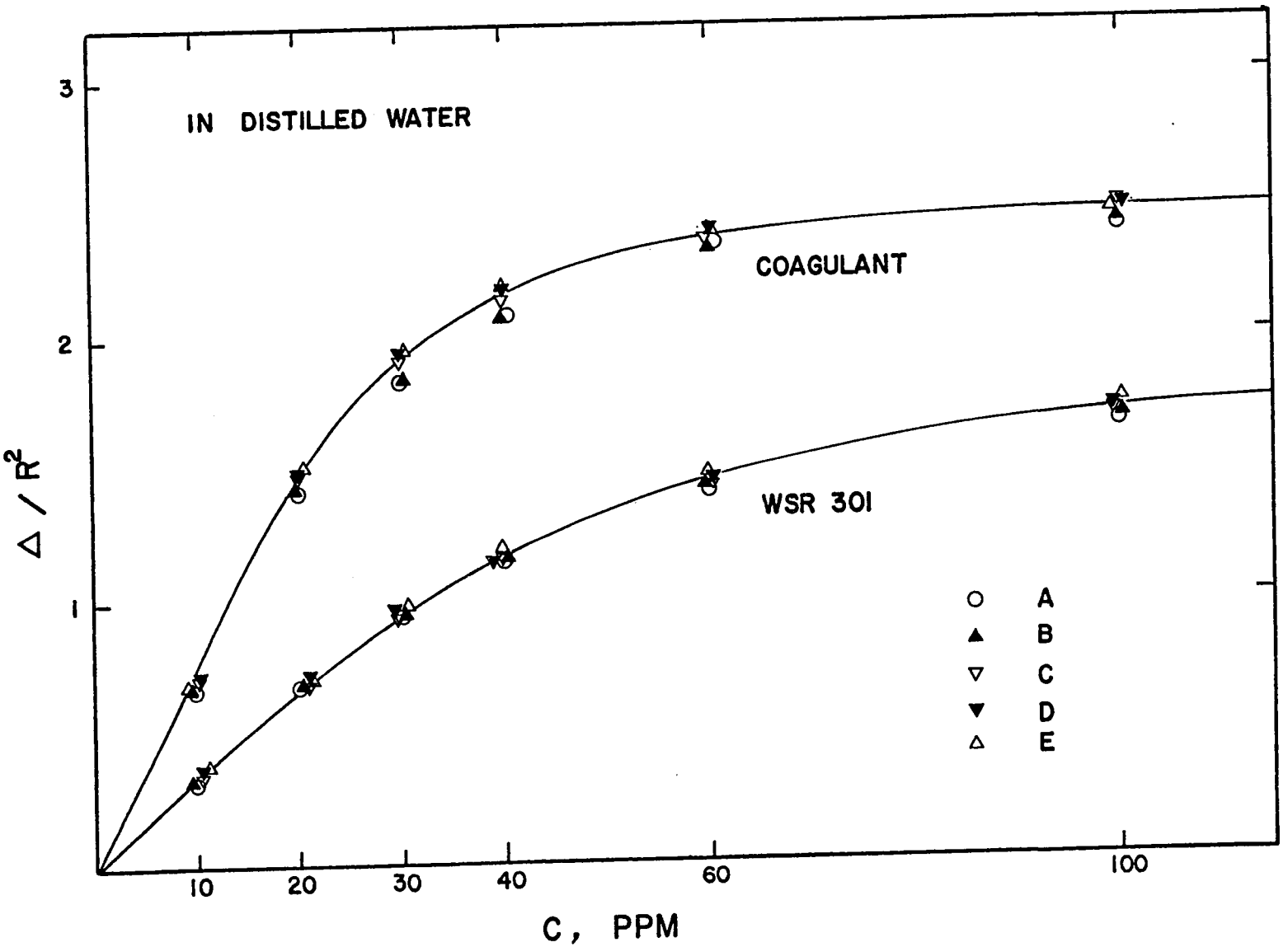

Figure 5.22 : Plot of Δ/R^2 for Polyox coagulant and Polyox WSR 301 in distilled water

in the concentrated layer. The adsorption of polymer in the adsorption zone is assumed to be of a multilayer character.

The location of the interface between adsorption zone and concentrated layer determined from the experimental data is shown in Figs. (5.23) and (5.24). The details of the evaluation procedure are shown in Appendix 3. The curves depicted are for the Polyox Coagulant and Polyox WSR 301, respectively, in distilled water, and for various tube diameters. For all curves, the dimensionless adsorption zone thicknesses $\tilde{\delta}_a$ are over 0.98, indicating that more than 98% of the anomalous zone is occupied by the adsorption zone. It is also illustrated that $\tilde{\delta}_a$ increases with increasing polymer concentration of the bulk solution, approaching unity asymptotically as the concentration is increased without limit.

The evaluations of the adsorption level index n indicating the level of polymer adsorption in the adsorption zone, from the experimental data, are shown in Figs. (5.25) and (5.26) as a function of the bulk polymer concentration. The curves depicted are for the Polyox Coagulant and Polyox WSR 301, respectively, in distilled water, for the various tubes employed. It is indicated that the adsorption level index increases with increasing polymer concentration and tube diameter. The details of the evaluation procedure are shown in Appendix 4.

Eq. (3.3-11) indicates that for values of the

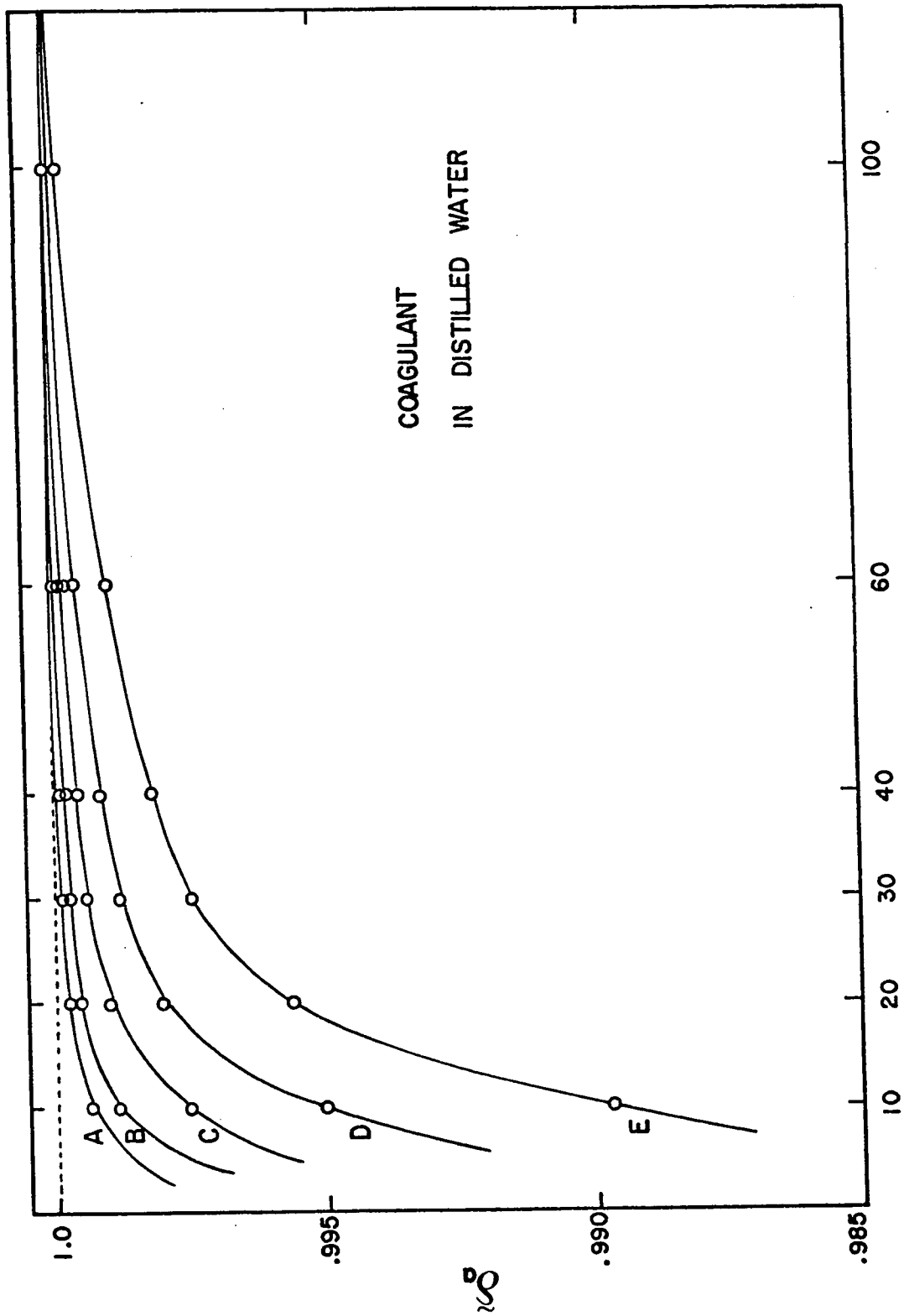

Figure 5.23 : Plot of $\tilde{\delta}_a$ vs. c for Polyox coagulant in distilled water

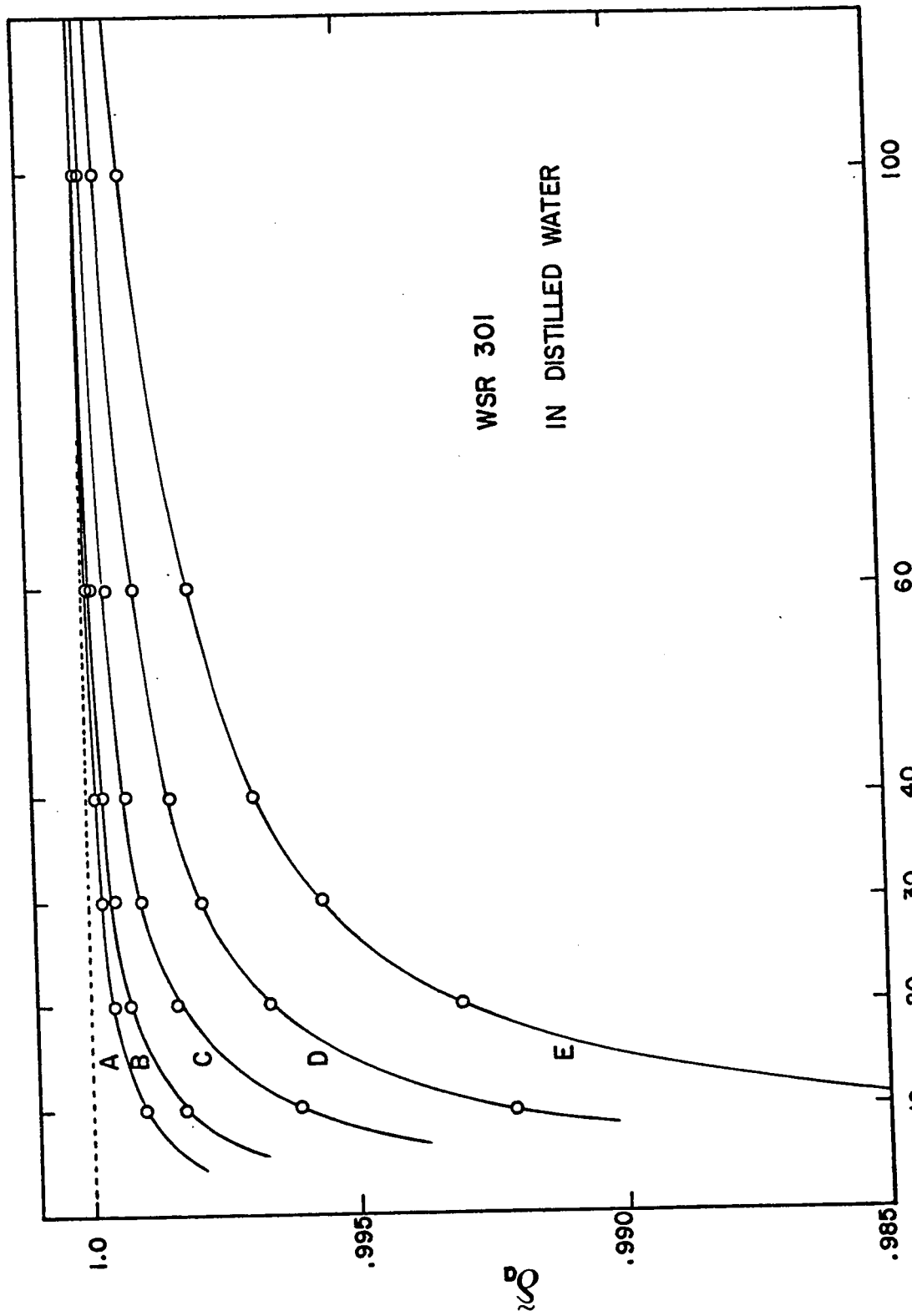

Figure 5.24 : Plot of $\tilde{\delta}_a$ vs. c for Polyox WSR 301 in distilled water

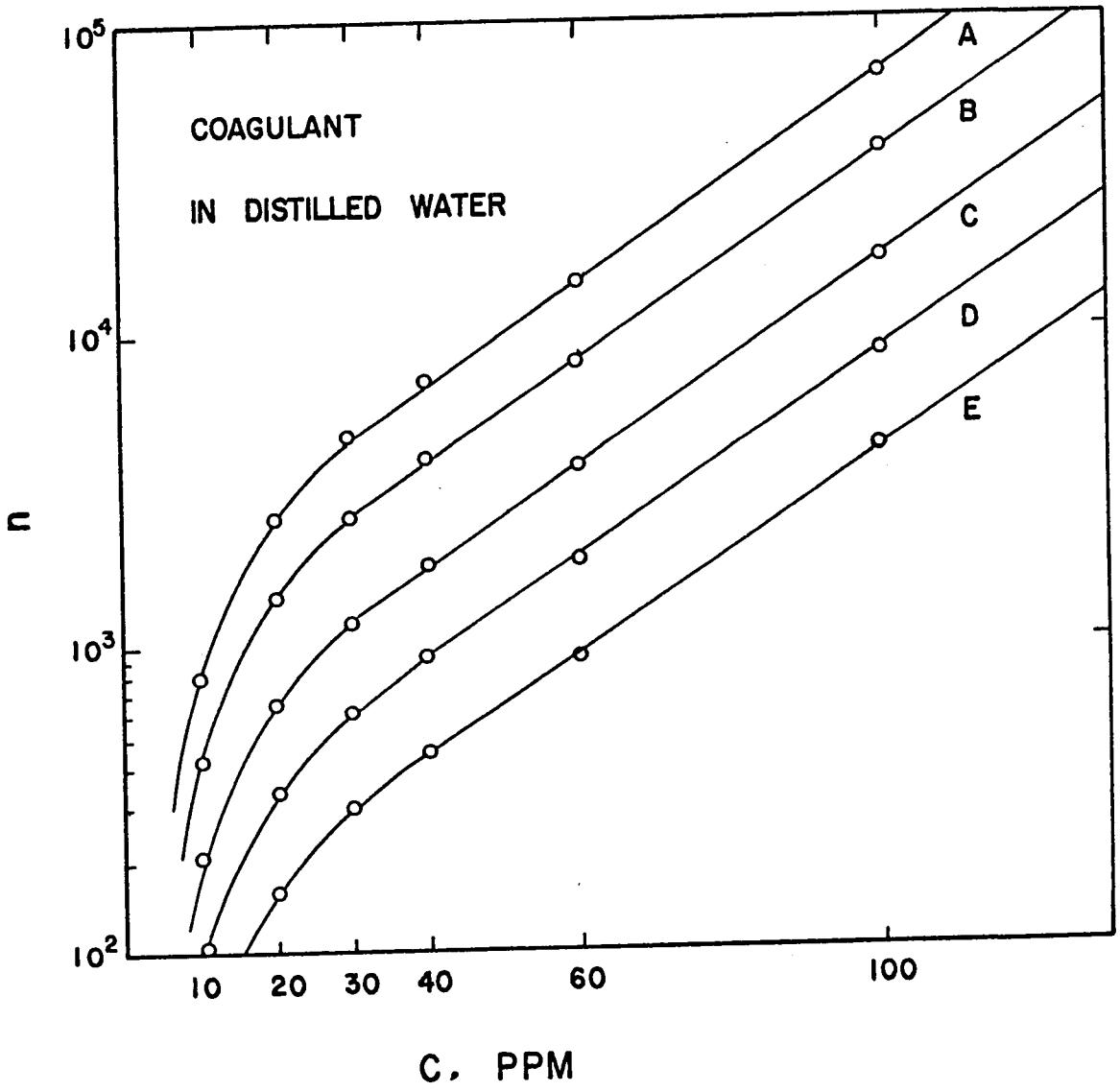

Figure 5.25 : Plot of n vs. c for Polyox coagulant in distilled water

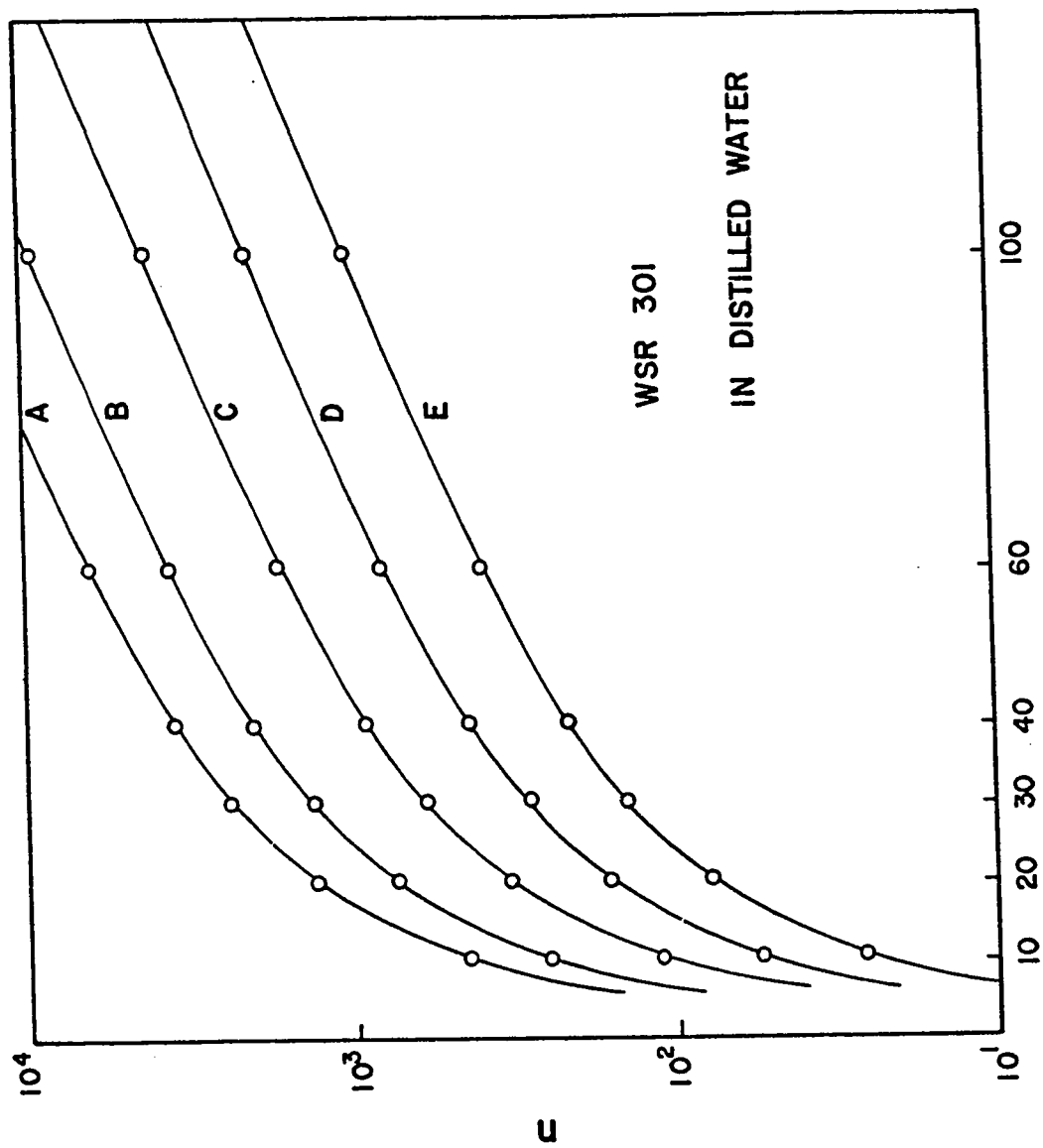

Figure 5.26 : Plot of n vs. c for Polyox WSR 301 in distilled water

adsorption level index n greater than 100, the computed value of the anomalous zone thickness $\overline{\Delta}$ differs from the value $\overline{\Delta}_{n=\infty}$ computed for a completely immobile anomalous zone (corresponding to n=∞) by less than 2%. In this regard, Figs. (5.25) and (5.26) indicate that for the most part, the anomalous zones for the system depicted may be considered to be immobile.

Porosity distribution in the adsorption zone in the vicinity of the interface with the concentrated fluid layer is seen in Fig. (5.27) for the Polyox Coagulant in distilled water as a function of the dimensionless distance from the wall $\tilde{y}$ at various polymer concentrations and two tubes. The data are calculated using the experimentally evaluated values of n and $\overline{\Delta}$. It is found that the region of low porosity corresponding to dense packing of the macromolecules moves progressively close to the concentrated layer interface with increasing polymer concentration.

In the latter calculation, the adsorbed macromolecules are assumed to be spherical. In dense packing, macromolecules in the same layer may overlap by the interpenetration of segments of adjacent macromolecules.

Fig. (5.28) shows the variation of the porosity in the adsorption zone at the interface with the concentrated layer, ε^*, with the polymer concentration in the mainstream for the aqueous solutions of two polymers in tube A. It is indicated that ε^* decreases as the bulk polymer concentration increases. In the limit when concentration equals zero,

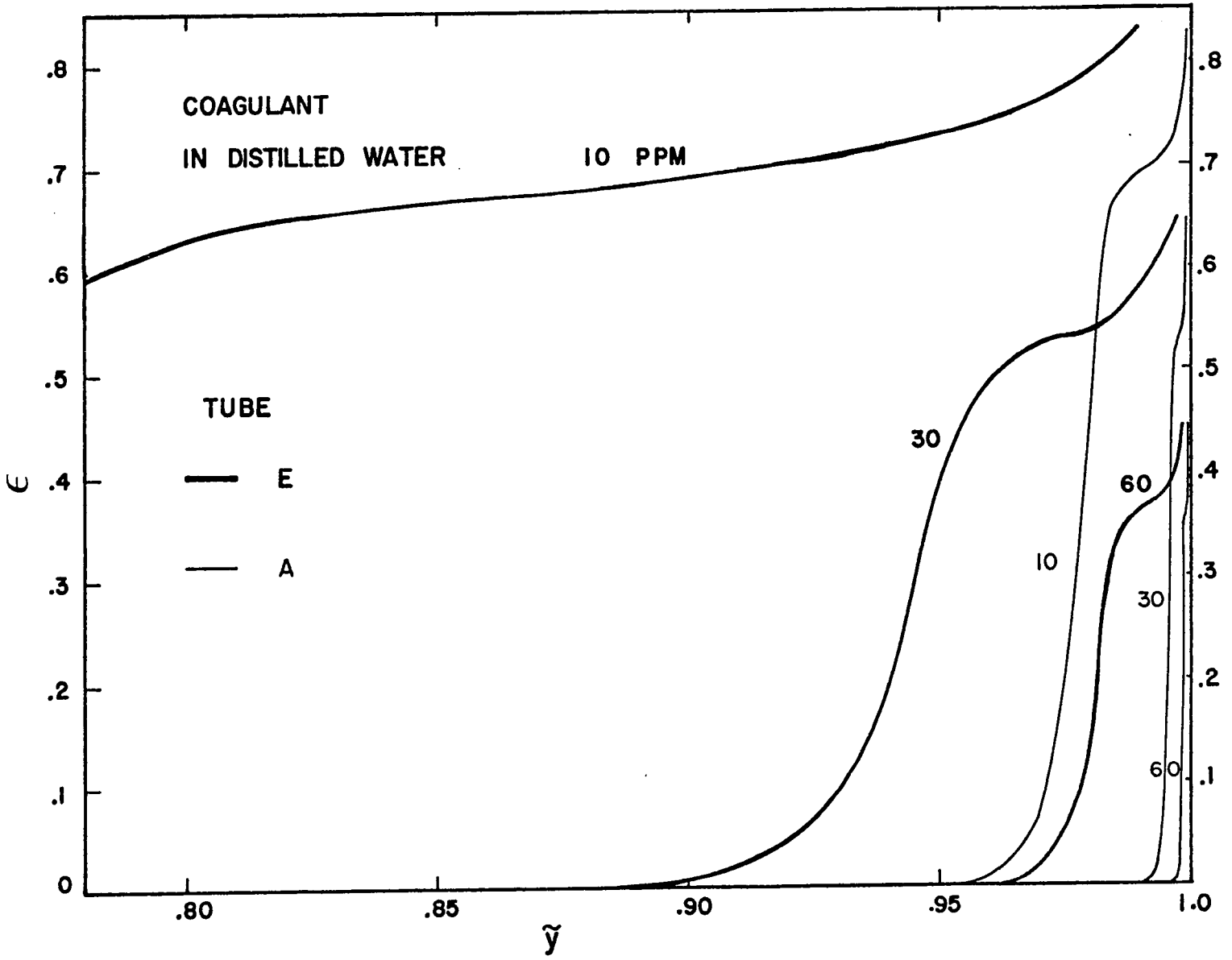

Figure 5.27 : Plot of ε vs. ỹ for Polyox coagulant in distilled water

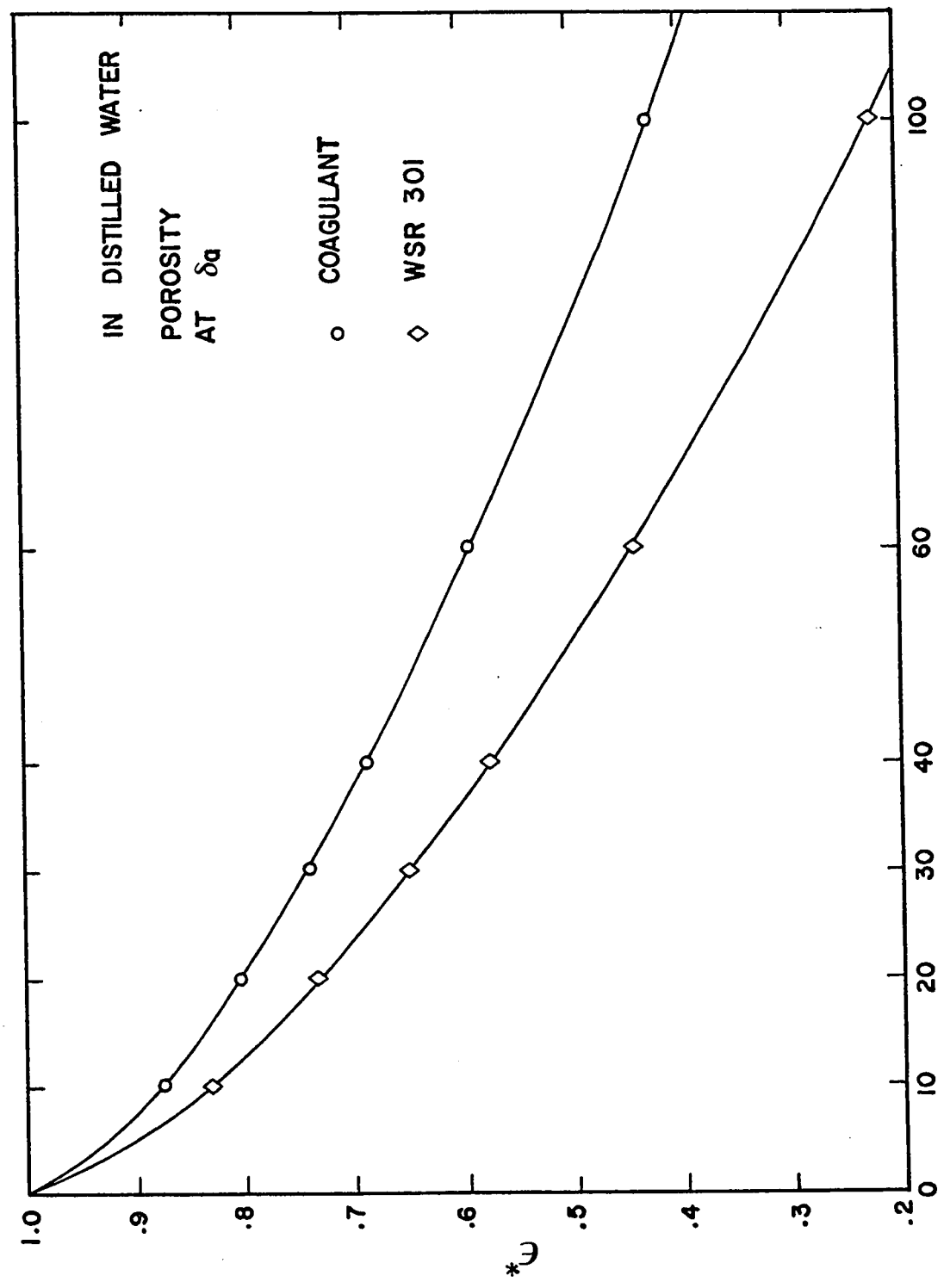

Figure 5.28 : Plot of ε^* vs. c for Polyox coagulant and Polyox WSR 301 in distilled water

ε^* becomes unity. It is shown that the variation of ε^* with tube diameter is negligible in the low range of $\overline{\Delta}$.

The enhancement of polymer concentration in the concentrated layer is seen in Fig. (5.29) from the data. The maximum polymer concentration, at the interface with the adsorption zone normalized with respect to the bulk polymer concentration, c_c^*/c, is plotted as a function of polymer concentration in the bulk solution. This data is based on the evaluations from the experimental data of n and $\overline{\Delta}$ required in the calculation.

It is indicated that the concentrating effect, represented by c_c^*/c, is greatest in the low bulk polymer concentration range and decreases rapidly until a concentration of about 40 ppm, beyond which point the decrease is more gradual. It has also been found by Kozicki et al. (44) that there is no significant variation in c_c^*/c with tube diameter in the range of small values of $\overline{\Delta}$, i.e. $\overline{\Delta}<<1$.

The variation of the maximum polymer concentration in the concentrated layer with the bulk polymer concentration is in qualitative agreement with the pattern determined by Arunachalam et al. (28) by measurement. They measured the polymer concentration of samples withdrawn from the pipe centreline and from the wall region, in the turbulent flow of dilute Polyox solutions. They found a higher polymer concentration in the liquid withdrawn from the wall region than in the core. Furthermore, the ratio of polymer

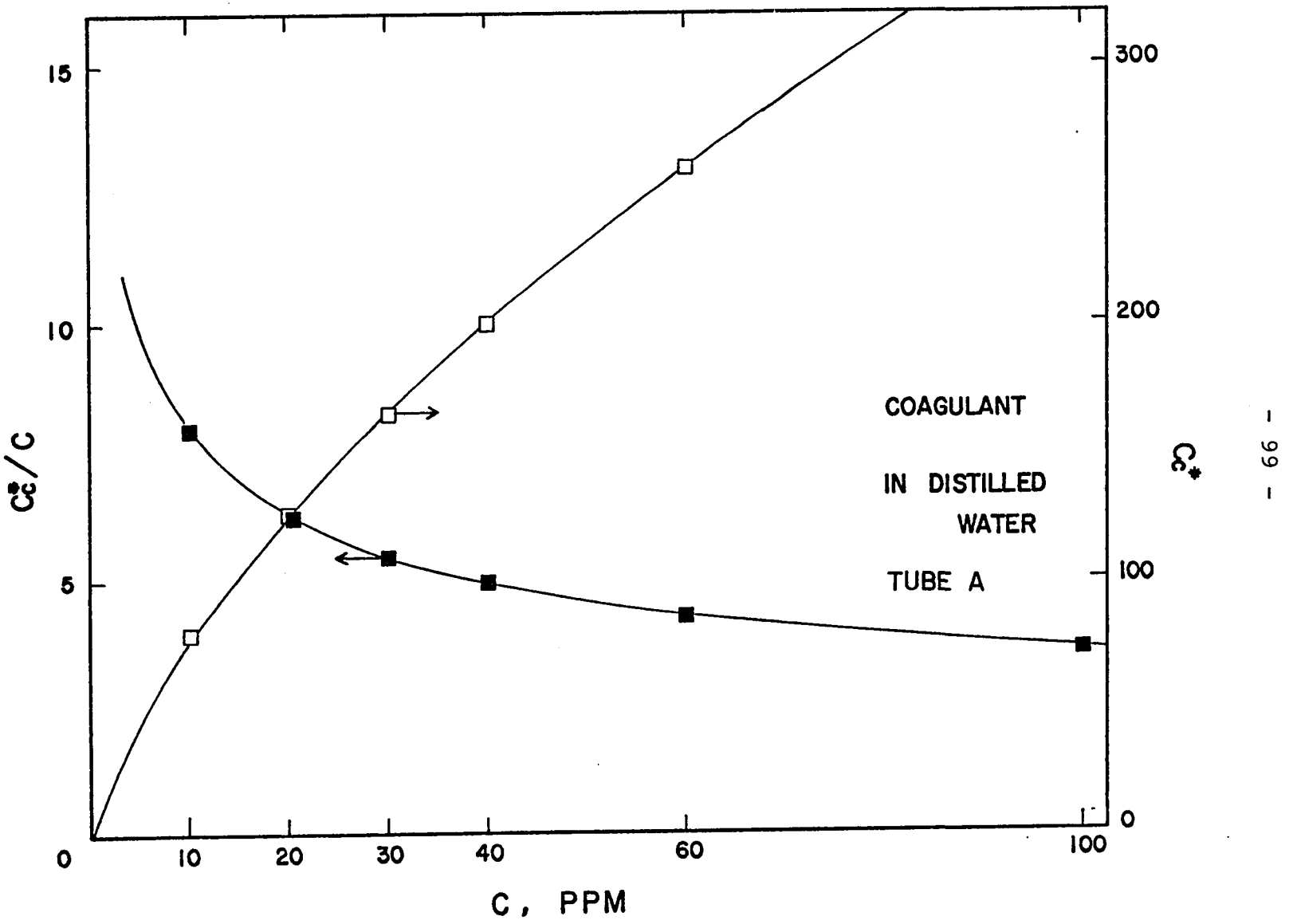

Figure 5.29 : Plot of c_c^*/c vs. c for Polyox coagulant in distilled water

concentration near the wall to concentration in the core was greatest for the lowest bulk polymer concentration (2-4 ppm) and decreased as the bulk polymer concentration increased, which is consistent with the behaviour depicted in Fig. (5.29).

Measurement of Goren and Norbury (98) also indicate a constant Polyox concentration across the pipe radius excluding the region very close to the wall, which support the assumption in the analysis that the anomalous flow behaviour is confined only to the wall region.

The above interpretation involving the formation of a concentrated layer adjacent to the adsorption zone could explain the meaning and significance of previous adsorption measurements, which were generally attributed to polymer adsorption.

Determination of the thickness of the concentrated layer indicates that the thickness is found to be much less than the diameters of a macromolecule in the coiled conformation, while the polymer concentration in the concentrated layer is many times greater than the bulk solution.

It is suggested from the above consideration that the abnormal state of polymer macromolecular conformation in the concentrated layer may give a basis for the turbulent drag reduction. Polymer macromolecules in the concentrated layer may be extended and aligned in a plane or planes parallel to the plane of the interface with the adsorption zone in such a high shear regime, rather than a spherical form assumed in

the present laminar flow regime. The interaction of these highly extended molecules with the adjacent flow field may be responsible for the drag reduction encountered in turbulent flow.

5.8 Correlation with drag reduction

In view of the independence of $\bar{\Delta}$ from the flow rate in laminar flow, and the similarity of its behaviour expressed as a function of the bulk polymer concentration as shown in Figs. (5.12) through (5.15) to drag reduction in turbulent flow, a correlation of drag reduction to $\bar{\Delta}$ with tube diameter and macromolecular size as parameters may be represented as follow:

$$DR = a' \, (\bar{\Delta})^{b'} \, (D_e/D)^{c'}, \qquad (5.8\text{-}1)$$

where D_e is the root mean square end to end distance of polymer macromolecule, D is the tube diameter, and DR represents drag reduction at a given flow rate defined by

$$DR = (f_s - f_a)/f_s, \qquad (5.8\text{-}2)$$

where f is the friction factor and the subscript s refers to solvent while a refers to solution. a', b' and c' are empirical constants to be evaluated at a given flow rate.

The recent drag reduction data by Arunachalam (48) was examined for this purpose because of the wide range of

molecular weights for the Polyox homologues employed and the extensive operating range, using various tube diameters covered experimentally. Furthermore, the author employed similar procedures in solution preparation and used test sections with tube diameters close to those in the present measurements.

The drag reduction data extends to a polymer concentration of 40 ppm. The data collected for the tubes with inside diameters of 0.489 and 0.946 cm using the polymers with molecular weights of 5.3×10^6 and 1.45×10^6 were chosen for the correlation because the molecular weights of these polymers matched most closely the molecular weights of the Polyox Coagulant and Polyox WSR 301, respectively, used in the present measurements. The former data were then adjusted by interpolation to obtain data corresponding to the molecular weights of the Polyox Coagulant and Polyox WSR 301, and to the tube diameters of tubes B and C.

Figs. (5.30) and (5.31) illustrate the success of Eq. (5.8-1) in the correlation of the drag reduction data for the two polymers and two tube sizes at the given Reynolds number. The variations of the indices b' and c' with Reynolds number are shown in Fig. (5.32). It is indicated that b' and c' are decreasing as Re increases until a Re of about 2×10^4. This curve then levels off at a constant value of b', while c' continue to decrease. The break in the b' curve corresponds to the Re at which Arunachalam's drag reduction data levels off.

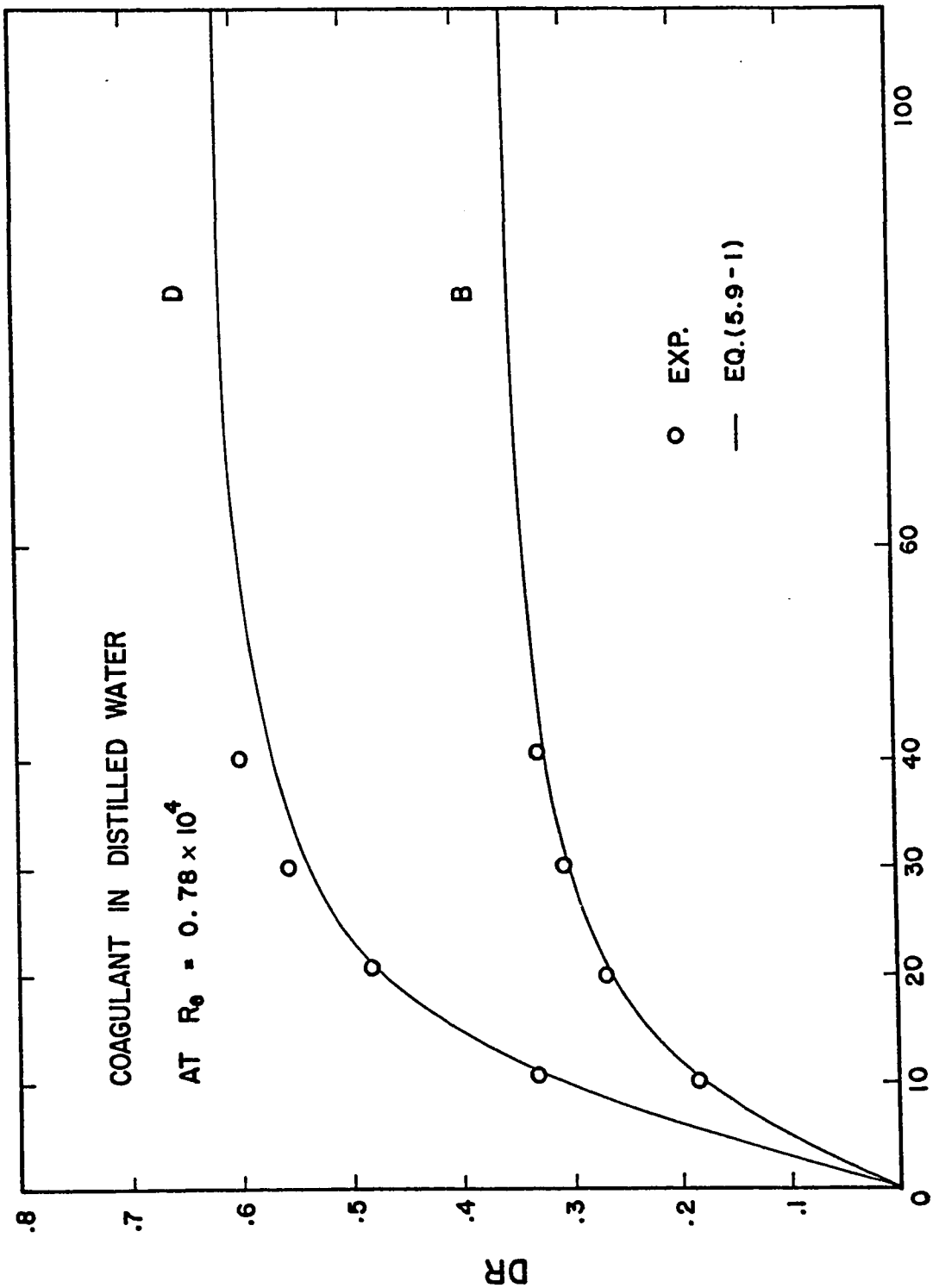

Figure 5.30 : Plot of DR vs. c for Polyox coagulant in distilled water

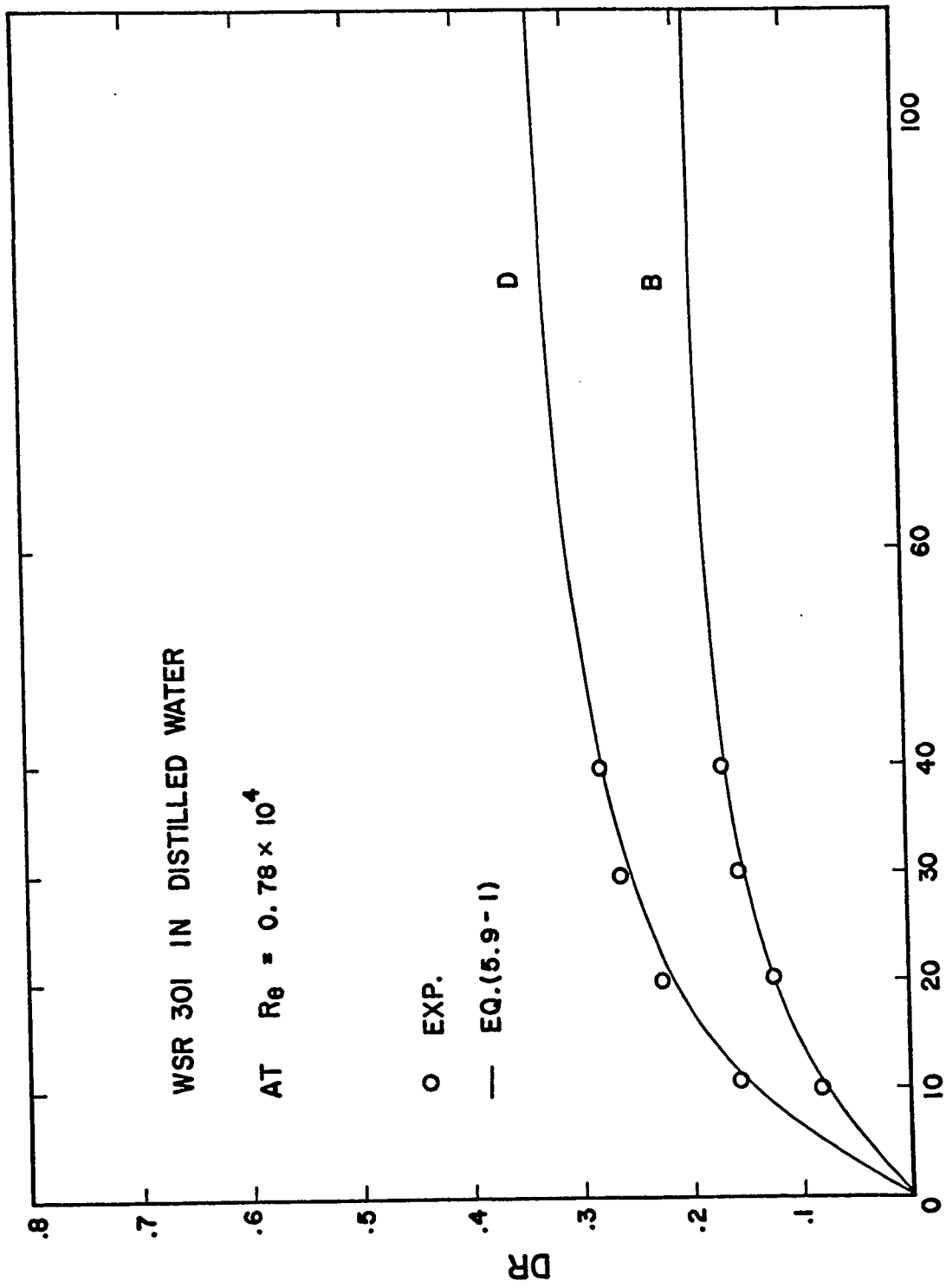

Figure 5.31 : Plot of DR vs. c for Polyox WSR 301 in distilled water

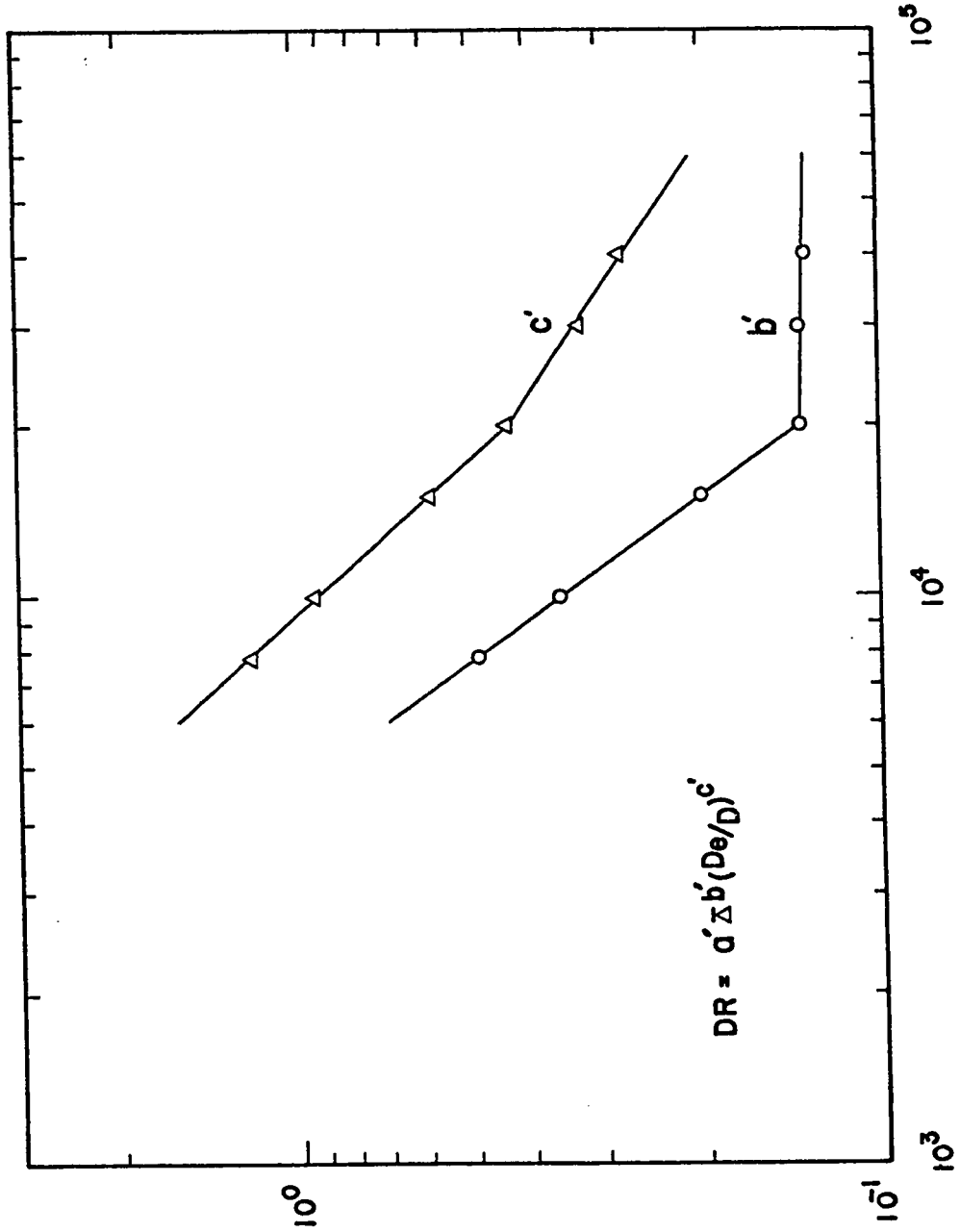

Figure 5.32 : Plot of b' and c' in Eq. (5.8-1) vs. Re

5.9 The effect of non-solvent

Both Polyox Coagulant and Polyox WSR 301 were used to measure the effect of a non-solvent on the polymer adsorption. The non-solvents considered for this series of tests included isopropanol, isobutanol, acetone, ethylene glycol, Na_2CO_3 and K_2SO_4. From these, the K_2SO_4 was selected because it produces a substantial reduction in viscosity at low concentration (e.g. at 0.6 Molar, the Polyox precipitates). For the investigation, 0.3 Molar concentration of K_2SO_4 was chosen to avoid any possibility of precipitation during the experimentation and also since a significant decrease in viscosity from that using distilled water as solvent could be achieved.

As shown in Figs. (5.12) through (5.15), the anomalous zone thickness is significantly reduced by the use of 0.3M K_2SO_4 (poor solvent) in place of distilled water (good solvent) with Polyox Coagulant and Polyox WSR 301, respectively.

The turbulent flow data of other investigators indicates that the drag reduction using high molecular weight polymer solutions decreases systematically with increasing coiling of polymer molecule by the addition of a non-solvent. The degree of coiling is inferred by the measurement of intrinsic viscosity in a capillary viscometer.

There is a similarity in the behaviours of $\overline{\Delta}$ and drag reduction, both decreasing as the coiling of polymer molecule increases. It therefore behoves us to determine if

a relationship between $\overline{\Delta}$ and drag reduction can be found incorporating the degree of polymer coiling as parameter.

According to Eq. (5.5-5),

$$\overline{\Delta}_\infty = a_1 [\eta]^{b_1} D^{c_1},$$

which indicates the dependence of the limiting anomalous zone thickness $\overline{\Delta}_\infty$ on the intrinsic viscosity of the polymer species $[\eta]$ and on tube diameter D. The values of a_1, b_1 and c_1 were determined as 0.003919, 0.5177 and 0.946, respectively. Also Eq. (5.5-1) gives

$$\frac{\overline{\Delta}}{\overline{\Delta}_\infty} = \frac{c^{n'}}{\alpha + c^{n'}},$$

which relates the anomalous zone thickness to the polymer concentration in the bulk solution, for a given polymer-solvent system. The values of α and n' are nearly the same for the two solvents: distilled water and 0.3M K_2SO_4. Therefore, the equality can be written:

$$\left[\frac{\overline{\Delta}}{\overline{\Delta}_\infty}\right]_w = \left[\frac{\overline{\Delta}}{\overline{\Delta}_\infty}\right]_k, \qquad (5.9\text{-}1)$$

where the subscript w refers to the distilled water and k to the 0.3M K_2SO_4 solution, as solvent. Rearranging,

$$\frac{\overline{\Delta}_k}{\overline{\Delta}_w} = \frac{\overline{\Delta}_{\infty k}}{\overline{\Delta}_{\infty w}}, \qquad (5.9\text{-}2)$$

and substitution for $\bar{\Delta}_\infty$ given by Eq. (5.5-5) into Eq. (5.9-2) leads to

$$\frac{\bar{\Delta}_k}{\bar{\Delta}_w} = \frac{a_1 [\eta]_k^{b_1} D^{c_1}}{a_1 [\eta]_w^{b_1} D^{c_1}}$$

or

$$\frac{\bar{\Delta}_k}{\bar{\Delta}_w} = \left[\frac{[\eta]_k}{[\eta]_w}\right]^{b_1} , \qquad (5.9\text{-}3)$$

with b_1=0.5177.

Eq. (5.9-3) incorporates the effect of polymer coiling on the anomalous zone thickness as reflected by the variation in the intrinsic viscosity.

Pruitt et al. (67) obtained extensive data in turbulent flow for the purpose of studying the effect of polymer coiling on drag reduction. They used three Polyox additives having different molecular weights with K_2SO_4 as the non-solvent. The flow condition corresponded to a velocity of 30 ft/sec at a Reynolds number of 4.17×10^4, in a tube with 0.45 cm inside diameter. Measurements were made by means of the air-driven system which effectively eliminated possible shear degradation of the polymer molecules.

The author employed the exponent "a" in the Mark-Houwink equation, $[\eta] = K M^a$, whose behaviour is such that in a poor solvent a lower value of "a" would be expected, while a higher value would be obtained in a good solvent, for the same polymer. It is generally considered that "a" is

dependent on the polymer and the solvent, while K is dependent on the temperature of the solvent.

They attempted a correlation between the parameter of polymer coiling and drag reduction where the incremental quantity (a-0.5) was assumed to be proportional to the drag reduction at a given flow rate and concentration, represented by

$$\frac{DR_k}{DR_w} = \frac{a_k - 0.5}{a_w - 0.5} \cdot \qquad (5.9\text{-}4)$$

The values of "a" for the polymer in distilled water and non-solvent, respectively, were calculated from the intrinsic viscosity determinations assuming a constant value of K at a given molecular weight in Mark-Houwink equation. Eq. (5.9-4) was found to give a reasonable representation of their experimental data.

Replacing (a-0.5) by "b" for simplification, which also defines the degree of molecular expansion of Flory (81), Eq. (5.9-4) becomes

$$\frac{DR_k}{DR_w} = \frac{b_k}{b_w} \cdot \qquad (5.9\text{-}5)$$

From a given set of experimental data, $[\eta]$ and "a", for a polymer in solvents with varying salt concentration, an attempt was made to express "b" as an exponent in $[\eta]$,

$$b = K_3 [\eta]^{a2}. \qquad (5.9\text{-}6)$$

The latter equation was found to give a good fit of the experimental data. The values of the K_3 and a_2 determined by least squares fitting were 0.147 and 0.254 for the Polyox Coagulant, and 0.171 and 0.236 for the Polyox WSR 301, respectively.

Substituting for "b" in Eq. (5.9-5) yields

$$\frac{DR_k}{DR_w} = \left[\frac{[\eta]_k}{[\eta]_w}\right]^{a_2} . \qquad (5.9\text{-}7)$$

It is seen from Eq. (5.9-3) and (5.9-7) that the effect of polymer coiling on both $\overline{\Delta}$ and DR is representable in terms of the intrinsic viscosity of the polymer in the solvent under consideration. Eq. (5.9-3) can be rearranged to

$$\frac{[\eta]_k}{[\eta]_w} = \left[\frac{\overline{\Delta}_k}{\overline{\Delta}_w}\right]^{1/b_1} . \qquad (5.9\text{-}8)$$

Substitution of Eq. (5.9-8) into Eq. (5.9-7) results in

$$\frac{DR_k}{DR_w} = \left[\frac{\overline{\Delta}_k}{\overline{\Delta}_w}\right]^{a_3} , \qquad (5.9\text{-}9)$$

where $a_3=a_2/b_1$ has the values of 0.4922 and 0.4574 for the Polyox Coagulant and Polyox WSR 301, respectively. Thus, Eq. (5.9-9) derived from Eq. (5.9-4) of Pruitt et al., based on the polymer coiling parameter, also illustrates the existence of a relationship between the drag reduction in

turbulent flow and the anomalous zone thickness in laminar flow. It is implied that as the polymer becomes more coiled the adsorption ability is decreased in an orderly fashion and as a consequence the drag reduction is also decreased.

A determination of $\overline{\Delta}$ in laminar flow for a polymer in aqueous and in a non-solvent enables one to predict the amount of drag reduction in turbulent flow utilizing Eq. (5.8-1) and (5.9-9). Furthermore, although the mechanism responsible for turbulent drag reduction is not known, a basis is provided for consideration of the role of polymer adsorption.

5.10 General discussion on drag reduction

It has been assumed in the earlier discussion that the anomalous zone is affected by the high shear stress fields accompanying turbulent flow, even though the anomalous zone thickness in laminar flow is found to be independent of flow rate. The increased shear associated with turbulent flow may produce an extension of the polymer macromolecules in the concentrated layer. These highly extended macromolecules could result in the formation of an abnormally flexible layer, capable of producing the eventual drag reduction.

The above consideration affords a possibility for resolution of the explanation of slip by Oldroyd (15) with the attribution of drag reduction to polymer adsorption proposed by Fulford (28). The effective slip at the wall is attributable to the unusual properties of the concentrated

layer associated with the polymer adsorption.

The drag reduction data of the previous investigators indicate an increase of drag reduction with decreasing tube diameter at a given Reynolds number. This diameter effect in drag reduction is attributable by similar reasoning to the increased shear stress prevailing in flow in smaller tubes: for a given R_e, the shear stress at the wall in a smaller tube is greater than in a larger tube.

The shear stress at the wall τ_w associated with the polymer adsorption is defined as the shear stress in the bulk flow region which is extrapolated to the tube wall. The momentum flux distribution in the bulk flow region cannot be applied in the adsorption zone due to the completely different flow geometries. By this consideration, the local shear stress in the concentrated fluid layer can be regarded as the shear stress at the wall τ_w due to the relatively small distance from the tube wall compared to the tube radius.

The above consideration of the effect of shear stress at the wall on the drag reduction is supported by Paterson et al. (58). Their experimental measurements indicate that the extent of drag reduction is relatively independent of tube diameter when the comparison is carried out at equal solvent wall shear stress.

Other indication of the effect of polymer adsorption on drag reduction could be found in the investigation describing increased laminar sublayer thickness, evaluated

from dispersion measurements by Arunachalam (48). He employed a Taylor axial tracer dispersion technique to study the changes in velocity profile in dilute solutions from those in the solvent alone.

A simple methematical model of the process has been proposed and solved in terms of the measurable dispersion parameters. The results show that the laminar sublayer thickness in the dilute solution is about three times greater than that expected in the solvent alone though there are some uncertainties due to the assumptions employed in the dispersion model that the tracer materials in the thickened sublayer are transported in and out of the layer entirely by the molecular diffusion with a constant diffusivity and that the velocity profiles in the core region for the polymer solutions are of the same shape as those for the solvent.

The measurements for the dispersion experiment were carried out with one tube, i.e. 1.233 cm inside diameter for a polymer additive having molecular weight of 5×10^6 at various concentrations and flow rates. Fig. (5.33) shows the comparison between laminar sublayer thickness in turbulent flow from the dispersion data and anomalous zone thickness from the present measurement in tube A for Polyox Coagulant at 30 ppm. The laminar sublayer thickness of the solvent was calculated from Eq. (A.10-5):

$$\delta/R = \frac{\delta^+}{0.0994\ R_e^{7/8}} \quad \text{for } \delta^+ = 5.$$

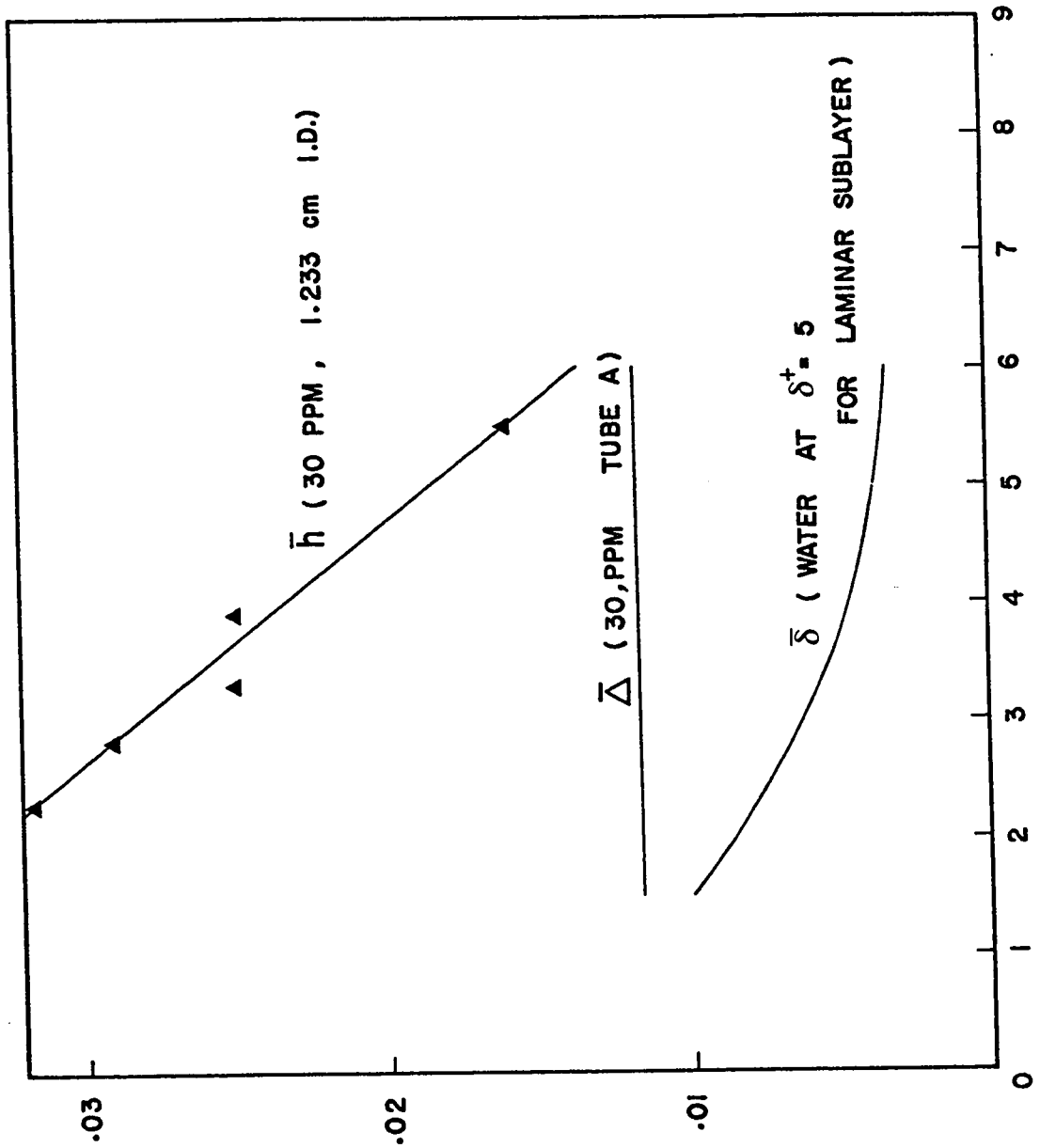

Figure 5.33 : Plot of $\bar{h}$, $\bar{\Delta}$ and $\bar{\delta}$ vs. Re for Polyox coagulant in distilled water

The derivation of the latter equation is described in Appendix 10.

By the consideration of the comparable amount of the anomalous zone thickness to the increased laminar sublayer, it is conceivable that the polymer adsorption represented by Δ may be responsible for or at least influence the increased laminar sublayer in turbulent flow, which is another manifestation of the drag reduction.

Though the analysis which relates the polymer adsorption to the drag reduction is admittedly rather speculative, however the sum of the available evidences is strongly in favor of the adsorption of polymer additives leading to a fundamental mechanism for the drag reduction in turbulent flow.

6. SUMMARY AND CONCLUSIONS

The results of experimental investigation are discussed for the characterization of the polymer adsorption and flow behaviour at the tube wall during steady uniform laminar tube flow. Pressure drop-flow rate measurements were carried out using a constant head device, for the Polyox homologues at various polymer concentrations with the tubes having five different tube diameters.

The analysis assumes a region of anomalous flow adjacent to the wall wherein the effects associated with inhomogeneities of the fluid are confined.

Polymer adsorption results in a negative effect on the velocity profile in the laminar flow investigated though it may cause a positive effect in the turbulent flow to give friction reduction.

The anomalous zone thickness can be represented reasonably well by the Langmuir type equation, $\overline{\Delta}/\overline{\Delta}_\infty = c^{n'}/(\alpha + c^{n'})$, which indicates a steep rise of the anomalous zone thickness at low concentration and a gradual increase at high concentration until it reaches a limiting value.

The limiting anomalous zone thickness can be expressed in terms of intrinsic viscosity and tube diameter by the equation, $\overline{\Delta}_\infty = a_1 [\eta]^{b1} D^{c1}$.

The thickness of the anomalous zone varies

approximately as the square of the tube radius in the range of tube radii investigated.

More than 98% of the anomalous zone is occupied by the adsorption zone, and less than one macromolecular diameter distance is attributed to the concentrated layer.

The concentrating effect, represented by c_c^*/c, is greatest in the low bulk solution concentration range and decreases rapidly until it reaches about 40 ppm, beyond which point the decrease in concentrating effect becomes more gradual. This phenomenon is in qualitative agreement with the experimental measurements for the concentration profile by other investigators.

Polymer degradation in the dilute solutions with duration of time results in a considerable reduction in the solution viscosity and in the anomalous zone thickness.

Polymer adsorption of a dilute aqueous solution is significantly decreased by the addition of a salt, K_2SO_4, which plays a role as non-solvent for the polymer molecules.

Correlation between the anomalous zone thickness in laminar flow and the drag reduction in turbulent flow was made with macromolecular dimension and tube diameter as parameters by the equation,

$$DR = a'(\bar{\Delta})^{b'}(D_e/D)^{c'} \quad \text{for aqueous solution,}$$

$$\frac{DR_k}{DR_w} = \left[\frac{\bar{\Delta}_k}{\bar{\Delta}_w}\right]^{a3} \quad \text{for non-solvent solution.}$$

It is suggested that the polymer adsorption could be a fundamental basis for the turbulent drag reduction by the discussions of the parameters associated with polymer adsorption in the present work and the increased laminar sublayer from the dispersion measurement in turbulent flow by other investigator.

Computer programs were developed for the evaluation of the parameters associated with polymer adsorption and for the various correlation procedures.

Future work should be aimed at collecting more reliable and sufficient drag reduction data in turbulent flow for the better and complete correlation with the anomalous zone thickness in the present laminar flow measurement.

Polymer degradation effect should be carefully considered to be same for both flow regimes either by aging or by mechanical shear during experimental procedures.

Measurement of point velocities in the core region of the mainstream will be of great value for the simple and accurate evaluation of the parameters.

REFERENCES

1. Toms, B.A., Proc. First Intern. Congr. on Rheol., North Holland Publ. Co., Amsterdam, Pt.2, P.135 (1949)
2. Mysels, K.J., U.S. Patent 2,492,173., Dec. 27 (1949)
3. Fabula, A.G., Proc. Fourth Intern. Congr. on Rheol., Brown Univ., Providence, Rhode Island, Pt.3 (1963), Ed. Interscience Publ. N.Y. (1965) P.455
4. Lumley, J.L., Ann. Rev. Fluid Mech., Vol. 1 (1969)
5. Hoyt, J.W., Trans. ASME J. Basic Eng., 94, 258 (1972)
6. Virk, P.S., AIChE J., No.4, 21, 625 (1975)
7. Dodge, D.W., Metzner, A.B., AIChE J., 5, 189 (1959)
8. Shaver, R.G., Merrill, E.W., AIChE J., 5, 181 (1959)
9. Metzner, A.B., Park, M.G., J. Fluid Mech., 20, 291 (1964)
10. Gadd, G., Nature, 212, 1348 (1966)
11. Gadd, G., ibid, No.4983, P.463 (1965)
12. Patterson, G.K., Zakin, J.L., AIChE J., 14, 434 (1968)
13. Astarita, G., I & E C Fundls., No.3, 4, 355 (1965)
14. Ruckenstein, E., Chem. Eng. Sci., 26, 1075 (1971)
15. Oldroyd, J.G., Proc. First Intern. Congr. on Rheol., North Holland Publ. Co., Amsterdam, Pt.2, P.130 (1949)
16. Kozicki, W., Tiu, C., Chem. Eng. Sci., 23, 231 (1968)
17. Ohrn, O.E., J. Polym. Sci., 17, 137 (1955)
18. Takeda, M., Endo, R., J. Phys. Chem., 60, 1202 (1956)
19. Maude, A.D., Whitemore, R.L., British J. of Appl. Phys., 7, 98 (1956)
20. Tuijnman, C.A.F., Hermans, J.J., J. Polym. Sci., 25, 385 (1957)

21. Astarita, G., Marrucci, G., Palumbo, G., I & E C Fundls., 3, 333 (1964)

22. Jastrzebski, Z.D., ibid, No.3, 6, 445 (1967)

23. Rowland, F.W., Eirich, F.R., J. Polym. Sci., A-1, 4, 2033 (1966)

24. El'rerin, I.T., Smol'skii, B.M., Levonthal, L.I., Intl. Chem. Eng., 7, 276 (1967)

25. Kowalski, T.Q., Quart. Trans. Royal Inst. Naval Architects, 110, 207 (1968)

26. David, G.A., Ponter, A.B., Nature, 212, 66 (1966)

27. Wells, C.S., Spangler, J.G., Phys. Fluids, 10, 1890 (1967)

28. Arunachalam, Vr., Fulford, G.D., Chem. Eng. Sci., 26, 1065 (1970)

29. Hand, J.H., Williams, M.C., ibid, 28, 63 (1973)

30. McComb, W.D., Nature, 251, 598 (1974)

31. Silberberg, A., J. Chem Phys., 48, 2835 (1968)

32. Diomarzio, E.A., ibid, 42, 2101 (1965)

33. Ellerstein, S., Ullmann, R., J. Polym. Sci., 55, 123 (1961)

34. Hoeve, C.A.J., Diomarzio, E.A., Peyser, P., J. Chem. Phys., 42, 2558 (1965)

35. Rowland, F., Bulas, R., I & E C, No.9, 57, 46 (1965)

36. Kipling, J.J., "Adsorption from Solutions of Non-electrolytes", Academic Press (1965)

37. Schofield, R.K., Blair, G.W.S., J. Phy. Chem., 34, 248 (1930)

38. Schofield, R.K., Blair, G.W.S., ibid, 35, 1212 (1931)

39. Oldroyd, J.G., J. Colloid Sci., 4, 333 (1949)

40. Toms, B.A., ibid, 4, 511 (1949)

41. Kozicki, W., Pasari, S.N., Rao, A.R., Tiu, C., Chem. Eng. Sci., 25, 41 (1970)

42. Pasari, S.N., M.A.Sc. Thesis, Univ. of Ottawa (1969)

43. Bhargava, B.K., ibid, (1972)

44. Kozicki, W., Wu, F., To be published

45. Hawkins, W.L., Winslow, F.H., "Chemical reaction of polymer", Interscience, N.Y. (1964) P.1055

46. Furukawa, J., Saegusa, T., "Polymerization of aldehydes and Oxides", Interscience, N.Y. (1963) P.286

47. Rodriquez, F., "Principles of polymer system", McGraw-Hill, N.Y. (1970) P.270

48. Arunachalam, Vr., Ph.D Thesis, Univ. of Waterloo (1969)

49. Nakano, A., Minoura, Y., J. Appl. Polym. Sci., 15, 927 (1971)

50. Minoura, Y., Kasuya, T., Kawamura, A., Nakano, A., J. Polym. Sci., 5, 43 (1967)

51. Fujiwara, H., Goto, K., J. Chem. Soc., Japan Ind. Chem. Soc., 71, 1430 (1968)

52. Harrington, R.E., J. Polym. Sci., 4, 489 (1966)

53. Rodriquez, F., Windring, C.C., I & E C, 51, 1281 (1959)

54. Arai, K., Nakamura, K., Kamatsu, T., Nakagawa, T., J. Chem. Soc., Japan Ind. Chem. Soc., 71, 1438 (1968)

55. Ram, A., Kadim, A., J. Appl. Polym. Sci., 14, 2145 (1970)

56. Patterson, G.K., Hershey, H.C., Green, C.D., Zakin, J.L., Trans. Soc. Rheol., 10, 489 (1966)

57. Kenis, P.R., J. Appl. Polym. Sci., 15, 607 (1971)

58. Paterson, R.W., Abernathy, F.H., J. Fluid Mech., 43, 689 (1970)

59. Fisher, D.H., Rodriquez, F., J. Appl. Polym. Sci., 15, 2975 (1971)

60. Bueche, F., ibid, 4, 101 (1960)

61. Bestal, A.B., J. Chem. Phys., 32, 350 (1960)

62. Goobermann, G., Lamb, J., J. Polym. Sci., 42, 35 (1960)

63. Ramakrishnan, B.C., Rodriquez, F., AIChE Symp. Ser., No. 130, 69, 52 (1973)

64. Lepera, M.E., Pigliacampi, J., I & E C, Prod. Res. Devl., 9, 525 (1970)

65. Crail, I.R.H., Neville, A.L., J. Inst. Petrol., 55, 100 (1969)

66. Ram, A., Timir, A., J. Appl. Polym. Sci., 8, 2751 (1964)

67. Pruitt, G.T., Rosen, B., Crawford, H.R., Report No.DTMB-2 (1966)

68. Hershey, H.C., Zakin, J.L., Chem. Eng. Sci., 22, 1847 (1967)

69. Persey, P., Little, R.C., J. Appl. Polym. Sci., 15, 2623 (1971)

70. White, W.D., "Viscous draf reduction", Ed. C.S. Wells, Plenum Press, N.Y. (1969) P.173

71. Shin, H., Sc.D Thesis, M.I.T. (1965)

72. Bailey, F.E., Callard, R.W., J. Appl. Polym. Sci., 1, 56 (1959)

73. Little, R.C., Patterson, R.L., ibid, 18, 1529 (1974)

74. Kraemer, E.O., I & E C, 30, 1200 (1938)

75. Huggins, M.L., J. Am. Chem. Soc., 64, 2716 (1942)

76. Schulz, G.L., Blaschke, F., J. Prakt. Chem., 158, 130 (1941)

77. Ibrahim, F.W., J. Polym. Sci., 3, Pt.A, 469 (1965)

78. Hanna, M.R., Ph.D Thesis, Univ. of Ottawa (1977)

79. Merrill, E.W., Smith, K.A., Shin, H., Mickley, H.S., Trans. Soc. Rheol., 10:1, 335 (1966)

80. Sever, E.T., "Rheology of polymer", Reinhold Pub. Corp., N.Y. (1962) P.84

81. Flory, P.J., "Principles of polymer chemistry", Cornell Univ. Press, Ithaca, N.Y. (1953)

82. Kirkwood, J.G., Riseman, J., J. Chem. Phys., 16 565 (1948)

83. Kirkwood, J.G., Zwanzig, R.W., Plock, R.J., ibid, 23, 213 (1955)

84. Yamakawa, H., "Modern theory of polymer solutions", Harper & Raw (1971)

85. Debye, P., Bueche, A.M., J. Chem. Phys., 16, No.6, 573 (1948)

86. Flory, P.J., ibid, 17, 303 (1949)

87. Flory, P.J., Fox, T.G. Jr., J. Am. Chem. Soc., 73, 1904 (1951)

88. Zimm, B.H., J. Chem. Phys., 24, 269 (1956)

89. Hearst, J.E., ibid, 37, 2547 (1962)

90. Tschoegl, N.W., ibid, 39, 149 (1963)

91. Fixman, M., ibid, 42, 3831 (1965)

92. Pyun, C.W., Fixman, M., ibid, 42, 3838 (1965)

93. Pyun, C.W., Fixman, M., ibid, 44, 2107 (1966)

94. Brinkman, H.C., Appl. Sci. Res., A1, 81 (1947)

95. Neale, G., Epstein, N., Nader, W., Chem. Eng. Sci., 28, 1865 (1973)

96. Neale, G., Nader, W., AIChE J., 20, 530 (1974)

97. Martin, J.J., McCabe, W.L., Monrad, C.C., Chem. Eng. Pro., 47, 91 (1951)

98. Goren, N.Y., Norbury, J.F., Trans. ASME J. Basic Eng., 89D, 814 (1967)

99. Huggins, M.L., New York, John Wiley & Sons, Inc., (1958)

100. Beech, D.R., Booth, C., J. Polym. Sci., Pt.A-2, 7, 575 (1969)

101. Union Carbide Corp., "Polyox", (1974)

APPENDICES

with

Computer Programmes

Appendix 1

Calibration of tube diameter

For a Newtonian laminar flow, Hagen-Poiseuille law can be used by the equation:

$$Q = \frac{\pi \Delta P R^4}{8 \eta L} \qquad \text{(A.1-1)}$$

Rearranging the latter equation, with substituting ΔP by $\rho g \Delta h$, and Q by w/ρ,

$$\frac{\Delta h}{w} = \frac{128 \eta L}{\pi \rho^2 g D^4} , \qquad \text{(A.1-2)}$$

where Δh = pressure drop, cm

w = mass flow rate, g/sec.

Let $\Delta h/w = s$ to obtain tube diameter as follow:

$$D = \left[\frac{128 \eta L}{\pi \rho^2 g s}\right]^{1/4} , \qquad \text{(A.1-3)}$$

where s can be evaluated by least squares fitting to a straight line with a set of data, Δh and w.

```
      C
      CC
      C   CALIBRATION OF TUBE DIAMETER
      CC
      CC
      CC       SL     = TEST TUBE LENGTH, CM
      C        H      = PRESSURE HEAD, CM
      C        W      = FLOW RATE, G/MIN.
      C        DIAM   = TUBE DIAMETER, CM
      CC
      C
 1            DIMENSION W(10), H(10)
 2            DOUBLE PRECISION W, H, DIAM, SL
 3            WRITE(6,4)
 4          4 FORMAT(1H1,//)
 5         10 READ (5,1) SL
 6          1 FORMAT (F7.3)
 7            IF(SL.EQ.0.0) GO TO 6
 8            READ (5,2) (H(I),W(I), I=1,10 )
 9          2 FORMAT (F6.3, 2X, F8.4)
10            CALL BESFIT(W,H, 10, DIAM, SL )
11            WRITE (6,3) DIAM
12          3 FORMAT(/ ,11X,'DIAM = ', F9.5,/)
13            WRITE(6,4)
14            GO TO 10
15          6 WRITE(6,4)
16            STOP
17            END

18            SUBROUTINE BESFIT (X,Y,NDATA, DIAM, SL)
      C
      C   BEST LEAST SQUARE FITTING
      C
19            DIMENSION X(10),Y(10)
20            DOUBLEPRECISION A,B,C,D,X,Y,SLOPE,XI,DSQRT,SL
             1,DIAM,D1,D2
21            A=0.0
22            B=0.0
23            C=0.0
24            D=0.0
25            DO 100 I=1,NDATA
26            WRITE(6,200) Y(I), X(I)
27       200  FORMAT(19X, F6.3,5X,F8.4,/)
28            A=A+X(I)
29            B=B+Y(I)
30            C=C+X(I)*X(I)
31       100  D=D+X(I)*Y(I)
32            SLOPE=D/C
33            WRITE (6,4) SLOPE
34          4 FORMAT(//11X,'SLOPE=',  1PD16.7,/)
35            XI=128.0*0.0089372*SL/(980.665*3.1416*0.997*0.997)
36            D1=SLOPE*60/XI
37            D2=DSQRT(D1)
38            DIAM =1/DSQRT(D2)
39            RETURN
40            END

      $ENTRY
```

Appendix 2

Treatment of solution measurement

The flow measurement of dilute polymer solution is expressed by the Eq. (3.3-6),

$$\tau_w = \eta_a \frac{8\langle u\rangle}{D}, \qquad (3.3\text{-}6)$$

where $$\tau_w = \frac{D\ \rho\ g}{4\ L}\ \Delta h, \qquad (A.2\text{-}1)$$

and $$\frac{8\langle u\rangle}{D} = \frac{32}{\rho\ \P\ D^3}\ w. \qquad (A.2\text{-}2)$$

Solving for viscosity coefficient η_a,

$$\eta_a = \frac{g\ \P\ \rho^2\ D^4}{128\ L}\ s, \qquad (A.2\text{-}3)$$

where $s = \Delta h/w$.

Subsequently, the average velocity deficiency can be evaluated by Eq. (3.3-8),

$$\bar{u}_w = \frac{1}{4}\left(\frac{\eta}{\eta_a} - 1\right).$$

```
C
C   EVALUATION OF B AND UW FROM ORIGINAL PRESSURE DROP
C   MEASUREMENT
C
C
C       CON    = SOLUTION CONCENTRATION, PPM
C       VISW   = VISCOSITY OF DISTILLED WATER, POISE
C       DEN    = SOLUTION DENSITY, G/CC
C       VIS    = RELATIVE VISCOSITY OF SOLUTION OVER DISTILLED
C                WATER
C       D      = TUBE DIAMETER, CM
C       L      = TEST TUBE LENGTH, CM
C       P      = PRESSURE DROP, CM
C       W      = FLOW RATE, G/MIN.
C       ST     = SHEAR STRESS AT WALL, DYNE/SQ. CM
C       SR     = SHEAR RATE, 8(U)/D, 1/SEC.
C       SRW    = SHEAR RATE OF DISTILLED WATER AT ST
C       RE     = REYNOLDS NUMBER
C       B      = RELATIVE viscosity coefficient, ηa/ηs
C       UW     = DIMENSIONLESS AVERAGE VELOCITY DEFICIENCY
C
C
 1          DIMENSION DIA(5),XL(5),CON(6),VIS(6),UW(6),SRW(6,7)
           1,SR(6,7),P(6,7),W(6,7),RE(6,7),B(6),WS(7),PS(7),
           2S(6),ST(6,7)
 2          DOUBLE PRECISION P,W,SR,ST,SRW,B,VISW,SLOPE,WS,PS
           1,CON,VIS,D,L,XL,UW,DEN,RE, S
 3          READ(5,1) D,L
 4        1 FORMAT(D12.5, 2X,F5.1)
 5          READ(5,11) (CON(I),I=1,6)
 6       11 FORMAT(6(D8.1,2X))
 7          READ(5,14) VISW, DEN
 8       14 FORMAT(2(D13.6))
 9          IF(VISW.EQ.0.) GO TO 888
10          READ(5,12)(VIS(I),I=1,6)
11       12 FORMAT(6(D12.5))
12          WRITE(6,6)
13        6 FORMAT(1H1)
14          WRITE (6,8) D, L
15        8 FORMAT(/////,10X,'POLYOX COAG. IN DISTILLED WATER'
           1,2X,'DIAM = ',F7.5,5X,'LENGTH = ',F5.1,////)
16          DO 200  I=1,6
17          READ(5,2) (P(I,J), J=1,7)
18        2 FORMAT (7(F6.3,2X))
19      200 READ(5,20) (W(I,J),J=1,7)
20       20 FORMAT (7(F8.4,2X))
21          DO 111 I=1,6
22      111 WRITE(6,13) (W(I,J),J=1,7),(P(I,J),J=1,7)
23       13 FORMAT(//10X,'W  = ',7(F8.4,2X),//10X,'P  = ',
           17(F8.4,2X),//)
24          WRITE(6,6)
25          DO 100  I=1, 6
26          DO 700 J=1,7
27          WS(J)=W(I,J)
28      700 PS(J)=P(I,J)
29          CALL BESFIT (WS, PS, 7, SLOPE )
30          S(I)=SLOPE
31          DO 999 J=1, 7
32          ST(I,J)= DEN*980.665*D/4./L*P(I,J)
```

```
33            SR(I,J)= 32.0*W(I,J)/D/D/(D*6).*3.14159*DEN)
34            SRW(I,J)= ST(I,J)/VISW
35            RE(I,J)= 4.0*W(I,J)/(D*3.14159)/(VIS(I)*VISW)/60.
36          999 CONTINUE
37            B(I)=980.665*60.*3.14159*DEN*DEN*D**4*S(I)/
             1(128.*VISW*L)
38            UW(I)=(VIS(I)/B(I)-1.)/4.
39            WRITE (6,3) CON(I), VIS(I)
40            3 FORMAT (//1X,'CONC = ', F4.0,'PPM',5X,'VISCOSITY = '
              1,1PD12.5,/)
41            WRITE (6,4) (ST(I,J), J=1, 7), (SR(I,J), J=1, 7),
              1(SRW(I,J), J=1,7), (RE(I,J), J=1,7)
42            4 FORMAT (1X,'SHEAR STRESS = ',7(1PD10.3,2X)/1X,
              1'SHEAR RATE   = ',7(1PD10.3,2X)/1X,'--- WATER       ',
              27(1PD10.3,2X)/1X,'REYNOLDS NO  = ',7(1PD10.3,2X))
43          100 CONTINUE
44            WRITE (6,18)(S(I),I=1,6)
45            18 FORMAT(//1X,'SLOPE              =',6(1PD12.5,2X),/  )
46            WRITE (6,17) (B(I), I=1, 6)
47            17 FORMAT (/1X,'COEFFICIENTS B =',6(1PD12.5,2X))
48            WRITE(6,27) (UW(I),I=1,6)
49            27 FORMAT(//,13X,'UW =', 6(1PD12.5,2X))
50          888 WRITE(6,6)
51            STOP
52            END

53            SUBROUTINE BESFIT (X,Y,NDATA,SLOPE )
          C
54            DIMENSION X( 7),Y( 7)
55            DOUBLEPRECISION A,B,C,D,X,Y,SLOPE
56            A=0.0
57            B=0.0
58            C=0.0
59            D=0.0
60            DO 100 I=1,NDATA
61            A=A+X(I)
62            B=B+Y(I)
63            C=C+X(I)*X(I)
64          100 D=D+X(I)*Y(I)
65            SLOPE=D/C
66            RETURN
67            END

          $ENTRY
```

Appendix 3

Determination of $\tilde{\delta}_a$ dependence

The velocity profile in the anomalous zone is shown in Eq. (3.2-15), or in the following general form:

$$\bar{u} = \bar{u}\,(n, \bar{\Delta}, \tilde{y}). \qquad \text{(A.3-1)}$$

The concentration in the concentrated layer is represented by Eq. (3.6-1). Multiplication of Eq. (3.6-4) by Eq. (3.4-3) gives

$$\frac{\eta_c}{\eta_s} = \frac{\left[1 + c\,[\eta]/(1-K_H c\,[\eta])\right](1-\tilde{y}\bar{\Delta})}{\left[(n+1) - n\bar{\Delta}\right]\tilde{y}^n - \left[n - (n-1)\bar{\Delta}\right]\tilde{y}^{n+1}}\,, \qquad \text{(A.3-2)}$$

or in general form,

$$\eta_c/\eta_s = F(K_H, c, [\eta], n, \bar{\Delta}, \tilde{y}). \qquad \text{(A.3-3)}$$

Therefore Eq. (3.6-1) can be expressed as

$$c_c = G(K_H, c, [\eta], n, \bar{\Delta}, \tilde{y}). \qquad \text{(A.3-4)}$$

Eq. (3.6-1) is rewritten for c_c/c as follow:

$$c_c/c = \frac{\eta_c/\eta_s - 1}{c[\eta]\left[1 + K_H(\eta_c/\eta_s - 1)\right]}\,. \qquad \text{(A.3-5)}$$

Since c and $[\eta]$ also enter in η_c/η_s as a single variable in the form of $c\,[\eta]$, it is concluded that

$$c_c/c = G'(c[\eta], K_H, n, \bar{\Delta}, \tilde{y}). \qquad \text{(A.3-6)}$$

Now the adsorption zone thickness in dimensionless form is given by Eq. (3.7-2). In view of the above determined dependence of $\overline{u^{<}}$ and c_c/c, the dependence of $\tilde{\delta}_a$ must be given by

$$\tilde{\delta}_a = \tilde{\delta}_a(c[\eta],\ K_H,\ n,\ \bar{\Delta}). \qquad \text{(A.3-6)}$$

Assuming K_H is a universal constant for a given polymer homologues (for Polyox, K_H=0.36),

$$\tilde{\delta}_a = \tilde{\delta}_a(c[\eta],\ n,\ \bar{\Delta}). \qquad \text{(A.3-7)}$$

The variation of $\tilde{\delta}_a$ with $\bar{\Delta}$ is proved to be negligible in the range of $\bar{\Delta} << 1$ to give

$$\tilde{\delta}_a = \tilde{\delta}_a(c[\eta],\ n). \qquad \text{(A.3-8)}$$

As it is indicated, $\tilde{\delta}_a$ can be evaluated for a given value of n in any polymer solutions in which c and $[\eta]$ are known.

Appendix 4

Determination of n and $\bar{\Delta}$ dependence

The porosity in the adsorption zone is given by Eq. (3.4-9) with Eq. (3.4-8) for $\alpha(\varepsilon)$ and Eq. (3.4-3) for η_r. Thus the porosity distribution can be represented as

$$\varepsilon = \varepsilon(\tilde{y},\ n,\ \bar{\Delta},\ c[\eta],\ \tilde{D}_e)\,. \qquad \text{(A.4-1)}$$

Eq. (3.5-7) also gives

$$\varepsilon = \varepsilon(c_a,[\eta])\,. \qquad \text{(A.4-2)}$$

Combination of Eq. (A.4-1) and Eq. (A.4-2) gives the expression of polymer concentration in the adsorption zone as follow:

$$c_a[\eta] = c_a[\eta]\,(\tilde{y},\ n,\ \bar{\Delta},\ c[\eta],\ \bar{D}_e)\,. \qquad \text{(A.4-3)}$$

It is found in Eq. (A.3-6) that

$$c_c/c = \frac{c_c[\eta]}{c[\eta]} = G'(c[\eta],\ n,\ \bar{\Delta},\ \tilde{y}) \text{ or}$$

$$c_c[\eta] = c_c[\eta]\,(\tilde{y},\ n,\ \bar{\Delta},\ c[\eta])\,. \qquad \text{(A.4-4)}$$

At the interface between adsorption zone and concentrated layer, i.e. $\tilde{y} = \tilde{\delta}_a = \tilde{\delta}_a\ (n,\ c[\eta])$,

$$c_a[\eta] = c_a[\eta](n,\ \bar{\Delta},\ c[\eta],\ \bar{D}_e)\,,$$

and $$c_c[\eta] = c_c[\eta](n,\ \bar{\Delta},\ c[\eta])\,.$$

Equating the polymer concentration on either side of the interface,

$$c_a[\eta](n, \bar{\Delta}, c[\eta], \bar{D}_e) = c_c[\eta](n, \bar{\Delta}, c[\eta]). \quad (A.4\text{-}5)$$

Eq. (3.3-3) can be used to express $\bar{\Delta}$ in terms of n and $\bar{u}_w$ as follow:

$$\bar{\Delta} = \bar{\Delta}(n, \bar{u}_w). \quad (A.4\text{-}6)$$

Substituting Eq. (A.4-6) into Eq. (A.4-5),

$$c_a[\eta](n, \bar{u}_w, c[\eta], \bar{D}_e) = c_c[\eta](n, \bar{u}_w, c[\eta]),$$

which can be solved for n as

$$n = n(c[\eta], \bar{u}_w, \bar{D}_e).$$

Thus n can be determined as a function of $c[\eta]$, $\bar{u}_w$ and $\bar{D}_e$, which are amenable to the experimental measurement. Once n is decided, $\bar{\Delta}$ can be evaluated subsequently by Eq. (A.4-6).

```
      C
      C   EVALUATION OF CHARACTERISTICS IN THE ANOMALOUS ZONE
      C
      C
      C       DP     = EFFECTIVE DIAMETER OF POLYMER MACROMOLECULE OR
      C                ROOT MEAN SQ. END TO END DISTANCE, CM
      C       VIN    = INTRINSIC VISCOSITY
      C       KH     = HUGGINS CONSTANT
      C       DIA    = TUBE DIAMETER, CM
      C       C      = SOLUTION CONCENTRATION, PPM
      C       UE     = AVERAGE VELOCITY DEFICIENCY(EXPERIMENTAL VALUE)
      C       N      = ADSORPTION INDEX
      C       DA     = ADSORPTION ZONE THICKNESS(DIMENSIONLESS FORM
      C                OVER ANOMALOUS ZONE THICKNESS)
      C       D = DEL = ANOMALOUS ZONE THICKNESS(DIMENSIONLESS FORM
      C                OVER TUBE RADIUS)
      C       NR     = RELATIVE VISCOSITY OF SOLUTION
      C       UW     = AVERAGE VELOCITY DEFICIENCY(CALCULATED VALUE)
      C       ADC    = CONCENTRATED FLUID LAYER, CM
      C       DC     = DIMENSIONLESS FORM, ADC/D
      C       Y      = DISTANCE FROM THE WALL
      C       CC     = CONCENTRATION AT THE INTERFACE BETWEEN ADSORPTION
      C                ZONE AND CONCENTRATED LAYER(DIMENSIONLESS
      C                FORM OVER BULK SOLUTION CONCENTRATION)
      C       E      = POROSITY IN THE ADSORPTION ZONE
      C       ALPH   = CONSTANT DEFINED IN EQ.(3.4-7)
      C       U      = VELOCITY PROFILE, CM/SEC.
      C
      C
 1          DOUBLE PRECISION  CIN,E,FB,CN,DEL,N,D,A,B,NEG,POS,
           1UW,K1,K2,K3,K4,NR,C1,C2,C3,C4,KH,DABS,UE,S,C,DA,
           2AS,BS,SS,NEGS,POSS,DIA,SIMPS,DC,CD,Y,NCS,CC,SA1,
           3SA2,SA3,PPOS,NNEG,SA,SB,DR,DRR,DP,DPR,ADC,VIN,U
 2          COMMON N,D,NR,C1,C2,C3,C4,CIN,KH,U
 3          EXTERNAL FB
 4          WRITE(6,7)
 5          READ(5,6) DP, VIN
 6        6 FORMAT(D12.5,2X,D10.3)
 7          KH=0.36D 00
 8        7 FORMAT(1H1)
 9       56 READ(5,4) DIA
10        4 FORMAT(    D12.5)
11          IF(DIA.LE.0) GO TO 3000
12          NN=0
13       55 READ(5,5) C,UE
14        5 FORMAT(D9.2,5X,D12.5)
15          CIN=C*1.D-4* VIN
      C
      C   EVALUATION OF N USING ROOT OF EQUATION
16          N=1.D 01
17          MM=0
      C
      C  EVALUATION OF THE ADSORBED SUBLAYER,  DA
18       99 DA=1.D0
19          D=1.D-04
20          C1=((N+1)-N*D)/(N+1)
21          C2=((N-1)*D-N)/(N+2)
22          NR=1+CIN/(1-KH*CIN)
23          C3=(N+1)-N*D
```

```
24            C4=N-(N-1)*D
25            MS=0
26            BS=1
27            SA1=C1*D/(N+2)
28            SA2=(C2*D-C1*D*D)/(N+3)
29            SA3=C2*D*D/(N+4)
30            SA=SA1+SA2-SA3
31         80 AS=DA
32            SB=SIMPS(AS,BS,FB)
      C
      C ROOT OF EQUATION FOR DA
33            SS=SB-SA
34            IF(SS)1,2,3
35          2 GO TO 1000
36          1 NEGS=DA
37            GO TO 70
38          3 POSS=DA
39         70 MS=MS+1
40            IF(MS.GE.2) GO TO 57
41            IF(N.LT.100) GO TO 66
42            IF(N.LT.1.5D4) GO TO 77
43            DA=0.999 D0
44            GO TO 80
45         77 DA=0.99D0
46            GO TO 80
47         66 DA=0.90D0
48            GO TO 80
49         57 IF(DABS(POSS-NEGS).LT.1.D-10) GO TO 1000
50            DA=(NEGS+POSS)/2
51            GO TO 80
52       1000 DEL=0.1D-5
      C
      C  EVALUATION OF DEL
53            M=0
54         90 A=DEL
55            DPR=DP*2/DIA
56            S=CN(A,DA, CIN,KH,N,DPR)
      C
      C  ROOT OF EQUATION FOR DEL
57            IF(S) 11,22,33
58         22 GO TO 2000
59         11 NEG=DEL
60            GO TO 100
61         33 POS=DEL
62        100 M=M+1
63            IF(M.GE.2) GO TO 44
64            DEL=0.5
65            GO TO 90
66         44 IF(DABS(POS-NEG).LT.1.D-9 )GO TO 2000
67            DEL=(POS+NEG)/2
68            GO TO 90
69       2000 K1=N/(N+2)
70            K2=(3*N*N+6*N-1)/(2*(N+1)*(N+3))
71            K3=(N*N+3*N-2)/((N+3)*(N+4))
72            K4=(N-1)*(N+2)/(4*(N+3)*(N+4))
73            UW=(-K1)*DEL*(1-K2*DEL+K3*DEL*DEL-K4*DEL**3)
74            S=DABS(UW)-DABS(UE)
75            IF(S) 110,222,333
76         222 GO TO 10
77         110 NNEG=N
```

```
 78          GO TO 200
 79      333 PPOS=N
 80      200 MM=MM+1
 81          IF(MM.GE.2) GO TO 444
 82          N=0.4D 05
 83          GO TO 99
       C
       C  ROOT OF EQUATION FOR N
 84      444 IF(DABS(S).LE.1.0D-06) GO TO 10
 85          N=(PPOS+NNEG)/2
 86          GO TO 99
 87       10 DC=1.D0-DA
 88          D=DEL
 89          Y=DA
 90          C3=(N+1)-N*D
 91          C4=N-(N-1)*D
 92          NCS=NR*(1-Y*D)/(C3*Y**N-C4*Y**(N+1))
 93          CC=(NCS-1)/(CIN*(1+KH*(NCS-1)))
 94          E=1.D0-1.5D0*CC*CIN
 95          CD=CC*DC
 96          DR=D/DPR
 97          DRR=D*2/DIA
 98          DZ=DRR/DP
 99          ADC=DC*D*DIA/2
100          WRITE(6,9)DIA,C,N,D,DA,UW,UE,DC,CC,CD,DR,DRR,ADC,E
101        9 FORMAT(     //////,30X,'DIA   = ',F 8.5,//,
             C30X,'CON   = ',D15.8,'  PPM',//,
             C30X,'N     = ',D15.8,//,
             C30X,'DEL   = ',D15.8,//,
             C30X,'DA    = ',D15.8,//,
             C30X,'UW    = ',D15.8,//,
             C30X,'UE    = ',D15.8,//,
             C30X,'DC    = ',D15.8,//,
             C30X,'CC    = ',D15.8,//,
             C30X,'CD    = ',D15.8,//,
             C30X,'DR    = ',D15.8,//,
             C30X,'DRR   = ',D15.8,//,
             C30X,'ADC   = ',D15.8,//
             C30X,'E     = ',D15.8,//)
102          WRITE(6,7)
103          NN=NN+1
104          IF(NN.LT.6) GO TO 55
105          GO TO 56
106     3000 WRITE(6,7)
107          STOP
108          END

109          FUNCTION CN(D,Y,CIN,KH,N,DIA)
       C
       C EVALUATION OF THE PERMEABILITY
110          DOUBLE PRECISION NR,CIN,KH,C3,N,C4,D,NCS,Y,CC,DS,
            1DIA,E,ALPH,A2,A3,A4,B0,B1,B2,L1,L2,L,R,RS,CN
111          NR=1+CIN/(1-KH*CIN)
112          C3=(N+1)-N*D
113          C4=N-(N-1)*D
114          NCS=NR*(1-Y*D)/(C3*Y**N-C4*Y**(N+1))
115          CC=(NCS-1)/      (1+KH*(NCS-1))
116          DS=DIA/D
117          E=1-1.5  *CC
118          ALPH=4*(1-E)**0.6/(E**1.92)
```

```
119           A2=C3/(N+1)
120           A3=C4/(N+2)
121           B0=N*C3
122           B1=(N+1)*(N+(2-N*D)*D)
123           B2=D*(N+2)*C4
124           L1=(1-Y*D)*(A2*Y*Y-A3*Y**3)
125           L2=B0-B1*Y+B2*Y*Y+2*NR*D*(1-Y*D)*Y**(1-N)
126           L=L1/L2
127           R=DS/(2*ALPH)
128           RS=R*R
129           CN=L-RS
130           RETURN
131           END

132           FUNCTION SIMPS(A,B,F)
      C
      C SIMPSON'S RULE BY REPEATED SUBDIVISION OF THE INTERVAL
133           DOUBLE PRECISION H,A,B,F,SUM1,TSUM1,SUM2,SUM21,
             1DABS,SIMPS,TSUM21
134           H=B-A
135           IF((B-A).GT.0) GO TO 40
136           TSUM21=0
137           GO TO 5
138        40 SUM1=F(A)+F(B)
139           TSUM1=SUM1*H/3
140           M=1
141         1 H=H/2
142           M=M*2
143           SUM2=0
144           J=1
145         4 SUM2=SUM2+2*F(A+J*H)
146           IF(J+1-M) 2,3,3
147         2 J=J+2
148           GO TO 4
149         3 SUM21=SUM1+SUM2*2
150           SUM1=SUM1+SUM2
151           TSUM21=SUM21*H/3
152           IF(DABS(TSUM21-TSUM1)-1.D-8 )5,6,6
153         6 TSUM1=TSUM21
154           GO TO 1
155         5 SIMPS=TSUM21
156           RETURN
157           END

158           FUNCTION FB(Y)
      C
      C FUNCTION FB
159           DOUBLE PRECISION NCS,NR,Y,D,C1,C2,C3,C4,N,CC,CIN,
             1KH,U,FB
160           COMMON N,D,NR,C1,C2,C3,C4,CIN,KH,U
161           NCS=NR*(1-Y*D)/(C3*Y**N-C4*Y**(N+1))
162           CC=(NCS-1)/(CIN*(1+KH*(NCS-1)))
163           U=D*(C1*Y**(N+1)+C2*Y**(N+2))
164           FB=CC*U*(1-Y*D)
165           RETURN
166           END

      $ENTRY
```

Appendix 5

Evaluation of $\bar{\Delta}_\infty$, n' and α in Eq. (5.5-1)

For the application to the least squares fitting, Eq. (5.5-1) is transformed into a standard simple form:

$$Y = A + BX.$$

Let $\bar{\Delta}/\bar{\Delta}_\infty = DR$, and rearranging Eq. (5.5-1),

$$(1/DR - 1) = \alpha(1/c^{n'}). \qquad \text{(A.5-1)}$$

Taking logarithms of both sides of Eq. (A.5-1),

$$\ln(1/DR - 1) = \ln \alpha - n' \ln c. \qquad \text{(A.5-2)}$$

This may be put into the desired form by placing,

$$\ln(1/DR - 1) = Y$$

$$\ln c = X$$

$$\ln \alpha = A$$

$$-n' = B.$$

Therefore the constants, A and B, are obtained by solving two normal equations:

$$A = \frac{\Sigma X_i^2 \, \Sigma Y_i - \Sigma X_i \, \Sigma(X_i Y_i)}{k \, \Sigma X_i^2 - (\Sigma Y_i)^2}$$

$$B = \frac{k \, \Sigma X_i Y_i - \Sigma Y_i \Sigma X_i}{k \, \Sigma X_i^2 - (\Sigma Y_i)^2} .$$

The above procedure is repeated with varing $\bar{\Delta}_\infty$ until the minimum standard deviation is obtained.

```
C
C   CORRELATION BETWEEN ANOMALOUS ZONE THICKNESS AND
C   SOLUTION CONCENTRATION
C
C
C       DEL    = ANOMALOUS ZONE THICKNESS
C       DMAX   = MAXIMUM(LIMITING) ANOMALOUS ZONE THICKNESS
C       DM     = INCREMENT
C       CON    = SOLUTION CONCENTRATION, PPM
C
C
 1          DIMENSION CON(60),DEL(60),DR(60)
 2          DOUBLE PRECISION DM,DMAX,DD,DR,X,Y,A,B,C,D,AA,BB,
           1CC,E,SLOPE,INT,CN,ALPH,DLOG,DEXP,CON,DEL,C1,D1,DRC
           2,DR1,Y2,YY,SY,SD,DSQRT,DABS,SY1
 3          WRITE(6,6)
 4          N=6
 5       20 READ(5,2) DMAX, DM
 6        2 FORMAT(D12.5,2X,D8.1)
 7          IF(DMAX.EQ.0.) GO TO 30
 8          DO 100 I=1, N
 9          READ(5,1) CON(I), DEL(I)
10        1 FORMAT(D9.2,1X,D12.5)
11      100 CONTINUE
12          NN=1
13       10 IF(NN.EQ.11)GO TO 20
14          A=0.
15          B=0.
16          C=0.
17          D=0.
18          WRITE(6,6)
19        6 FORMAT(1H1)
20          WRITE(6,4)     DMAX
21        4 FORMAT(///,5X,'DEL AT MAXIMUM OF TUBE',I2,' = ',D12.5,/)
22          DO 400 I=1, N
23          DR(I)=DEL(I)/DMAX
24          DD=1/DR(I)-1.
25          Y=DLOG(DD)
26          X=DLOG(CON(I))
27          A=A+X
28          B=B+Y
29          C=C+X*X
30      400 D=D+X*Y
31          E=N
32          AA=(E*D-A*B)
33          BB=(C*B-A*D)
34          CC=(E*C-A*A)
35          SLOPE=AA/CC
36          INT=BB/CC
37          CN=(-SLOPE)
38          ALPH=DEXP(INT)
39          WRITE(6,5) ALPH,CN
40        5 FORMAT(///,5X,'ALPH = ',D12.5,//5X,'CN   = ',
           1D12.5,///)
41          SY=0.0
42          DO 200 I=1,N
43          C1=CON(I)
44          D1=DEL(I)
45          DR1=DR(I)
```

```
46            DRC=C1**CN/(ALPH+C1**CN)
47            YY=DABS(DRC-DR1)
48            Y2=YY *YY
49            SY=SY+Y2
50            WRITE(6,3) C1,D1,DR1,DRC
51          3 FORMAT(  5X,4(D12.5,3X),/)
52        200 CONTINUE
53            SY1=SY/(N -2)
54            SD=DSQRT(SY1)
55            WRITE(6,8) SD
56          8 FORMAT(/  ,5X,'STANDARD DEVIATION = ',D13.6)
57            NN=NN+1
58            DMAX=DMAX+DM
59            GO TO 10
60         30 WRITE(6,6)
61            STOP
62            END

      $ENTRY
```

Appendix 6

Evaluation of a_1, b_1 and c_1 in Eq. (5.5-5)

Taking logarithms of both sides of Eq. (5.5-5) for the least squares fitting,

$$\ln \bar{\Delta}_\infty = \ln a_1 + b_1 \ln [\eta] + c_1 \ln D. \qquad (A.6\text{-}1)$$

Now, let $\ln [\eta] = X$

$\ln D = Z$

$\ln \bar{\Delta}_\infty = Y$

$\ln a_1 = A$

$b_1 = B$

$c_1 = C.$

So, $Y = A + BX + CZ$, which is linear in X, Z and Y.

Thus the desired values of a_1, b_1 and c_1 can be obtained by solving three normal equations:

$$kA + (\Sigma X_i)B + (\Sigma Z_i)C = \Sigma Z_i$$

$$(\Sigma X_i)A + (\Sigma X_i^2)B + (\Sigma X_i Z_i)C = \Sigma X_i Y_i$$

$$(\Sigma Z_i)A + (\Sigma X_i Z_i)B + (\Sigma Z_i^2)C = \Sigma Z_i Y_i$$

```
      C  CORRELATION OF DMAX WITH INTRINSIC VISCO. AND TUBE DIAM.
      C
      C
      C      VIN    = INTRINSIC VISCOSITY
      C      DIA    = TUBE DIAMETER, CM
      C      DMAX   = MAXIMUM ANOMALOUS ZONE THICKNESS
      C
      C
 1            DIMENSION A(10,10),ADIA(20),AVIN(20),ADMAX(20),
             1XX(3),CDMAX(20)
 2            DOUBLE PRECISION A,DIA,VIN,DMAX,NN,X,Y,Z,SX,SXX,
             1SXY,SXZ,SY,SYZ,SZ,SZZ,ADIA,ADMAX,AVIN,XX,AX,BX,CX
             2,CDMAX,DLOG
 3            COMMON A,XX, N,M,N1
 4            SX=0.
 5            SXX=0.
 6            SY=0.
 7            SXY=0.
 8            SZ=0.
 9            SYZ=0.
10            SXZ=0.
11            SZZ=0.
12            NN=0
13            WRITE(6,3)
14          3 FORMAT(1H1,/////)
15         31 IF(NN.GE.20) GO TO 32
16            READ(5,11) VIN,DIA,DMAX
17         11 FORMAT(3(D12.5,3X))
18            I=NN+1
19            ADIA(I)=DIA
20            AVIN(I)=VIN
21            ADMAX(I)=DMAX
22            X=DLOG(VIN)
23            Y=DLOG(DMAX)
24            Z=DLOG(DIA)
25            SX=SX+X
26            SXX=SXX+X*X
27            SXY=SXY+X*Y
28            SXZ=SXZ+X*Z
29            SY=SY+Y
30            SYZ=SYZ+Y*Z
31            SZ=SZ+Z
32            SZZ=SZZ+Z*Z
33            NN=NN+1
34            GO TO 31
35         32 A(1,1)=NN
36            A(1,2)=SX
37            A(1,3)=SZ
38            A(1,4)=SY
39            A(2,1)=SX
40            A(2,2)=SXX
41            A(2,3)=SXZ
42            A(2,4)=SXY
43            A(3,1)=SZ
44            A(3,2)=SXZ
45            A(3,3)=SZZ
46            A(3,4)=SYZ
47            CALL MATRIX
```

```
48            CALL SOLUTS
49            AX=XX(1)
50            BX=XX(2)
51            CX=XX(3)
52            K=NN
53            DO 100 I=1,K
54            CDMAX(I)=AX*AVIN(I)**BX*ADIA(I)**CX
55          100 WRITE(6,4) AVIN(I),ADIA(I),ADMAX(I),CDMAX(I)
56            4 FORMAT(     5X,4(D12.5,5X),/)
57            WRITE(6,3)
58            STOP
59            END

60            SUBROUTINE MATRIX
      C
      C   GAUSS ELIMINATION MATHOD PART 1
61            DIMENSION A(10,10),X(3)
62            DOUBLE PRECISION A,X
63            COMMON A,X   ,N,M,N1
64           21 FORMAT(1H1,/5X,'ORIGINAL MATRIX', 6X,I6,//)
65           22 FORMAT(5X,4(D11.4,3X),//)
66           23 FORMAT(5X,'NEW MATRIX',//)
67            N=3
68            M=4
69            WRITE(6,21) N
70            DO 100 I=1,N
71          100 WRITE(6,22) (A(I,J),J=1,M)
72            N1=N-1
73            DO 200 L=1,N1
74            I1=L+1
75            DO 200 I=I1,N
76            J1=L+1
77            DO 200 J=J1,M
78          200 A(I,J)=A(I,J)-A(I,L)*A(L,J)/A(L,L)
79            WRITE(6,23)
80            DO 300 I=1,N
81          300 WRITE(6,22) (A(I,J),J=1,M)
82            RETURN
83            END

84            SUBROUTINE SOLUTS
      C
      C   GAUSS ELIMINATION MATHOD PART 2, SOLUTION
85            DIMENSION A(10,10),X(3)
86            DOUBLE PRECISION A, X,DEXP
87            COMMON A,X   ,N,M,N1
88           10 FORMAT(////,5X,'SOLUTION',//)
89           11 FORMAT(5X,D11.4,/)
90            X(3)=A(N,M)/A(N,N)
91            X(2)=(A(2,4)-A(2,3)*X(N))/A(2,2)
92            X(1)=(A(1,4)-A(1,2)*X(2)-A(1,3)*X(3))/A(1,1)
93            X(1)=DEXP(X(1))
94          600 WRITE(6,10)
95            WRITE(6,11)(X(I),I=1,N)
96            WRITE(6,3)
97            3 FORMAT(1H1)
98            RETURN
99            END

      $ENTRY
```

Appendix 7

Evaluation of a', b' and c' in Eq. (5.8-1)

With the same procedure as in Appendix 6, Eq. (5.8-1) is transformed into the equation,

$$\ln DR = \ln a' + b' \ln \bar{\Delta} + c' \ln(D_e/D). \qquad (A.7\text{-}1)$$

Setting $\ln \bar{\Delta} = X$,

$\ln DR = Y$,

$\ln(D_e/D) = Z$,

$\ln a' = A$,

$b' = B$,

and $c' = C$,

one get

$$Y = A + BX + CZ,$$

which is linear in X, Z and Y.

The three normal equations are given in Appendix 6 for the evaluation of the desired constants, a', b' and c'.

```
C   CORRELATION OF DEL WITH DRAG REDUCTION
C
C
C      RE     = REYNOLDS NUMBER
C      DP     = EFFECTIVE DIAMETER OF POLYMER MACROMOLECULE
C               OR SQ. ROOT END TO END DISTANCE, CM
C      D      = TUBE DIAMETER, CM
C      DEL    = ANOMALOUS ZONE THICKNESS(DIMENSIONLESS FORM
C               OVER TUBE RADIUS)
C      DR     = DRAG REDUCTION
C
C
      DIMENSION A(10,10),ADP(20),AD(20),ADEL(20),ADR(20),
     1XX(3),CDR(20)
      DOUBLE PRECISION A,DP,NN ,X,Y,Z,SX,SXX,SXY,SXZ,SY,
     1SYZ,SZ,SZZ,DEL,DR,D,DPR,ADP,AP,ADEL,ADR,XX,AX,BX,
     2CX,CDR,RE
      COMMON A,XX,RE,N,M,N1
      MM=0
   33 IF(MM.EQ.1) GO TO 44
      SX=0.
      SXX=0.
      SY=0.
      SXY=0.
      SZ=0.
      SYZ=0.
      SXZ=0.
      SZZ=0.
      NN=0
      WRITE(6,3)
    3 FORMAT(1H1,/////)
      READ(5,1) RE
    1 FORMAT(D9.2)
   31 IF(NN.GE.16) GO TO 32
      READ(5,11) DP,D,DEL,DR
   11 FORMAT(4(D12.5,2X))
      I=NN+1
      ADP(I)=DP
      AD(I)=D
      ADEL(I)=DEL
      ADR(I)=DR
      X=DLOG(DEL)
      Y=DLOG(DR)
      DPR=DP/R
      Z=DLOG(DPR)
      SX=SX+X
      SXX=SXX+X*X
      SXY=SXY+X*Y
      SXZ=SXZ+X*Z
      SY=SY+Y
      SYZ=SYZ+Y*Z
      SZ=SZ+Z
      SZZ=SZZ+Z*Z
      NN=NN+1
      GO TO 31
   32 A(1,1)=NN
      A(1,2)=SX
      A(1,3)=SZ
```

```
44            A(1,4)=SY
45            A(2,1)=SX
46            A(2,2)=SXX
47            A(2,3)=SXZ
48            A(2,4)=SXY
49            A(3,1)=SZ
50            A(3,2)=SXZ
51            A(3,3)=SZZ
52            A(3,4)=SYZ
53            CALL MATRIX
54            CALL SOLUTS
55            AX=XX(1)
56            BX=XX(2)
57            CX=XX(3)
58            K=NN
59            WRITE(6,6) RE
60          6 FORMAT(///,5X, 'RE   = ',D9.2,//)
61            DO 100 I=1,K
62            CDR(I)=AX*ADEL(I)**BX*(ADP(I)/AD(I))**CX
63        100 WRITE(6,4) ADP(I),AD(I),ADEL(I),CDR(I),ADR(I)
64          4 FORMAT(     5X,5(D12.5,5X),/)
65            MM=MM+1
66            GO TO 33
67         44 WRITE(6,3)
68            STOP
69            END

70            SUBROUTINE MATRIX
      C
      C   GAUSS ELIMINATION MATHOD PART 1
71            DIMENSION A(10,10),X(3)
72            DOUBLE PRECISION A,X,RE
73            COMMON A, X,RE,N,M,N1
74         21 FORMAT(1H1,/5X,'ORIGINAL MATRIX', 6X,I6,//)
75         22 FORMAT(5X,4(D11.4,3X),//)
76         23 FORMAT(5X,'NEW MATRIX',//)
77            N=3
78            M=4
79            WRITE(6,21) N
80            DO 100 I=1,N
81        100 WRITE(6,22) (A(I,J),J=1,M)
82            N1=N-1
83            DO 200 L=1,N1
84            I1=L+1
85            DO 200 I=I1,N
86            J1=L+1
87            DO 200 J=J1,M
88        200 A(I,J)=A(I,J)-A(I,L)*A(L,J)/A(L,L)
89            WRITE(6,23)
90            DO 300 I=1,N
91        300 WRITE(6,22) (A(I,J),J=1,M)
92            RETURN
93            END

94            SUBROUTINE SOLUTS
      C
      C   GAUSS ELIMINATION MATHOD PART 2, SOLUTION
95            DIMENSION A(10,10),X(3)
96            DOUBLE PRECISION A, X,DEXP,RE
97            COMMON A, X,RE,N,M,N1
```

```
 98            WRITE(6,6) RE
 99          6 FORMAT(///,5X, 'RE  = ',D9.2,///)
100         10 FORMAT(////,5X,'SOLUTION',//)
101         11 FORMAT(5X,D11.4,/)
102            X(3)=A(N,M)/A(N,N)
103            X(2)=(A(2,4)-A(2,3)*X(N))/A(2,2)
104            X(1)=(A(1,4)-A(1,2)*X(2)-A(1,3)*X(3))/A(1,1)
105            X(1)=DEXP(X(1))
106        600 WRITE(6,10)
107            WRITE(6,11)(X(I),I=1,N)
108            WRITE(6,3)
109          3 FORMAT(1H1)
110            RETURN
111            END

       $ENTRY
```

Appendix 8

Evaluation of the porosity distribution in the adsorption zone

The porosity distribution is given by Eq. (3.4-9). When $\overline{\Delta}$, n, $\tilde{D}_e$, c and $[\eta]$ are known, ε can be evaluated by the numerical method as a function of $\tilde{y}$.

```
C
C   POROCITY DISTRIBUTION IN THE ADSORPTION ZONE
C
C
C       DP      = EFFECTIVE DIAMETER OF POLYMER MACROMOLECULE
C       VIN     = INTRINSIC VISCOSITY
C       DIA     = TUBE DIAMETER
C       C       = SOLUTION CONCNENTRATION, PPM
C       N       = ADSORPTION INDEX
C       D       = ANOMALOUS ZONE THICKNESS
C       DA      = ADSORPTION ZONE THICKNESS
C       Y       = DISTANCE FROM THE WALL
C       Y1      = LOW LIMIT OF Y
C       KH      = HUGGINS CONSTANT
C       NR      = RELATIVE VISCOSITY
C       YO      = DISTANCE FROM THE WALL IN TERMS OF
C                 MCROMOLECULAR DIAMETER
C       E       = POROSITY
C
C
 1          DOUBLE PRECISION DIA,DP,N,D,C,DA,KH,DS,CIN,Y,YY,H,
           1K,YO,YDA,NR,CA,C3,C4,B0,B1,B2,A2,A3,L1,L2,LL,E,ALPH
           2,R,RR,S,NEG,POS,DABS,Y1,NC,NCS,CC,VIN
 2          J=0
 3        9 READ(5,17) DP,VIN
 4       17 FORMAT(2(D12.5,2X))
 5          J=J+1
 6          IF(J.EQ.4) GO TO 16
 7          I=0
 8       15 READ(5,1)DIA
 9        1 FORMAT(D12.5)
10          I=I+1
11          WRITE(6,7)
12        7 FORMAT(1H1)
13          WRITE(6,6)
14        6 FORMAT(/////////,10X,'TUBE',/)
15          M=0
16       12 READ(5,2) C,N,D,DA,Y1
17        2 FORMAT(D8.1,2X, 2(D12.5,2X),D15.8,2X,D12.5)
18          IC=C
19          WRITE(6,3)IC,N,D,DA
20        3 FORMAT(10X,'CON= ',I3,' PPM',//,10X,'    = ',D12.5,//,
           110X,'    = ',D12.5,//,10X,'    = ',D12.5,////)
21          KH=0.36D 00
22          CIN=C*1.D-04* VIN
23          C3=(N+1)-N*D
24          C4=N-(N-1)*D
25          B0=N*C3
26          B1=(N+1)*(N+(2-N*D)*D)
27          B2=D*(N+2)*C4
28          A2=C3/(N+1)
29          A3=C4/(N+2)
30          NR=1+CIN/(1-KH*CIN)
31          DS=DP*2./(D*DIA)
32          K=0
33          H=(DA-Y1)/9
34       13 Y=Y1+H*K
35          YO=Y/DS
36          YDA=Y/DA
```

```
37            MM=0
38            L1=(1-Y*D)*(A2*Y**2-A3*Y**3)
39            L2=B0-B1*Y+B2*Y*Y+2*NR*D*(1-Y*D)*Y**(1-N)
40            LL=L1/L2
41            E=1.D0-1.D-15
42         11 ALPH=4*(1.D0-E)**0.6/E**1.92
43            R=DS/(2*ALPH)
44            RR=R*R
45            S=LL-RR
      C
      C   ROOT OF EQUATION FOR E
      C
46            IF(S) 10,20,30
47         20 GO TO 100
48         10 NEG=E
49            GO TO 40
50         30 POS=E
51         40 MM=MM+1
52            IF(MM.GE.2) GO TO 50
53            E=1.D-15
54            GO TO 11
55         50 IF(DABS(POS-NEG).LT.1.D-8) GO TO 100
56            E=(POS+NEG)/2
57            GO TO 11
58        100 CA=(1.-E)/(1.5*CIN)
59            WRITE(6,4) Y,YO,E
60          4 FORMAT(10X,3(D12.5,10X),/)
61            K=K+1
62            IF(K.GE.10) GO TO 14
63            GO TO 13
64         14 WRITE(6,7)
65            M=M+1
66            IF(M.LT.4) GO TO 12
67            IF(I.EQ.2) GO TO 9
68            GO TO 15
69         16 WRITE(6,7)
70            STOP
71            END

      $ENTRY
```

Appendix 9

Evaluation of the maximum length of polymer macromolecule in a fully extended configuration

Polyox homologues are high polymers with the common formula:

$$-\left[CH_2 - O - CH_2\right]_n ,$$

which can be expressed at its fully extended configuration as

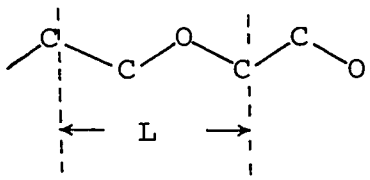

To an approximation which is adequate for all ordinary purpose, it is permissible to consider the length (l) of the valence bonds in the chain and the valence angle (θ) between successive bonds with fixed valence angles but free rotation about chain bonds.

Taking l_{c-c} = 1.53 Å, l_{c-o} = 1.43 Å, and the valence angles as $\theta = 110^{\circ}$ from Beech and Booth (100), the length (L) of the repeading unit can be calculated as follow:

$$L = 1.53 \cos 35 + 2(1.43) \cos 35$$
$$= 4.39 \cos 35$$
$$= 3.595 \text{ Å}.$$

Since the molecular weight of the repeating unit is 44, the degree of polymerization, n, can be obtained from the molecular weight divided by 44 to give:

9.1×10^4 for Polyox Coagulant,

and 4.96×10^4 for Polyox WSR 301.

Thus the length of the fully extended configuration of the polymer macromolecule can be evaluated by the multiplication of n by L to give:

3.27×10^5 Å for Polyox Coagulant,

and 1.783×10^5 Å for Polyox WSR 301.

It may be of interest if the fully extended length of the polymer macromolecule is expressed in terms of the multiples of root-mean-square end-to-end distance, $\sqrt{\overline{r^2}}$, of the polymer macromolecule in solution to give:

103.7 for Polyox Coagulant,

and 81.6 for Polyox WSR 301.

Appendix 10

Evaluation of δ^*/R (turbulent boundary layer thickness) as a function of Re

Let $\delta = R - r$ be the distance from the tube wall. In dimensionless form,

$$\delta^+ = \delta u^* \rho / \eta \ , \qquad \text{(A.10-1)}$$

where ρ = density, η = viscosity, and $u^* = \sqrt{\tau_w/\rho}$, which has dimensions of a velocity and τ_w is shear stress at the wall.

The friction factor is expressed by

$$f = \frac{2\ \tau_w}{\rho \langle u \rangle^2} \ ,$$

or $$\tau_w = \frac{1}{2}\ f\ \rho \langle u \rangle^2 \ . \qquad \text{(A.10-2)}$$

Thus, $$u^* = \sqrt{f/2}\ \langle u \rangle . \qquad \text{(A.10-3)}$$

Substituting Eq. (A.10-3) into Eq. (A.10-1),

$$\delta^+ = \frac{1}{2}\ (\frac{\delta}{R})\ \mathrm{Re}\ \sqrt{f/2} \ , \qquad \text{(A.10-4)}$$

where $\mathrm{Re} = \rho \langle u \rangle D/\eta$.

Now the Blasius formula gives, $f = \frac{0.0791}{\mathrm{Re}^{\frac{1}{4}}}$, which is good up to about $\mathrm{Re} = 10^5$.

Therefore Eq. (A.10-4) can be written as follow:

$$\delta^+ = \left(\frac{\delta}{R}\right) \mathrm{Re}\left(\frac{1}{2}\right) \sqrt{\frac{0.0791}{2\ \mathrm{Re}^{\frac{1}{4}}}}$$

$$= \left(\frac{\delta}{R}\right) (0.0994)\ \mathrm{Re}^{7/8} \qquad \text{(A.10-5)}$$

Letting $\delta^+ = 5$ for the boundary layer thickness (laminar sublayer thickness),

$$\bar{\delta}^* = \frac{\delta^*}{R} = \frac{50.28}{\mathrm{Re}^{7/8}} \quad ,$$

where δ^* = thickness of the laminar sublayer in turbulent flow.

Appendix 11

TABLES

of

the experimental data

Table 5.1

Calibration of tube diameters

Distilled water at 25° C

Tube A	No	Δh, cm water	w, g/min.
	1	0.086	58.5031
	2	0.152	103.0175
	3	0.248	168.7306
	4	0.312	212.4725
	5	0.392	266.6079
	6	0.427	290.3216
	7	0.615	418.4968
	8	0.682	464.1436
	9	0.743	504.7212
	10	0.796	542.3269

Slope = 0.0014697

Diameter = 1.26718 cm

Tube B	No	Δh, cm water	w, g/min.
	1	0.189	39.1457
	2	0.305	63.9048
	3	0.546	113.5963
	4	0.813	169.0945
	5	1.052	218.5036
	6	1.215	253.3259
	7	1.409	293.6960
	8	1.698	354.1568
	9	1.863	381.9577
	10	2.087	433.9804

Slope = 0.0048035

Diameter = 0.94311 cm

Tube C	No	Δh, cm water	w, g/min.
	1	0.496	27.0328
	2	0.932	51.5579
	3	1.453	79.9660
	4	1.917	105.5389
	5	2.408	133.3076
	6	3.014	166.7867
	7	3.638	200.1175
	8	4.005	220.1673
	9	4.534	249.0937
	10	4.896	270.5359

Slope = 0.0181466

Diameter = 0.62711 cm

Tube D	No	Δh, cm water	w, g/min.
	1	0.937	17.4033
	2	2.045	38.8857
	3	2.968	55.3210
	4	4.157	77.0786
	5	5.934	111.1614
	6	6.821	126.1618
	7	7.573	140.5901
	8	8.871	164.6037
	9	9.733	181.2754
	10	10.838	202.4429

Slope = 0.0537187

Diameter = 0.43887 cm

Tube E	No	Δh, cm water	w, g/min.
	1	1.836	12.2394
	2	3.273	20.1064
	3	6.076	38.2601
	4	8.363	53.1420
	5	10.927	68.7158
	6	12.131	76.3878
	7	15.360	97.4741
	8	17.673	112.0605
	9	19.201	121.7836
	10	21.535	135.9755

Slope = 0.1580572

Diameter = 0.30521 cm

Table 5.2

Tube flow measurement

of distilled water

Tube A	Δh(cm)	w(g/min.)	τ_w(dyne/cm^2)	$8\langle u\rangle/D$(sec^{-1})
	0.152	103.0175	0.07734	8.62084
	0.312	212.4725	0.15876	17.78039
	0.427	290.3216	0.21728	24.29507
	0.682	464.1434	0.34704	38.84105
	0.796	542.3269	0.40505	45.38370

Tube B	Δh(cm)	w(g/min.)	τ_w(dyne/cm^2)	$8\langle u\rangle/D$(sec^{-1})
	0.305	63.9048	0.11519	12.97180
	0.813	169.0945	0.30704	34.32386
	1.215	253.3259	0.45886	51.42168
	1.698	354.1568	0.64127	71.88897
	2.087	433.9804	0.78818	88.09206

Tube C	Δh(cm)	w(g/min.)	τ_w(dyne/cm^2)	$8\langle u\rangle/D$(sec^{-1})
	0.932	51.5579	0.31690	35.59736
	1.917	105.5389	0.65184	72.86770
	3.014	166.7867	1.02485	115.15530
	4.005	220.1673	1.36181	152.01111
	4.896	270.5359	1.66478	186.78733

Tube D	Δh(cm)	w(g/min.)	τ_w(dyne/cm^2)	$8\langle u\rangle/D$(sec^{-1})
	2.045	38.8857	0.68533	78.33141
	4.157	77.0789	1.39311	155.26724
	6.821	126.1618	2.28588	254.14051
	8.871	164.6037	2.97289	331.57792
	10.836	202.4429	3.63208	407.80126

Tube E	Δh(cm)	w(g/min.)	τ_w(dyne/cm^2)	$8\langle u\rangle/D$(sec^{-1})
	1.836	12.2394	0.62174	73.30229
	6.078	38.2601	2.05826	229.14138
	10.927	68.7158	3.70034	411.54187
	15.360	97.4741	5.20153	583.77656
	19.201	121.7836	6.50225	729.36720

Table 5.3

Viscosity measurement from tube flow (η_r)

Conc. (ppm)	In distilled water		In 0.3M K_2SO_4	
	Coagulant	WSR 301	Coagulant	WSR 301
10	1.0143	1.0089	1.0073	1.0047
20	1.0286	1.0179	1.0147	1.0095
30	1.0433	1.0274	1.0221	1.0141
40	1.0579	1.0361	1.0289	1.0188
60	1.0879	1.0547	1.0445	1.0291
100	1.1497	1.0919	1.0748	1.0472
[η]	14.2	8.9	7.3	4.7

Table 5.4

Viscosity measurement from Cannon Fenske viscometer (η_r)

Conc. (ppm)	In distilled water		In 0.3M K_2SO_4	
	Coagulant	WSR 301	Coagulant	WSR 301
10	1.0139	1.0091	1.0076	1.0042
20	1.0298	1.0175	1.0157	1.0094
30	1.0443	1.0284	1.0242	1.0149
40	1.0591	1.0373	1.0301	1.0191
60	1.0889	1.0565	1.0462	1.0305
100	1.1518	1.0921	1.0764	1.0469

Table 5.6

Degradation by aging

Measurement by Cannon Fenske viscometer (η_r)

Coagulant in distilled water

Conc. ppm	Fresh	Oneday	Two days
10	1.01394	1.01286	1.01175
20	1.02980	1.02583	1.02361
30	1.04425	1.03894	1.03558
40	1.05910	1.05216	1.04756
60	1.08892	1.07898	1.07210
100	1.15188	1.13414	1.12645
[η]	14.2	12.8	11.7

Coagulant in 0.3M K_2SO_4

Conc. ppm	Fresh	Oneday	Two days
10	1.00761	1.00342	1.00190
20	1.01573	1.00678	1.00382
30	1.02422	1.01028	1.00570
40	1.03014	1.01371	1.00765
60	1.04622	1.02056	1.01143
100	1.07635	1.03445	1.01915
[η]	7.3	3.4	1.9

Table 5.7

Tube flow measurement of degraded polymer solutions

in tube B

after oneday and two days

h = pressure drop, cm

w = mass flow rate, g/min.

Polyox Coagulant

in distilled water

		oneday		two days	
10 PPM		h	w	h	w
	1	0.298	60.4943	0.386	78.4903
	2	0.526	106.6784	0.613	124.5490
	3	0.608	123.4245	0.796	161.9607
	4	0.853	173.2596	0.941	191.3454
	5	1.286	261.0591	1.374	279.3928
	6	1.747	354.7422	1.635	332.6653
	7	1.848	375.0454	1.906	387.3711
20 PPM					
	1	0.305	60.4381	0.328	65.2075
	2	0.465	91.8909	0.488	96.8673
	3	0.595	117.7088	0.618	122.5721
	4	0.787	155.5922	0.807	160.1884
	5	0.974	192.6864	0.996	197.7046
	6	1.436	284.1838	1.456	289.1140
	7	1.872	370.3376	1.894	375.8562
30 PPM					
	1	0.302	58.5550	0.303	59.0299
	2	0.404	78.2319	0.405	78.8014
	3	0.598	115.9467	0.599	116.7961
	4	0.779	151.1410	0.780	151.9582
	5	1.077	208.9204	1.078	210.1141
	6	1.446	280.3662	1.447	281.8020
	7	1.870	362.4758	1.871	364.5049

		oneday		two days	
40 PPM		h	w	h	w
	1	0.312	59.3477	0.221	42.3672
	2	0.506	96.4119	0.415	79.6582
	3	0.730	139.1923	0.639	122.4005
	4	0.879	167.4824	0.788	151.0648
	5	1.148	218.6370	1.057	202.8339
	6	1.749	333.2500	1.658	317.8496
	7	1.916	365.1096	1.822	349.0896
60 PPM					
	1	0.427	79.0460	0.426	79.4114
	2	0.659	121.8938	0.678	126.5464
	3	0.807	149.4914	0.826	154.2701
	4	0.935	173.0867	0.985	183.8469
	5	1.174	217.4303	1.194	222.3560
	6	1.659	307.0132	1.567	292.4751
	7	1.858	343.9519	1.878	350.8223
100 PPM					
	1	0.468	82.0969	0.389	68.9273
	2	0.646	113.4599	0.568	100.5444
	3	0.855	150.2674	0.775	137.4229
	4	1.104	193.9004	1.024	181.4435
	5	1.456	255.9238	1.374	243.1603
	6	1.784	313.3318	1.708	302.6421
	7	2.006	352.1228	1.925	341.3926

Polyox Coagulant

in 0.3M K_2SO_4

		oneday		two days	
10 PPM		h	w	h	w
	1	0.213	44.5007	0.298	62.4958
	2	0.474	99.2522	0.432	90.8429
	3	0.687	143.9529	0.784	164.6815
	4	0.938	196.4105	0.968	203.5312
	5	1.097	229.5040	1.039	218.2450
	6	1.328	278.0737	1.298	272.4487
	7	1.815	380.2480	1.796	377.2549
20 PPM					
	1	0.324	67.1948	0.309	64.5182
	2	0.511	105.8769	0.475	99.0785
	3	0.769	159.5838	0.683	142.7082
	4	0.961	199.3030	0.874	182.4884
	5	1.096	227.1008	1.185	247.7242
	6	1.404	291.1772	1.433	299.2058
	7	1.789	371.2229	1.906	397.6667
30 PPM					
	1	0.315	64.7671	0.315	65.3509
	2	0.487	100.3866	0.462	95.9946
	3	0.648	133.4409	0.644	133.9107
	4	0.898	184.7228	0.923	191.7815
	5	1.305	268.7351	1.268	263.5659
	6	1.506	310.3267	1.501	311.7788
	7	1.809	372.5227	1.858	386.0564

		oneday		two days	
40 PPM		h	w	h	w
	1	0.287	58.7452	0.257	53.1830
	2	0.425	86.8920	0.424	87.9417
	3	0.587	120.1514	0.607	125.6113
	4	0.819	167.7388	0.852	176.3111
	5	0.995	203.8637	0.986	204.0408
	6	1.357	277.5605	1.276	264.1526
	7	1.629	333.4358	1.709	353.5569
60 PPM					
	1	0.307	62.1969	0.310	63.7187
	2	0.494	100.2432	0.512	105.5038
	3	0.654	132.8106	0.661	136.0780
	4	0.787	159.6991	0.784	161.5996
	5	0.897	182.3205	0.910	187.3388
	6	1.208	245.1290	1.196	246.0167
	7	1.569	318.0835	1.467	302.0066
100 PPM					
	1	0.278	55.5730	0.276	56.2267
	2	0.510	101.8505	0.494	100.8166
	3	0.692	138.3328	0.661	134.9984
	4	0.804	160.8220	0.783	159.7964
	5	1.015	202.7015	0.888	181.5250
	6	1.358	271.4683	1.267	258.2722
	7	1.496	299.2549	1.481	302.2458

Table 5.8

Tube flow measurement of polymer solutions

h = pressure drop, cm water

w = mass flow rate, g/min.

T = τ_w = shear stress at the wall, dyne/cm^2

U = 8<u>/D, sec^{-1}

Table 5.8-1

POLYOX Coagulant in distilled water

TUBE A

		h	w	T	U
10 PPM					
	1	0.095	62.6372	0.04834	5.2417
	2	0.185	121.8777	0.09414	10.1991
	3	0.286	188.5709	0.14553	15.7802
	4	0.353	232.8466	0.17962	19.4854
	5	0.547	360.6583	0.27634	30.1811
	6	0.657	433.0856	0.33432	36.2421
	7	0.721	475.4833	0.36688	39.7900
20 PPM					
	1	0.121	77.1833	0.06157	6.4590
	2	0.200	127.4757	0.10177	10.6676
	3	0.281	179.2438	0.14299	14.9997
	4	0.378	241.2180	0.19235	20.1859
	5	0.495	315.7498	0.25188	26.4230
	6	0.706	450.2421	0.35925	37.6778
	7	0.736	469.5785	0.37451	39.2959
30 PPM					
	1	0.151	93.9591	0.07684	7.8628
	2	0.216	134.5050	0.10991	11.2558
	3	0.292	181.6957	0.14858	15.2049
	4	0.363	225.9751	0.18471	18.9104
	5	0.458	284.9884	0.23305	23.8488
	6	0.528	328.4456	0.26867	27.4854
	7	0.697	433.8050	0.35467	36.3023

		h	w	T	U
40 PPM					
	1	0.109	66.4984	0.05546	5.5648
	2	0.182	111.1341	0.09261	9.3001
	3	0.357	217.7999	0.18166	18.2262
	4	0.403	245.7612	0.20507	20.5661
	5	0.509	310.7294	0.25901	26.0029
	6	0.570	347.7442	0.29005	29.1004
	7	0.788	480.5411	0.40097	40.2133
60 PPM					
	1	0.125	73.7628	0.06361	6.1727
	2	0.198	116.8404	0.10075	9.7776
	3	0.286	168.9694	0.14553	14.1399
	4	0.345	203.3855	0.17555	17.0200
	5	0.409	241.2520	0.20812	20.1888
	6	0.521	307.4436	0.26511	25.7279
	7	0.705	416.1225	0.35874	34.8225
100 PPM					
	1	0.128	71.1248	0.06513	5.9520
	2	0.196	109.1630	0.09973	9.1351
	3	0.275	152.8221	0.13993	12.7887
	4	0.356	198.2941	0.18115	16.5939
	5	0.507	282.1171	0.25799	23.6085
	6	0.598	332.6535	0.30429	27.8376
	7	0.715	397.9575	0.36383	33.3024

Table 5.8-2

POLYOX Coagulant in distilled water

TUBE B

		h	w	T	U
10 PPM					
	1	0.301	60.9910	0.11368	12.3803
	2	0.435	88.0431	0.16428	17.8716
	3	0.786	159.2655	0.29684	32.3287
	4	0.975	197.6621	0.36822	40.1227
	5	1.045	211.5461	0.39466	42.9410
	6	1.376	279.0159	0.51966	56.6364
	7	1.860	376.8878	0.70245	76.5031
20 PPM					
	1	0.307	60.4723	0.11594	12.2751
	2	0.485	94.5344	0.18317	19.1892
	3	0.693	137.5059	0.26172	27.9118
	4	0.884	174.1288	0.33385	35.3458
	5	1.195	235.4890	0.45131	47.8011
	6	1.443	284.2396	0.54497	57.6968
	7	1.916	377.3103	0.72360	76.5889
30 PPM					
	1	0.320	61.8465	0.12085	12.5540
	2	0.467	89.7653	0.17637	18.2211
	3	0.649	125.0268	0.24510	25.3787
	4	0.928	178.7748	0.35047	36.2889
	5	1.275	244.6227	0.48152	49.6551
	6	1.506	291.1237	0.56876	59.0942
	7	1.862	358.7054	0.70321	72.8123

		h	w	T	U
40 PPM					
	1	0.247	46.7247	0.09328	9.4845
	2	0.414	78.3160	0.15635	15.8971
	3	0.597	112.7339	0.22546	22.8835
	4	0.842	159.2803	0.31799	32.3317
	5	0.976	184.8289	0.36860	37.5178
	6	1.266	239.3879	0.47812	48.5925
	7	1.699	321.4981	0.64165	65.2598
60 PPM					
	1	0.312	57.1570	0.11783	11.6021
	2	0.514	94.1425	0.19412	19.1096
	3	0.663	121.4586	0.25039	24.6544
	4	0.786	144.0917	0.29684	29.2487
	5	0.912	166.9743	0.34443	33.8935
	6	1.198	219.4682	0.45244	44.5491
	7	1.469	269.1342	0.55479	54.6306
100 PPM					
	1	0.287	49.4131	0.10839	10.0302
	2	0.505	87.5983	0.19072	17.7813
	3	0.672	116.1673	0.25379	23.5804
	4	0.794	137.2572	0.29986	27.8613
	5	0.899	155.1083	0.33952	31.4849
	6	1.278	221.1253	0.48265	44.8854
	7	1.492	257.9190	0.56347	52.3541

Table 5.8-3

POLYOX Coagulant in distilled water

TUBE C

		h	w	T	U
10 PPM					
	1	0.644	34.6803	0.21898	23.9445
	2	1.334	71.8177	0.45360	49.5855
	3	1.947	104.8786	0.66204	72.4119
	4	2.408	129.6741	0.81879	89.5316
	5	3.112	167.6055	1.05817	115.7207
	6	3.634	195.6959	1.23566	135.1153
	7	4.404	237.1314	1.49749	163.7238
20 PPM					
	1	0.629	33.0634	0.21388	22.8281
	2	1.221	64.2114	0.41518	44.3338
	3	1.783	93.7519	0.60627	64.7296
	4	2.769	145.5767	0.94154	100.5113
	5	3.851	202.5093	1.30945	139.8195
	6	4.043	212.5848	1.37474	146.7760
	7	4.923	258.8561	1.67396	178.7233
30 PPM					
	1	0.676	34.8528	0.22986	24.0636
	2	1.346	69.4063	0.45768	47.9205
	3	1.939	99.9798	0.65932	69.0296
	4	2.829	145.8359	0.96194	100.6902
	5	3.755	193.5980	1.27681	133.6669
	6	4.016	207.0545	1.36556	142.9577
	7	4.910	253.1468	1.66954	174.7814

		h	w	T	U
40 PPM					
	1	0.927	46.9979	0.31521	32.4490
	2	1.628	82.5378	0.55357	56.9870
	3	2.328	118.0170	0.79159	81.4831
	4	2.863	145.1609	0.97350	100.2242
	5	3.453	175.0632	1.17412	120.8698
	6	4.006	203.0797	1.36216	140.2134
	7	4.729	239.7750	1.60800	165.5491
60 PPM					
	1	0.691	33.9628	0.23496	23.4491
	2	1.439	70.7580	0.48930	48.8538
	3	2.439	119.9326	0.82933	82.8057
	4	2.975	146.2649	1.01159	100.9864
	5	3.219	158.2411	1.09455	109.2552
	6	4.150	204.0334	1.41112	140.8718
	7	4.672	229.6973	1.58861	158.5911
100 PPM					
	1	0.818	37.9885	0.27814	26.2286
	2	1.255	58.2931	0.42674	40.2476
	3	1.997	92.7321	0.67904	64.0255
	4	2.565	119.1005	0.87217	82.2312
	5	3.007	139.6673	1.02247	96.4312
	6	4.019	186.6453	1.36658	128.8665
	7	4.587	213.0237	1.55971	147.0790

Table 5.8-4

POLYOX Coagulant in distilled water

TUBE D

		h	w	T	U
10 PPM					
	1	1.563	28.5050	0.52380	57.4206
	2	2.887	52.6412	0.96750	106.0406
	3	4.215	76.8704	1.41255	154.8480
	4	5.850	106.6385	1.96048	214.9136
	5	7.431	135.5317	2.49031	273.0155
	6	8.690	158.4725	2.91223	319.2275
	7	9.135	166.6081	3.06136	335.6159
20 PPM					
	1	1.825	32.5881	0.61160	65.6456
	2	3.015	53.8273	1.01040	108.4299
	3	4.536	80.9969	1.52012	163.1604
	4	5.090	90.8994	1.70578	183.1080
	5	7.436	132.7807	2.49199	267.4738
	6	8.680	154.9742	2.90888	312.1805
	7	10.051	179.4954	3.36834	361.5761
30 PPM					
	1	1.490	26.1278	0.49934	52.6319
	2	2.863	50.2340	0.95946	101.1915
	3	4.027	70.5852	1.34955	142.1870
	4	5.542	97.1814	1.85726	195.7625
	5	7.042	123.4846	2.35995	248.7478
	6	8.949	156.9046	2.99903	316.0691
	7	9.540	167.3081	3.19709	337.0259

		h	w	T	U
40 PPM					
	1	1.642	28.3373	0.55027	57.0827
	2	2.875	49.6161	0.96348	99.9468
	3	3.934	67.8821	1.31838	136.7419
	4	5.194	89.6468	1.74064	180.5848
	5	6.482	111.8649	2.17228	225.3410
	6	7.475	129.0078	2.50506	259.8737
	7	9.110	157.2123	3.05298	316.6889
60 PPM					
	1	1.839	30.6993	0.61629	61.8408
	2	2.926	49.0042	0.98057	98.7142
	3	4.095	68.6824	1.37233	138.3540
	4	5.669	94.9435	1.89982	191.2545
	5	6.708	112.4445	2.24801	226.5085
	6	7.651	128.1377	2.56404	258.1210
	7	9.036	151.2335	3.02818	304.6452
100 PPM					
	1	1.549	24.5170	0.51911	49.3871
	2	2.877	45.5461	0.96415	91.7482
	3	4.315	68.2962	1.44606	137.5761
	4	5.749	90.9732	1.92663	183.2567
	5	7.428	117.5577	2.48930	236.8086
	6	8.510	134.6932	2.85191	271.3264
	7	9.678	153.1998	3.24333	308.6061

Table 5.8-5

POLYOX Coagulant in distilled water

TUBE E

		h	w	T	U
10 PPM					
	1	3.175	19.7190	1.07519	118.0980
	2	5.250	32.6012	1.77787	195.2501
	3	8.369	51.9823	2.83409	311.3245
	4	10.293	63.9267	3.48564	382.8601
	5	12.145	75.4239	4.11280	451.7173
	6	14.010	87.0169	4.74437	521.1484
	7	17.697	109.9107	5.99294	658.2604
20 PPM					
	1	3.751	22.8569	1.27024	136.8911
	2	6.360	38.7600	2.15376	232.1355
	3	8.613	52.4837	2.91672	314.3274
	4	10.511	64.0443	3.55946	383.5644
	5	11.469	69.8889	3.88388	418.5680
	6	13.938	84.9319	4.71998	508.6612
	7	18.094	110.2547	6.12738	660.3207
30 PPM					
	1	4.003	23.9811	1.35558	143.6240
	2	5.931	35.5342	2.00848	212.8160
	3	7.490	44.8766	2.53642	268.7681
	4	9.164	54.9040	3.10331	328.8227
	5	12.249	73.3971	4.14802	439.5787
	6	13.910	83.3286	4.71050	499.0590
	7	16.455	98.5864	5.57235	590.4387

		h	w	T	U
40 PPM					
	1	2.808	16.5645	0.95091	99.2056
	2	4.806	28.3542	1.62751	169.8147
	3	6.258	36.9227	2.11922	221.1318
	4	7.586	44.7556	2.56893	268.0434
	5	9.280	54.7517	3.14259	327.9105
	6	11.590	68.3782	3.92485	409.5203
	7	14.787	87.2377	5.00749	522.4707
60 PPM					
	1	3.186	18.2521	1.07891	109.3127
	2	5.015	28.7201	1.69829	172.0060
	3	7.234	41.4424	2.44973	248.2005
	4	8.015	45.9267	2.71421	275.0572
	5	9.525	54.5672	3.22556	326.8056
	6	13.724	78.6326	4.64752	470.9344
	7	15.437	88.4261	5.22761	529.5881
100 PPM					
	1	3.176	17.2019	1.07553	103.0230
	2	6.718	36.3811	2.27499	217.8881
	3	8.026	43.4755	2.71794	260.3768
	4	9.024	48.8759	3.05590	292.7201
	5	10.998	59.5775	3.72438	356.8125
	6	12.136	65.7211	4.10975	393.6068
	7	16.733	90.6294	5.66649	542.7838

Table 5.8-6

POLYOX WSR 301 in distilled water

TUBE A

		h	w	T	U
10 PPM					
	1	0.191	129.4182	0.10115	10.4063
	2	0.302	204.4298	0.15993	16.4378
	3	0.443	300.1689	0.23460	24.1360
	4	0.551	373.5477	0.29180	30.0363
	5	0.607	411.7923	0.32145	33.1115
	6	0.687	465.4989	0.36382	37.4299
	7	0.740	500.9107	0.39189	40.2773
20 PPM					
	1	0.108	71.5600	0.05719	5.7540
	2	0.215	142.6566	0.11386	11.4708
	3	0.278	184.5583	0.14722	14.8400
	4	0.353	234.2222	0.18694	18.8334
	5	0.487	323.5337	0.25790	26.0147
	6	0.548	363.6084	0.29021	29.2371
	7	0.758	502.5474	0.40142	40.4089
30 PPM					
	1	0.121	79.1045	0.06408	6.3606
	2	0.196	128.6362	0.10380	10.3434
	3	0.286	186.9743	0.15146	15.0343
	4	0.356	232.2372	0.18853	18.6738
	5	0.507	331.4544	0.26850	26.6516
	6	0.615	402.1601	0.32569	32.3370
	7	0.771	503.9461	0.40830	40.5214

		h	w	T	U
40 PPM					
	1	0.151	97.4809	0.07997	7.8383
	2	0.216	139.7290	0.11439	11.2354
	3	0.278	180.0363	0.14722	14.4764
	4	0.375	242.5850	0.19859	19.5058
	5	0.489	316.5308	0.25896	25.4517
	6	0.607	392.6642	0.32145	31.5734
	7	0.779	503.7299	0.41254	40.5040
60 PPM					
	1	0.098	62.2033	0.05190	5.0017
	2	0.182	115.2203	0.09638	9.2647
	3	0.357	226.5976	0.18906	18.2203
	4	0.413	262.4423	0.21872	21.1025
	5	0.531	337.0401	0.28121	27.1008
	6	0.695	441.3354	0.36806	35.4870
	7	0.807	512.0248	0.42737	41.1710
100 PPM					
	1	0.138	84.8152	0.07308	6.8198
	2	0.207	127.3728	0.10962	10.2418
	3	0.358	220.3872	0.18959	17.7209
	4	0.508	312.5863	0.26903	25.1345
	5	0.597	367.0505	0.31616	29.5139
	6	0.705	433.8058	0.37335	34.8815
	7	0.815	501.7919	0.43161	40.3482

Table 5.8-7

POLYOX WSR 301 in distilled water

TUBE B

		h	w	T	U
10 PPM					
	1	0.287	59.6809	0.11280	11.6403
	2	0.514	106.7850	0.20203	20.8276
	3	0.597	124.1446	0.23465	24.2134
	4	0.842	175.1918	0.33094	34.1697
	5	1.275	265.3330	0.50113	51.7511
	6	1.736	360.9968	0.68233	70.4095
	7	1.837	381.7995	0.72202	74.4669
20 PPM					
	1	0.307	62.7237	0.12066	12.2338
	2	0.467	95.8135	0.18355	18.6877
	3	0.597	121.9740	0.23465	23.7900
	4	0.786	160.5889	0.30893	31.3216
	5	0.975	199.4038	0.38322	38.8921
	6	1.437	293.5958	0.56481	57.2635
	7	1.873	382.4756	0.73617	74.5988
30 PPM					
	1	0.312	62.9241	0.12263	12.2728
	2	0.414	83.5055	0.16272	16.2871
	3	0.608	122.6114	0.23897	23.9144
	4	0.789	159.1255	0.31011	31.0361
	5	1.087	219.1261	0.42724	42.7388
	6	1.456	293.6460	0.57227	57.2733
	7	1.880	379.2583	0.73893	73.9713

		h	w	T	U
40 PPM					
	1	0.320	63.8248	0.12577	12.4485
	2	0.514	102.6793	0.20203	20.0268
	3	0.738	147.5267	0.29007	28.7739
	4	0.887	177.1917	0.34863	34.5598
	5	1.156	230.8285	0.45436	45.0212
	6	1.757	350.9874	0.69058	68.4573
	7	1.921	383.8489	0.75504	74.8666
60 PPM					
	1	0.527	103.3903	0.20713	20.1654
	2	0.759	148.8056	0.29832	29.0233
	3	0.907	177.9412	0.35649	34.7060
	4	1.036	203.3493	0.40719	39.6616
	5	1.275	250.1379	0.50113	48.7874
	6	1.658	325.3774	0.65167	63.4622
	7	1.959	384.2296	0.76998	74.9409
100 PPM					
	1	0.489	93.1628	0.19220	18.1707
	2	0.667	126.9384	0.26216	24.7583
	3	0.876	166.6136	0.34431	32.4966
	4	1.125	214.1014	0.44218	41.7588
	5	1.475	280.6108	0.57974	54.7309
	6	1.809	344.2751	0.71102	67.1491
	7	2.026	385.6729	0.79631	75.2224

Table 5.8-8

POLYOX WSR 301 in distilled water

TUBE C

		h	w	T	U
10 PPM					
	1	0.754	41.6314	0.26682	27.6188
	2	1.424	78.6247	0.50392	52.1606
	3	1.895	104.5805	0.67060	69.3600
	4	2.796	154.3783	0.98945	102.4165
	5	3.248	179.3851	1.14940	119.0064
	6	4.236	233.8865	1.49903	155.1633
	7	4.901	270.6038	1.73436	179.5220
20 PPM					
	1	0.629	34.2380	0.22259	22.7139
	2	1.728	94.1093	0.61150	62.4333
	3	2.318	126.1744	0.82029	83.7057
	4	2.976	161.9410	1.05314	107.4337
	5	3.875	210.9258	1.37128	139.9309
	6	4.263	232.1456	1.50859	154.0084
	7	4.975	270.7015	1.76055	179.5869
30 PPM					
	1	0.809	43.5002	0.28629	28.8586
	2	1.238	66.6442	0.43810	44.2126
	3	2.075	111.7516	0.73430	74.1374
	4	2.865	154.2290	1.01386	102.3175
	5	3.197	172.2013	1.13135	114.2406
	6	4.069	219.0429	1.43993	145.3159
	7	4.932	265.4000	1.74533	176.0698

		h	w	T	U
40 PPM					
	1	0.907	48.4091	0.32097	32.1152
	2	1.563	83.3717	0.55311	55.3099
	3	2.256	120.4090	0.79835	79.8809
	4	2.747	146.6650	0.97211	97.2994
	5	3.068	163.7477	1.08570	108.6323
	6	3.965	211.6031	1.40313	140.3802
	7	4.977	265.6564	1.76126	176.2399
60 PPM					
	1	0.758	39.7260	0.26824	26.3547
	2	1.375	72.1349	0.48658	47.8552
	3	2.136	112.0983	0.75589	74.3675
	4	2.956	155.0770	1.04607	102.8801
	5	3.257	170.9080	1.15258	113.3826
	6	4.259	223.4347	1.50717	148.2295
	7	5.069	265.8887	1.79381	176.3940
100 PPM					
	1	0.736	37.4766	0.26045	24.8625
	2	1.258	64.1065	0.44518	42.5291
	3	2.037	103.7226	0.72085	68.8109
	4	2.856	145.3755	1.01068	96.4440
	5	3.133	159.5302	1.10870	105.8344
	6	4.836	246.2257	1.71136	163.3493
	7	5.132	261.3378	1.81611	173.3749

Table 5.8-9

POLYOX WSR 301 in distilled water

TUBE D

		h	w	T	U
10 PPM					
	1	1.643	30.7023	0.57304	59.4262
	2	2.865	53.5575	0.99924	103.6639
	3	3.924	73.3267	1.36859	141.9235
	4	5.084	94.9833	1.77317	183.8462
	5	6.382	119.2586	2.22588	230.8326
	6	7.405	138.3352	2.58268	267.7565
	7	9.549	178.4795	3.33045	345.4584
20 PPM					
	1	1.368	25.2429	0.47712	48.8592
	2	2.787	51.4573	0.97204	99.5989
	3	4.236	78.1955	1.47741	151.3523
	4	5.709	105.3667	1.99116	203.9439
	5	7.328	135.2731	2.55582	261.8296
	6	8.419	155.4326	2.93633	300.8496
	7	9.679	178.6719	3.37579	345.8308
30 PPM					
	1	1.399	25.5679	0.48794	49.4683
	2	2.775	50.7354	0.96785	98.2016
	3	3.284	60.0178	1.14538	116.1682
	4	5.194	94.9047	1.81154	183.6941
	5	6.381	116.6181	2.22553	225.7217
	6	7.375	134.7743	2.57221	260.8642
	7	10.186	186.1677	3.55262	360.3394

		h	w	T	U
40 PPM					
	1	1.768	32.0449	0.61663	62.0249
	2	2.787	50.5300	0.97204	97.8040
	3	4.326	78.4430	1.50880	151.8314
	4	5.749	104.2328	2.00511	201.7492
	5	7.428	134.6641	2.59070	260.6509
	6	8.688	157.5187	3.03016	304.8374
	7	10.372	188.0606	3.61749	364.0032
60 PPM					
	1	1.896	33.8177	0.66128	65.4563
	2	3.123	55.6864	1.08922	107.7846
	3	4.527	80.7112	1.57890	156.2216
	4	5.109	91.0989	1.78189	176.3277
	5	7.451	132.8393	2.59872	257.1189
	6	8.718	155.4513	3.04062	300.8858
	7	10.755	191.7931	3.75107	371.2277
100 PPM					
	1	1.511	26.1594	0.52700	50.6332
	2	2.793	48.3641	0.97413	93.6118
	3	4.058	70.2446	1.41533	135.9629
	4	5.492	95.0809	1.91547	184.0351
	5	7.083	122.6213	2.47037	237.3413
	6	9.849	170.5120	3.43508	330.0368
	7	11.006	190.5467	3.83862	368.8152

Table 5.8-10

POLYOX WSR 301 in distilled water

TUBE E

		h	w	T	U
10 PPM					
	1	2.908	18.4906	1.02488	106.4069
	2	4.878	31.0198	1.71918	178.5080
	3	6.369	40.4997	2.24466	233.0615
	4	8.537	54.2877	3.00874	312.4066
	5	12.356	78.5703	4.35469	452.1444
	6	16.757	106.5537	5.90575	613.1791
	7	18.559	118.0144	6.54084	679.1314
20 PPM					
	1	3.276	20.6041	1.15458	118.5693
	2	5.028	31.6211	1.77204	181.9683
	3	7.358	46.2794	2.59322	266.3217
	4	9.123	57.3782	3.21527	330.1914
	5	13.507	84.9539	4.76034	488.8798
	6	15.136	95.1963	5.33446	547.8212
	7	18.793	118.1937	6.62331	680.1632
30 PPM					
	1	3.951	24.6235	1.39247	141.6996
	2	6.237	38.8656	2.19814	223.6579
	3	8.633	53.7932	3.04257	309.5609
	4	10.627	66.2217	3.74533	381.0826
	5	11.568	72.0845	4.07697	414.8209
	6	16.368	101.9965	5.76866	586.9540
	7	19.298	120.2557	6.80129	692.0292

		h	w	T	U
40 PPM					
	1	3.897	24.1006	1.37344	138.6905
	2	5.288	32.7071	1.86368	188.2179
	3	9.378	57.9972	3.30514	333.7535
	4	11.283	69.7745	3.97652	401.5277
	5	13.247	81.9246	4.66871	471.4473
	6	15.019	92.8844	5.29322	534.5170
	7	19.887	122.9880	7.00888	707.7527
60 PPM					
	1	3.286	19.9964	1.15810	115.0722
	2	6.818	41.4857	2.40290	238.7356
	3	9.036	54.9837	3.18460	316.4119
	4	12.124	73.7711	4.27292	424.5267
	5	14.136	86.0160	4.98202	494.9918
	6	16.837	102.4487	5.93395	589.5562
	7	20.529	124.9115	7.23514	718.8217
100 PPM					
	1	4.129	24.3994	1.45520	140.4100
	2	6.931	40.9591	2.44273	235.7052
	3	9.490	56.0790	3.34461	322.7149
	4	13.164	77.7876	4.63946	447.6403
	5	15.910	94.0175	5.60724	541.0376
	6	19.351	114.3502	6.81997	658.0452
	7	22.089	130.5288	7.78494	751.1473

Table 5.8-11

POLYOX Coagulant in 0.3M K_2SO_4

TUBE A

		h	w	T	U
10 PPM					
	1	0.095	63.5324	0.04834	5.3166
	2	0.225	150.6714	0.11449	12.6087
	3	0.296	197.7535	0.15062	16.5487
	4	0.386	258.1420	0.19642	21.6022
	5	0.485	324.0494	0.24679	27.1175
	6	0.558	373.4690	0.28394	31.2531
	7	0.718	480.1709	0.36536	40.1823
20 PPM					
	1	0.243	159.5228	0.12365	13.3494
	2	0.334	219.3992	0.16996	18.3601
	3	0.396	260.2260	0.20151	21.7766
	4	0.468	307.4217	0.23814	25.7261
	5	0.561	368.7119	0.28547	30.8551
	6	0.632	415.1506	0.32159	34.7412
	7	0.730	479.3253	0.37146	40.1116
30 PPM					
	1	0.112	72.3835	0.05699	6.0573
	2	0.275	177.4275	0.13993	14.8477
	3	0.327	211.3341	0.16639	17.6851
	4	0.401	259.4589	0.20405	21.7124
	5	0.466	301.3672	0.23712	25.2194
	6	0.622	401.7872	0.31651	33.6229
	7	0.731	472.4319	0.37197	39.5347

		h	w	T	U
40 PPM					
	1	0.128	81.4139	0.06513	6.8130
	2	0.208	132.8226	0.10584	11.1150
	3	0.331	211.0485	0.16843	17.6612
	4	0.396	252.2931	0.20151	21.1127
	5	0.523	333.4694	0.26613	27.9058
	6	0.709	452.2646	0.36078	37.8470
	7	0.856	545.7931	0.43558	45.6738
60 PPM					
	1	0.206	128.1749	0.10482	10.7261
	2	0.387	240.5946	0.19693	20.1338
	3	0.449	279.5715	0.22847	23.3955
	4	0.519	322.7261	0.26409	27.0068
	5	0.622	387.2135	0.31651	32.4033
	6	0.723	449.8565	0.36790	37.6455
	7	0.870	541.3212	0.44270	45.2996
100 PPM					
	1	0.239	142.7681	0.12162	11.9473
	2	0.326	194.6381	0.16589	16.2880
	3	0.389	232.4716	0.19794	19.4540
	4	0.481	287.3283	0.24476	24.0446
	5	0.639	381.3106	0.32516	31.9094
	6	0.709	423.5256	0.36078	35.4420
	7	0.873	521.7920	0.44423	43.6653

Table 5.8-12

POLYOX Coagulant in 0.3M K_2SO_4

TUBE B

		h	w	T	U
10 PPM					
	1	0.235	48.0850	0.08875	9.7606
	2	0.425	87.1430	0.16051	17.6888
	3	0.638	130.9171	0.24095	26.5744
	4	0.936	191.9197	0.35349	38.9571
	5	1.285	263.3795	0.48530	53.4625
	6	1.541	315.9704	0.58198	64.1377
	7	1.907	391.1159	0.72020	79.3912
20 PPM					
	1	0.439	88.6074	0.16579	17.9861
	2	0.694	140.1765	0.26210	28.4539
	3	0.936	188.9216	0.35349	38.3485
	4	1.107	223.5361	0.41807	45.3748
	5	1.420	286.6118	0.53628	58.1783
	6	1.698	342.9231	0.64127	69.6087
	7	1.937	390.7627	0.73153	79.3195
30 PPM					
	1	0.503	100.1583	0.18996	20.3308
	2	0.702	139.6440	0.26512	28.3458
	3	0.911	181.1190	0.34405	36.7647
	4	1.047	208.2725	0.39541	42.2765
	5	1.210	240.5970	0.45697	48.8379
	6	1.629	324.0457	0.61521	65.7769
	7	1.928	383.6238	0.72813	77.8704

		h	w	T	U
40 PPM					
	1	0.408	80.1713	0.15409	16.2737
	2	0.700	137.3489	0.26436	27.9800
	3	0.910	178.8135	0.34367	36.2967
	4	1.226	241.1070	0.46301	48.9414
	5	1.419	278.8312	0.53590	56.5989
	6	1.736	341.0212	0.65562	69.2227
	7	2.037	400.3672	0.76930	81.2691
60 PPM					
	1	0.357	68.4679	0.13483	13.8981
	2	0.515	98.9144	0.19450	20.0783
	3	0.729	140.1167	0.27532	28.4418
	4	1.008	193.6034	0.38068	39.2989
	5	1.328	255.1648	0.50154	51.7950
	6	1.697	325.9374	0.64089	66.1609
	7	1.912	367.1318	0.72209	74.5228
100 PPM					
	1	0.297	54.8490	0.11217	11.1336
	2	0.603	111.4601	0.22773	22.6249
	3	0.815	150.5116	0.30779	30.5518
	4	0.983	181.4373	0.37124	36.8293
	5	1.225	226.3291	0.46264	45.9417
	6	1.487	274.6144	0.56158	55.7430
	7	1.851	341.7367	0.69905	69.3679

Table 5.8-13

POLYOX Coagulant in 0.3M K_2SO_4

TUBE C

		h	w	T	U
10 PPM					
	1	0.524	28.4595	0.17818	19.6494
	2	1.285	69.8891	0.43694	48.2539
	3	1.999	108.7624	0.67972	75.0934
	4	2.617	142.3345	0.88986	98.2727
	5	3.308	179.8569	1.12482	124.1795
	6	3.860	211.0270	1.31931	145.7005
	7	4.756	258.7213	1.61718	178.6303
20 PPM					
	1	0.576	30.9094	0.19586	21.3409
	2	1.108	59.4078	0.37675	41.0172
	3	1.824	97.8799	0.62021	67.5797
	4	2.378	127.6588	0.80859	88.1401
	5	3.128	167.8655	1.06361	115.9002
	6	3.587	192.4864	1.21968	132.8994
	7	4.897	262.7740	1.66512	181.4284
30 PPM					
	1	0.765	40.5739	0.26012	28.0136
	2	1.543	81.7363	0.52466	56.4336
	3	2.133	112.9400	0.72528	77.9777
	4	2.886	152.8782	0.98132	105.5525
	5	3.497	185.2843	1.18908	127.9268
	6	4.174	221.1066	1.41928	152.6598
	7	4.906	259.8824	1.66818	179.4319

		h	w	T	U
40 PPM					
	1	0.535	28.0305	0.18192	19.3532
	2	1.340	70.1572	0.45564	48.4390
	3	1.997	104.6297	0.67904	72.2400
	4	2.896	151.7815	0.98472	104.7953
	5	3.773	197.6805	1.28293	136.4856
	6	4.691	245.7277	1.59508	169.6590
	7	5.087	266.5756	1.72973	184.0532
60 PPM					
	1	0.345	17.6958	0.11731	12.2178
	2	1.188	60.9751	0.40395	42.0993
	3	1.913	98.1219	0.65048	67.7468
	4	2.608	133.7299	0.88680	92.3318
	5	3.335	171.0593	1.13400	118.1053
	6	4.711	241.6873	1.60188	166.8694
	7	5.218	267.5924	1.77427	184.7552
100 PPM					
	1	0.439	21.6839	0.14927	14.9713
	2	1.239	61.2491	0.42130	42.2885
	3	2.580	127.3864	0.87727	87.9520
	4	3.301	163.0494	1.12244	112.5750
	5	3.887	191.9242	1.32169	132.5112
	6	4.457	220.1488	1.51551	151.9985
	7	5.017	247.8794	1.70592	171.1446

Table 5.8-14

POLYOX Coagulant in 0.3M K_2SO_4

TUBE D

		h	w	T	U
10 PPM					
	1	1.604	29.5074	0.53754	59.4398
	2	2.824	51.9608	0.94639	104.6700
	3	4.213	77.4930	1.41188	156.1021
	4	5.375	98.8794	1.80129	199.1830
	5	6.701	123.2527	2.24567	248.2806
	6	7.861	144.6122	2.63441	291.3073
	7	9.047	166.4501	3.03187	335.2976
20 PPM					
	1	1.425	25.8896	0.47755	52.1521
	2	2.645	48.0733	0.88640	96.8390
	3	3.945	71.7110	1.32207	144.4549
	4	5.356	97.3462	1.79493	196.0945
	5	7.490	136.1220	2.51008	274.2046
	6	8.215	149.3090	2.75305	300.7685
	7	9.156	166.4219	3.06840	335.2408
30 PPM					
	1	1.221	21.9315	0.40919	44.1789
	2	2.907	52.2053	0.97421	105.1625
	3	4.950	88.9215	1.65887	179.1237
	4	6.263	112.4955	2.09988	226.6113
	5	7.601	136.5486	2.54728	275.0639
	6	8.667	155.6760	2.90452	313.5942
	7	9.376	168.3910	3.14213	339.2073

40 PPM		h	w	T	U
	1	0.873	15.5109	0.29256	31.2452
	2	2.226	39.5756	0.74599	79.7212
	3	3.578	63.6226	1.19908	128.1616
	4	5.047	89.7296	1.69137	180.7516
	5	6.838	121.5815	2.29158	244.9141
	6	8.945	159.0214	2.99769	320.3332
	7	10.125	180.0104	3.39313	362.6135
60 PPM					
	1	1.325	23.0841	0.44404	46.5007
	2	2.702	47.0642	0.90551	94.8063
	3	3.943	68.6948	1.32140	138.3790
	4	5.325	92.7820	1.78454	186.9003
	5	6.575	114.5495	2.20344	230.7489
	6	8.845	154.0873	2.96418	310.3939
	7	10.709	186.5819	3.58885	375.8511
100 PPM					
	1	1.381	23.1792	0.46281	46.6923
	2	2.594	43.5573	0.86931	87.7420
	3	4.817	80.8950	1.61429	162.9551
	4	5.543	93.0757	1.85759	187.4920
	5	6.928	116.3520	2.32174	234.3798
	6	8.379	140.6966	2.80801	283.4197
	7	10.786	181.0939	3.61465	364.7961

Table 5.8-15

POLYOX Coagulant in 0.3M K_2SO_4

TUBE E

		h	w	T	U
10 PPM					
	1	3.271	20.4729	1.10770	122.6132
	2	5.483	34.3142	1.85677	205.5094
	3	7.848	49.1171	2.65766	294.1647
	4	9.930	62.1449	3.36271	372.1888
	5	12.229	76.5367	4.14125	458.3819
	6	16.650	104.2006	5.63838	624.0624
	7	18.539	116.0186	6.27807	694.8409
20 PPM					
	1	2.452	15.1755	0.83035	90.8868
	2	4.884	30.2262	1.65392	181.0262
	3	7.117	44.0473	2.41011	263.8014
	4	9.261	57.3176	3.13616	343.2778
	5	11.421	70.6859	3.86762	423.3412
	6	15.420	95.4348	5.22185	571.5636
	7	18.425	114.0318	6.23947	682.9419
30 PPM					
	1	2.160	13.2200	0.73147	79.1752
	2	4.465	27.3244	1.51203	163.6471
	3	7.693	47.0810	2.60517	281.9704
	4	9.914	60.6773	3.35729	363.3992
	5	12.299	75.2724	4.16495	450.8100
	6	15.387	94.1741	5.21068	564.0132
	7	19.124	117.0479	6.47618	701.0055

40 PPM		h	w	T	U
	1	2.212	13.4087	0.74907	80.3053
	2	5.613	34.0223	1.90079	203.7612
	3	7.634	46.2713	2.58519	277.1210
	4	10.098	61.2075	3.41960	366.5746
	5	13.578	82.3029	4.59807	492.9160
	6	15.704	95.1874	5.31803	570.0819
	7	18.860	114.3150	6.38678	684.6380
60 PPM					
	1	3.281	19.5016	1.11108	116.7960
	2	6.642	39.4767	2.24926	236.4278
	3	8.734	51.9131	2.95769	310.9100
	4	11.101	65.9841	3.75926	395.1819
	5	13.358	79.3972	4.52357	475.5136
	6	15.850	94.2071	5.36747	564.2108
	7	19.325	114.8658	6.54425	687.9368
100 PPM					
	1	3.081	17.6645	1.04335	105.7935
	2	7.105	40.7256	2.40605	243.9076
	3	8.380	48.0373	2.83782	287.6977
	4	9.480	54.3410	3.21032	325.4508
	5	12.857	73.7032	4.35391	441.4120
	6	16.368	93.8276	5.54298	561.9380
	7	20.423	117.0724	6.91607	701.1522

Table 5.8-16

POLYOX WSR 301 in 0.3M K_2SO_4

TUBE A

		h	w	T	U
10 PPM					
	1	0.131	89.4637	0.06937	7.1936
	2	0.116	79.3083	0.06143	6.3770
	3	0.268	183.3296	0.14193	14.7412
	4	0.388	265.2727	0.20548	21.3301
	5	0.499	341.5625	0.26426	27.4644
	6	0.627	428.6752	0.33205	34.4690
	7	0.808	552.0235	0.42790	44.3872
20 PPM					
	1	0.162	109.5321	0.08579	8.8073
	2	0.226	152.6040	0.11968	12.2706
	3	0.268	181.4012	0.14193	14.5861
	4	0.367	248.1374	0.19436	19.9523
	5	0.589	398.3369	0.31192	32.0295
	6	0.653	441.4089	0.34581	35.4929
	7	0.817	552.3932	0.43267	44.4169
30 PPM					
	1	0.128	85.6214	0.06779	6.8847
	2	0.217	145.3245	0.11492	11.6853
	3	0.368	246.5489	0.19488	19.8245
	4	0.587	393.1128	0.31086	31.6095
	5	0.698	467.7493	0.36965	37.6109
	6	0.724	484.8615	0.38341	38.9868
	7	0.839	561.5768	0.44432	45.1554

40 PPM		h	w	T	U
	1	0.107	71.0707	0.05666	5.7147
	2	0.206	136.6277	0.10909	10.9860
	3	0.289	191.9573	0.15305	15.4349
	4	0.364	241.9732	0.19277	19.4566
	5	0.479	318.3576	0.25367	25.5985
	6	0.639	424.4316	0.33840	34.1278
	7	0.843	559.7309	0.44643	45.0069
60 PPM					
	1	0.188	123.1548	0.09956	9.9027
	2	0.313	204.8732	0.16576	16.4735
	3	0.463	303.0553	0.24519	24.3681
	4	0.572	374.3009	0.30292	30.0968
	5	0.618	404.2101	0.32728	32.5018
	6	0.709	464.3739	0.37547	37.3395
	7	0.860	562.9105	0.45544	45.2626
100 PPM					
	1	0.178	113.9827	0.09426	9.1651
	2	0.225	144.2792	0.11916	11.6012
	3	0.269	172.0547	0.14246	13.8346
	4	0.342	219.0004	0.18112	17.6094
	5	0.476	304.6076	0.25208	24.4929
	6	0.689	441.2026	0.36488	35.4763
	7	0.858	549.6221	0.45438	44.1941

Table 5.8-17

POLYOX WSR 301 in 0.3M K_2SO_4

TUBE B

		h	w	T	U
10 PPM					
	1	0.490	102.5572	0.19259	20.0030
	2	0.678	142.0441	0.26648	27.7046
	3	0.865	181.3214	0.33998	35.3653
	4	1.126	235.9021	0.44257	46.0108
	5	1.464	306.5146	0.57542	59.7832
	6	1.819	381.0887	0.71495	74.3283
	7	2.102	440.5785	0.82618	85.9313
20 PPM					
	1	0.427	88.6077	0.16783	17.2822
	2	0.748	155.3191	0.29400	30.2937
	3	0.906	188.0060	0.35610	36.6691
	4	1.027	213.0149	0.40366	41.5468
	5	1.286	266.6606	0.50546	52.0100
	6	1.669	346.3377	0.65599	67.5504
	7	2.068	429.3350	0.81282	83.7383
30 PPM					
	1	0.297	61.0193	0.11673	11.9013
	2	0.523	107.6276	0.20556	20.9919
	3	0.606	124.8081	0.23819	24.3428
	4	1.264	260.1171	0.49681	50.7337
	5	1.745	359.4016	0.68586	70.0984
	6	1.924	395.9378	0.75622	77.2245
	7	2.215	455.5224	0.87060	88.8460

		h	w	T	U
40 PPM					
	1	0.318	64.9630	0.12499	12.6705
	2	0.478	97.5487	0.18788	19.0261
	3	0.608	124.2059	0.23897	24.2254
	4	0.897	183.2446	0.35256	35.7404
	5	1.237	252.9018	0.48620	49.3265
	6	1.873	382.6278	0.73617	74.6285
	7	2.010	410.4149	0.79002	80.0481
60 PPM					
	1	0.323	65.1999	0.12695	12.7167
	2	0.425	85.6578	0.16704	16.7069
	3	0.718	144.6112	0.28221	28.2052
	4	0.989	199.3307	0.38872	38.8778
	5	1.398	281.5637	0.54948	54.9167
	6	1.781	358.9564	0.70001	70.0116
	7	1.989	401.0783	0.78177	78.2271
100 PPM					
	1	0.329	64.9461	0.12931	12.6672
	2	0.388	76.4930	0.15250	14.9193
	3	0.605	119.4298	0.23779	23.2938
	4	0.975	192.5696	0.38322	37.5591
	5	1.437	283.6705	0.56481	55.3276
	6	1.856	366.5831	0.72949	71.4991
	7	2.181	430.3396	0.85723	83.9343

Table 5.8-18

POLYOX WSR 301 in 0.3M K_2SO_4

TUBE C

		h	w	T	U
10 PPM					
	1	0.669	37.1011	0.23674	24.6133
	2	1.386	76.9677	0.49048	51.0614
	3	2.147	119.2778	0.75978	79.1304
	4	2.967	164.7642	1.04996	109.3067
	5	3.268	181.5794	1.15648	120.4621
	6	4.271	237.1783	1.51142	157.3471
	7	5.073	281.6152	1.79523	186.8271
20 PPM					
	1	0.745	41.0396	0.26364	27.2262
	2	1.247	68.5930	0.44129	45.5055
	3	2.025	111.6505	0.71660	74.0704
	4	2.847	156.8317	1.00749	104.0442
	5	3.142	173.1822	1.11189	114.8913
	6	4.827	265.9032	1.70817	176.4036
	7	5.097	280.6766	1.80372	186.2045
30 PPM					
	1	0.745	40.7179	0.26364	27.0128
	2	1.415	77.3937	0.50074	51.3440
	3	1.884	103.0757	0.66671	68.3817
	4	2.787	152.4354	0.98626	101.1276
	5	3.251	177.8140	1.15046	117.9641
	6	4.227	231.0965	1.49585	153.3124
	7	4.956	271.1693	1.75382	179.8972

		h	w	T	U
40 PPM					
	1	0.638	34.6711	0.22577	23.0013
	2	1.727	93.7510	0.61115	62.1956
	3	2.319	126.1223	0.82065	83.6712
	4	2.967	161.2369	1.04096	106.9666
	5	3.874	210.5863	1.37093	139.7057
	6	4.275	232.3180	1.51283	154.1227
	7	4.997	271.5039	1.76833	180.1192
60 PPM					
	1	0.818	43.9481	0.28947	29.1557
	2	1.229	65.9695	0.43492	43.7650
	3	2.086	111.9310	0.73819	74.2565
	4	2.877	154.4298	1.01811	102.4507
	5	3.209	172.1506	1.13560	114.2069
	6	4.088	219.4330	1.44666	145.5747
	7	5.246	281.6914	1.85645	186.8777
100 PPM					
	1	0.909	47.8426	0.32168	31.7394
	2	1.574	82.7929	0.55701	54.9259
	3	2.247	118.2643	0.79517	78.4581
	4	2.758	145.2093	0.97600	96.3337
	5	3.079	162.0543	1.08959	107.5089
	6	3.967	208.7516	1.40384	138.4885
	7	5.298	278.8849	1.87485	185.0158

Table 5.8-19

POLYOX WSR 301 in 0.3M K_2SO_4

TUBE D

		h	w	T	U
10 PPM					
	1	1.874	35.1789	0.65360	68.0910
	2	3.112	58.4354	1.08539	113.1054
	3	4.516	84.8090	1.57507	164.1532
	4	5.098	95.7275	1.77805	185.2866
	5	7.449	139.8632	2.59802	270.7141
	6	8.709	163.5328	3.03748	316.5281
	7	9.298	174.6028	3.24291	337.9548
20 PPM					
	1	1.428	26.6219	0.49805	51.5284
	2	2.784	51.9075	0.97099	100.4703
	3	4.049	75.4904	1.41219	146.1164
	4	5.483	102.2362	1.91233	197.8846
	5	7.079	131.9824	2.46898	255.4603
	6	9.839	183.4304	3.43160	355.0411
	7	10.367	193.2845	3.61575	374.1144
30 PPM					
	1	1.629	30.1767	0.56815	58.4089
	2	2.854	52.8595	0.99540	102.3129
	3	3.936	72.9232	1.37278	141.1475
	4	5.096	94.4019	1.77736	182.7209
	5	6.482	120.0971	2.26076	232.4655
	6	8.653	160.2742	3.01795	310.2209
	7	10.135	187.7478	3.53483	363.3977

		h	w	T	U
40 PPM					
	1	1.468	27.0225	0.51200	52.3038
	2	2.887	53.1627	1.00691	102.8998
	3	4.336	79.8554	1.51229	154.5652
	4	5.718	105.2943	1.99429	203.8038
	5	7.628	140.4860	2.66045	271.9195
	6	8.819	162.3977	3.07584	314.3310
	7	10.310	189.8338	3.59587	367.4353
60 PPM					
	1	1.598	29.0843	0.55734	56.2945
	2	2.745	49.9403	0.95739	96.6626
	3	3.283	59.7721	1.14503	115.6927
	4	5.093	92.7049	1.77631	179.4362
	5	7.274	132.3901	2.53699	256.2494
	6	8.351	151.9820	2.91262	294.1708
	7	9.396	171.0115	3.27709	331.0036
100 PPM					
	1	1.667	29.7578	0.58141	57.5981
	2	2.786	49.7499	0.97169	96.2941
	3	4.205	75.0992	1.46660	145.3593
	4	5.648	100.8570	1.96988	195.2151
	5	7.419	132.4619	2.58756	256.3884
	6	8.687	155.1248	3.02981	300.2539
	7	10.139	181.0733	3.53623	350.4798

Table 5.8-20

POLYOX WSR 301 in 0.3M K_2SO_4

TUBE E

		h	w	T	U
10 PPM					
	1	3.187	20.3520	1.12321	117.1186
	2	6.538	41.7575	2.30422	240.2997
	3	9.025	57.6389	3.18073	331.6916
	4	12.133	77.4904	4.27609	445.9300
	5	14.126	90.2148	4.97850	519.1544
	6	16.848	107.6011	5.93783	619.2065
	7	19.465	124.3148	6.86015	715.3879
20 PPM					
	1	3.928	24.9259	1.38436	143.4398
	2	6.832	43.3508	2.40784	249.4686
	3	9.391	59.5955	3.30972	342.9511
	4	12.963	82.2593	4.56862	473.3733
	5	14.998	95.1758	5.28582	547.7032
	6	16.352	103.7649	5.76302	597.1305
	7	18.375	116.5993	6.47599	670.9380
30 PPM					
	1	2.987	18.8416	1.05272	108.4268
	2	4.876	30.7598	1.71847	177.0118
	3	6.358	40.1076	2.24078	230.8051
	4	8.548	53.9246	3.01261	310.3171
	5	12.367	78.0136	4.35856	448.9408
	6	17.356	109.4833	6.11686	630.0379
	7	20.036	126.3913	7.06139	727.3375

		h	w	T	U
40 PPM					
	1	3.476	21.8055	1.22506	125.4830
	2	5.027	31.5332	1.77169	181.4625
	3	7.347	46.0890	2.58934	265.2260
	4	9.136	57.3137	3.21985	329.8202
	5	12.887	80.8423	4.54183	465.2190
	6	17.106	107.3098	6.02875	617.5301
	7	19.525	122.4826	6.88129	704.8443
60 PPM					
	1	3.856	23.9208	1.35899	137.6558
	2	6.237	38.6902	2.19814	222.6485
	3	8.633	53.5541	3.04257	308.1850
	4	10.727	66.5431	3.78057	382.9321
	5	11.567	71.7549	4.07662	412.9242
	6	16.478	102.2184	5.80743	588.2309
	7	19.257	119.4565	6.78684	687.4301
100 PPM					
	1	2.197	13.3778	0.77430	76.9845
	2	5.387	32.8010	1.89857	188.7582
	3	10.078	61.3660	3.55184	353.1397
	4	12.282	74.7874	4.32861	430.3752
	5	14.148	86.1487	4.98625	495.7555
	6	17.119	104.2374	6.03334	599.8496
	7	20.514	124.9139	7.22985	718.8356

Table 5.9

Characteristics in the anomalous zone

CON: polymer concentration of solution

A, B, C, D and E: tube diameters of test sections

Table 5.9-1

Average velocity deficiency, $-\bar{u}_w \times 10^2$

Polyox Coagulant in distilled water

CON	A	B	C	D	E
10	0.42607	0.31678	0.21972	0.15642	0.10752
20	0.89033	0.66591	0.46220	0.33186	0.23251
30	1.14332	0.86017	0.59637	0.42950	0.30011
40	1.28785	0.96589	0.66777	0.48121	0.33817
60	1.41016	1.06576	0.73402	0.52983	0.37226
100	1.49184	1.13059	0.77653	0.56066	0.39391

Polyox WSR 301 in distilled water

CON	A	B	C	D	E
10	0.20720	0.15530	0.10403	0.07281	0.04967
20	0.43284	0.32713	0.21962	0.15449	0.10762
30	0.60226	0.45675	0.30882	0.21615	0.15320
40	0.72509	0.55030	0.37244	0.26170	0.18512
60	0.88447	0.67153	0.45562	0.32002	0.22658
100	1.03343	0.78577	0.53176	0.37658	0.26722

Polyox Coagulant in 0.3M K_2SO_4

CON	A	B	C	D	E
10	0.30585	0.23211	0.15415	0.10759	0.07787
20	0.64312	0.48551	0.32739	0.22944	0.16924
30	0.82713	0.62450	0.42225	0.29855	0.21928
40	0.92396	0.69874	0.47234	0.33529	0.24677
60	1.01212	0.76901	0.52138	0.37028	0.27143
100	1.07020	0.81271	0.55248	0.39310	0.28821

Polyox WSR 301 in 0.3M K_2SO_4

CON	A	B	C	D	E
10	0.15000	0.10872	0.07681	0.05155	0.03399
20	0.30583	0.22861	0.15948	0.11138	0.07604
30	0.42746	0.32272	0.22022	0.15628	0.10848
40	0.51669	0.39101	0.26621	0.18975	0.13220
60	0.63018	0.47416	0.32352	0.23220	0.16241
100	0.73859	0.55768	0.37966	0.27247	0.19183

Table 5.9-2

Anomalous zone thickness, $\overline{\Delta} \times 10^2$

Polyox Coagulant in distilled water

CON	A	B	C	D	E
10	0.42979	0.31968	0.22265	0.15981	0.11224
20	0.90311	0.67351	0.46681	0.33546	0.23621
30	1.16396	0.87224	0.60277	0.43382	0.30360
40	1.31396	0.98078	0.67539	0.48576	0.34150
60	1.44116	1.08348	0.74273	0.53464	0.37512
100	1.52646	1.15035	0.78580	0.56558	0.39640

Polyox WSR 301 in distilled water

CON	A	B	C	D	E
10	0.20876	0.15696	0.10607	0.07563	0.05367
20	0.43630	0.32958	0.22171	0.15675	0.11058
30	0.60825	0.46058	0.31129	0.21835	0.15569
40	0.73361	0.55543	0.37545	0.26391	0.18739
60	0.89677	0.67878	0.45934	0.32228	0.22847
100	1.05006	0.79531	0.53629	0.37903	0.26875

Polyox Coagulant in 0.3M K_2SO_4

CON	A	B	C	D	E
10	0.30847	0.23438	0.15685	0.11109	0.08275
20	0.65021	0.49013	0.33072	0.23269	0.17311
30	0.83836	0.63135	0.42620	0.30178	0.22284
40	0.93759	0.70690	0.47683	0.33854	0.24995
60	1.02825	0.77856	0.52633	0.37357	0.27417
100	1.08804	0.82316	0.55751	0.39611	0.29037

Polyox WSR 301 in 0.3M K_2SO_4

CON	A	B	C	D	E
10	0.15121	0.11027	0.07880	0.05439	0.03812
20	0.30796	0.23033	0.16140	0.11372	0.07928
30	0.43076	0.32514	0.22227	0.15837	0.11124
40	0.52116	0.39396	0.26836	0.19173	0.13466
60	0.63660	0.47812	0.32590	0.23410	0.16439
100	0.74721	0.56283	0.38227	0.27438	0.19337

Table 5.9-3

Anomalous zone thickness, Δ/D_e

Polyox Coagulant in distilled water

CON	A	B	C	D	E
10	91.19	50.48	23.37	11.74	5.73
20	191.61	106.35	49.01	24.65	12.07
30	246.96	137.73	63.29	31.87	15.51
40	278.78	154.87	70.91	35.69	17.45
60	305.77	171.10	77.98	39.28	19.17
100	323.87	181.65	82.51	41.56	20.25

Polyox WSR 301 in distilled water

CON	A	B	C	D	E
10	63.03	35.27	15.85	7.90	3.90
20	131.74	74.06	33.13	16.39	8.04
30	183.66	103.50	46.51	22.83	11.32
40	221.51	124.82	56.10	27.59	13.62
60	270.78	152.54	68.64	33.70	16.61
100	317.07	178.73	80.14	39.63	19.54

Polyox Coagulant in 0.3M K_2SO_4

CON	A	B	C	D	E
10	81.70	46.20	20.55	10.19	5.27
20	172.21	96.61	43.34	21.34	11.04
30	222.04	124.45	55.86	27.68	14.21
40	248.32	139.34	62.50	31.05	15.94
60	272.33	153.47	68.98	34.26	17.49
100	288.17	162.26	73.07	36.33	18.52

Polyox WSR 301 in 0.3M K_2SO_4

CON	A	B	C	D	E
10	56.48	30.65	14.56	7.03	3.42
20	115.04	64.03	29.83	14.71	7.13
30	160.91	90.39	41.09	20.48	10.00
40	194.68	109.53	49.61	24.80	12.11
60	237.80	132.93	60.24	30.28	14.79
100	279.12	156.48	70.67	35.49	17.39

Table 5.9-4

Adsorption level, n

Polyox Coagulant in distilled water

CON	A	B	C	D	E
10	804	444	204	101	48
20	2583	1432	658	329	159
30	4664	2599	1192	598	289
40	7165	3978	1819	913	444
60	14395	8052	3667	1844	897
100	67428	37813	17169	8643	4207

Polyox WSR 301 in distilled water

CON	A	B	C	D	E
10	445	248	110	53	25
20	1314	738	328	161	77
30	2369	1333	597	291	143
40	3563	2006	899	440	215
60	6472	3644	1637	802	393
100	16229	9146	4097	2023	995

Polyox Coagulant in 0.3M K_2SO_4

CON	A	B	C	D	E
10	531	299	131	64	32
20	1543	864	386	188	96
30	2511	1406	629	310	157
40	3417	1916	857	424	216
60	5283	2975	1335	661	335
100	10434	5873	2642	1311	666

Polyox WSR 301 in 0.3M K_2SO_4

CON	A	B	C	D	E
10	309	167	78	36	16
20	834	463	214	104	49
20	1416	794	359	177	85
40	2006	1127	509	253	122
60	3190	1781	805	403	195
100	5810	3255	1468	735	358

Table 5.9-5

Adsorption zone thickness, δ_a

Polyox Coagulant in distilled water

CON	A	B	C	D	E
10	0.99936	0.99884	0.99750	0.99501	0.98967
20	0.99975	0.99954	0.99902	0.99804	0.99599
30	0.99984	0.99971	0.99938	0.99877	0.99746
40	0.99988	0.99979	0.99955	0.99911	0.99818
60	0.99993	0.99988	0.99974	0.99949	0.99896
100	0.99998	0.99997	0.99993	0.99987	0.99974

Polyox WSR 301 in distilled water

CON	A	B	C	D	E
10	0.99901	0.99824	0.99607	0.99206	0.98363
20	0.99957	0.99925	0.99832	0.99660	0.99301
30	0.99973	0.99952	0.99894	0.99784	0.99562
40	0.99980	0.99965	0.99922	0.99842	0.99860
60	0.99987	0.99978	0.99951	0.99901	0.99798
100	0.99994	0.99989	0.99977	0.99953	0.99905

Polyox Coagulant in 0.3M K_2SO_4

CON	A	B	C	D	E
10	0.99923	0.99863	0.99692	0.99375	0.98779
20	0.99966	0.99940	0.99866	0.99728	0.99472
30	0.99976	0.99957	0.99906	0.99810	0.99628
40	0.99980	0.99966	0.99924	0.99847	0.99701
60	0.99985	0.99974	0.99944	0.99887	0.99779
100	0.99991	0.99985	0.99966	0.99933	0.99868

Polyox WSR 301 in 0.3M K_2SO_4

CON	A	B	C	D	E
10	0.99886	0.99790	0.99556	0.99071	0.98050
20	0.99946	0.99903	0.99793	0.99579	0.99123
30	0.99963	0.99935	0.99858	0.99715	0.99413
40	0.99971	0.99950	0.99889	0.99778	0.99545
60	0.99979	0.99963	0.99920	0.99840	0.99673
100	0.99986	0.99976	0.99948	0.99896	0.99788

Table 5.9-6

Concentration in the concentrated layer at the interface, c_c^*/c

Polyox Coagulant in distilled water

CON	A	B	C	D	E
10	8.06520	8.05380	8.02410	7.96910	7.86730
20	6.33240	6.32970	6.32270	6.30980	6.28270
30	5.50060	5.49940	5.49610	5.49010	5.47730
40	4.98110	4.98040	4.97850	4.97510	4.96775
60	4.33700	4.33680	4.33600	4.33450	4.33150
100	3.65230	3.65220	6.65210	3.65180	3.65130

Polyox WSR 301 in distilled water

CON	A	B	C	D	E
10	9.49350	9.46920	9.40170	9.29210	9.03790
20	7.45490	7.44830	7.43090	7.39860	7.33120
30	6.47010	6.46720	6.45910	6.44380	6.41310
40	5.85370	5.85200	5.84720	5.83820	5.82010
60	5.08800	5.08720	5.08500	5.08080	5.07240
100	4.27340	4.27310	4.27240	4.27110	4.26840

Polyox Coagulant in 0.3M K_2SO_4

CON	A	B	C	D	E
10	10.18520	10.16380	10.10220	10.00260	9.79350
20	7.99350	7.98780	7.97180	7.94180	7.88650
30	6.93500	6.93210	6.92370	6.90830	6.87920
40	6.27210	6.27010	6.26470	6.25460	6.23570
60	5.44810	5.44710	5.44410	5.43870	5.42830
100	4.57110	4.57070	4.56950	4.56730	4.56310

Polyox WSR 301 in 0.3M K_2SO_4

CON	A	B	C	D	E
10	11.86940	11.82170	11.70640	11.48380	11.00720
20	9.32650	9.31370	9.28050	9.21650	9.09530
30	8.09140	8.08510	8.06780	8.03590	7.96910
40	7.31540	7.31150	7.30060	7.28060	7.23370
60	6.34860	6.34650	6.34070	6.33010	6.30780
100	5.31700	5.31610	5.31350	5.30870	5.29890

Table 5.9-7

Concentrated layer thickness, $\delta_c \times 10^6$

Polyox Coagulant in distilled water

CON	A	B	C	D	E
10	1.73220	1.73410	1.73910	1.74850	1.76820
20	1.43000	1.43070	1.43250	1.43580	1.44270
30	1.16750	1.16790	1.16890	1.17080	1.17480
40	0.94300	0.94330	0.94400	0.94520	0.94780
60	0.58760	0.58770	0.58800	0.58860	0.58970
100	0.15660	0.15660	0.15660	0.15670	0.15690

Polyox WSR 301 in distilled water

CON	A	B	C	D	E
10	1.29790	1.30000	1.30600	1.31710	1.34090
20	1.16110	1.16190	1.16430	1.16870	1.17780
30	1.02880	1.02930	1.03070	1.03340	1.03870
40	0.90770	0.90810	0.90900	0.91080	0.91450
60	0.69820	0.69840	0.69890	0.69990	0.70200
100	0.38510	0.38520	0.38540	0.38570	0.38650

Polyox Coagulant in o.3M K_2SO_4

CON	A	B	C	D	E
10	1.50360	1.50550	1.51100	1.52130	1.54080
20	1.37970	1.38050	1.38270	1.38680	1.39440
30	1.25260	1.25310	1.25450	1.25720	1.26230
40	1.13270	1.13310	1.13420	1.13630	1.14020
60	0.91890	0.91920	0.92000	0.92130	0.92400
100	0.58200	0.58210	0.58250	0.58320	0.58450

Polyox WSR 301 in 0.3M K_2SO_4

CON	A	B	C	D	E
10	1.08880	1.09110	1.09680	1.10870	1.13400
20	1.04230	1.04330	1.04570	1.05050	1.06060
30	0.98450	0.98510	0.98670	0.98980	0.99620
40	0.92590	0.92640	0.92760	0.92980	0.93460
60	0.81440	0.81470	0.81550	0.81700	0.82030
100	0.62140	0.62160	0.62210	0.62300	0.62480

Table 5.9-8

Concentrated layer thickness

in dimensionless form, $\tilde{\delta}_c \times 10^3$ $(=\delta_c/\Delta)$

Polyox Coagulant in distilled water

CON	A	B	C	D	E
10	0.63613	1.15039	2.49118	4.98600	10.32282
20	0.24992	0.45049	0.97869	1.95048	4.00220
30	0.15832	0.28396	0.61850	1.22995	2.53579
40	0.11328	0.20396	0.44576	0.88677	1.81874
60	0.06435	0.11503	0.25250	0.50171	1.03029
100	0.01619	0.02887	0.06358	0.12630	0.25938

Polyox WSR 301 in distilled water

CON	A	B	C	D	E
10	0.98126	1.75640	3.92659	7.93644	16.36992
20	0.42004	0.74766	1.67481	3.39774	6.98003
30	0.26697	0.47395	1.05603	2.15682	4.37160
40	0.19530	0.34672	0.77220	1.57289	3.19813
60	0.12288	0.21819	0.48528	0.98976	2.01344
100	0.05789	0.10272	0.22920	0.46384	0.94244

Polyox Coagulant in 0.3M K_2SO_4

CON	A	B	C	D	E
10	0.76935	1.36217	3.07242	6.24089	12.20162
20	0.33492	0.59731	1.33340	2.71599	5.27862
30	0.23581	0.42091	0.93878	1.89856	3.71214
40	0.19068	0.33993	0.75864	1.52963	2.98936
60	0.14106	0.25038	0.55746	1.12397	2.20849
100	0.05789	0.10272	0.22920	0.46384	0.94244

Polyox WSR 301 in 0.3M K_2SO_4

CON	A	B	C	D	E
10	1.13653	2.09850	4.43912	9.28915	19.49448
20	0.53421	0.96053	2.06637	4.20955	8.76641
30	0.36073	0.64253	1.41588	2.84824	5.86859
40	0.28042	0.49866	1.10237	2.21013	4.54816
60	0.20191	0.36136	0.79810	1.59057	3.26972
100	0.13127	0.23422	0.51902	1.03472	2.11741

Table 5.9-9

Porosity in the adsorption zone at the interface, ε^*

Polyox Coagulant in distilled water

CON	A	B	C	D	E
10	0.82820	0.82840	0.82900	0.83020	0.83240
20	0.73020	0.73030	0.73060	0.73110	0.73230
30	0.64850	0.64850	0.64870	0.64910	0.64990
40	0.57560	0.57560	0.57580	0.57610	0.57670
60	0.44570	0.44570	0.44580	0.44600	0.44640
100	0.22200	0.22200	0.22200	0.22210	0.22220

Polyox WSR 301 in distilled water

CON	A	B	C	D	E
10	0.87320	0.87350	0.87440	0.87590	0.87930
20	0.80090	0.80110	0.80150	0.80240	0.80420
30	0.74080	0.74090	0.74130	0.74190	0.74310
40	0.68740	0.68750	0.68770	0.68820	0.68920
60	0.59240	0.59250	0.59260	0.59300	0.59370
100	0.42940	0.42950	0.42960	0.42980	0.43010

Polyox Coagulant in 0.3M K_2SO_4

CON	A	B	C	D	E
10	0.88840	0.88870	0.88930	0.89040	0.89270
20	0.82490	0.82500	0.82540	0.82600	0.82720
30	0.77210	0.77220	0.77250	0.77300	0.77400
40	0.72520	0.72530	0.72560	0.72600	0.72680
60	0.64200	0.64210	0.64230	0.64260	0.64330
100	0.49940	0.49950	0.49960	0.49980	0.50030

Polyox WSR 301 in 0.3M K_2SO_4

CON	A	B	C	D	E
10	0.91630	0.91660	0.91740	0.91910	0.92230
20	0.86840	0.86860	0.86910	0.87000	0.87170
30	0.82880	0.82890	0.82930	0.83000	0.83140
40	0.79370	0.79380	0.79410	0.79460	0.79580
60	0.73140	0.73150	0.73170	0.73220	0.73310
100	0.62510	0.62520	0.62530	0.62570	0.62640

Table 5.9-10

Anomalous zone thickness, $\Delta/R^2 \times 10^2$

Polyox Coagulant in distilled water

CON	A	B	C	D	E
10	0.67830	0.67790	0.71000	0.72820	0.73550
20	1.42530	1.42820	1.48870	1.52870	1.54790
30	1.83710	1.84970	1.92230	1.97700	1.98940
40	2.07380	2.07980	2.15390	2.21370	2.23780
60	2.27450	2.29760	2.36870	2.43640	2.45810
100	2.40920	2.43940	2.50610	2.57740	2.59750

Polyox WSR 301 in distilled water

CON	A	B	C	D	E
10	0.32940	0.33280	0.33830	0.34460	0.35170
20	0.68860	0.69890	0.70710	0.71430	0.72460
30	0.96000	0.97670	0.99270	0.99500	1.02020
40	1.15780	1.17780	1.19740	1.20260	1.22790
60	1.41530	1.43940	1.46490	1.46860	1.49710
100	1.65730	1.68650	1.71030	1.72730	1.76100

Polyox Coagulant in 0.3M K_2SO_4

CON	A	B	C	D	E
10	0.48680	0.49700	0.50020	0.50620	0.54220
20	1.02620	1.03930	1.05470	1.06040	1.13430
30	1.32310	1.33880	1.35920	1.37530	1.46020
40	1.47980	1.49900	1.52070	1.54270	1.63790
60	1.62280	1.65100	1.67860	1.70240	1.79660
100	1.71720	1.74560	1.77800	1.80510	1.90270

Polyox WSR 301 in 0.3M K_2SO_4

CON	A	B	C	D	E
10	0.23860	0.23380	0.25130	0.24780	0.24970
20	0.48600	0.48840	0.51470	0.51820	0.51950
30	0.67980	0.68950	0.70880	0.72170	0.72890
40	0.82250	0.83540	0.85580	0.87370	0.88240
60	1.00470	1.01390	1.03930	1.06680	1.07720
100	1.17930	1.19350	1.21910	1.25040	1.26710

Table 5.10

Porosity distribution in the adsorption zone at a given polymer solution

$\tilde{y}$ = distance from the wall

= y/Δ

D_e= effective diameter of polymer molecule

$\overset{o}{y} = y/D_e$

ε = porosity

Table 5.10-1

Polyox Coagulant in distilled water

TUBE A

CON= 10 PPM

n = 0.80456D 03

$\bar{\Delta}$ = 0.42980D-02

$\tilde{\delta}_a$ = 0.99936D 00

$\tilde{y}$	$\overset{o}{y}$	ε
0.95000D 00	0.86632D 02	0.10474D-02
0.95548D 00	0.87132D 02	0.34025D-02
0.96097D 00	0.87633D 02	0.10920D-01
0.96645D 00	0.88133D 02	0.34472D-01
0.97194D 00	0.88633D 02	0.10567D 00
0.97742D 00	0.89133D 02	0.30117D 00
0.98291D 00	0.89633D 02	0.61760D 00
0.98839D 00	0.90133D 02	0.68756D 00
0.99388D 00	0.90634D 02	0.70564D 00
0.99936D 00	0.91134D 02	0.82821D 00

CON= 30 PPM

n = 0.46642D 04

$\bar{\Delta}$ = 0.11640D-01

$\tilde{\delta}_a$= 0.99984D 00

$\tilde{y}$	$\overset{o}{y}$	ε
0.99100D 00	0.24475D 03	0.68858D-03
0.99198D 00	0.24499D 03	0.22289D-02
0.99296D 00	0.24523D 03	0.71730D-02
0.99395D 00	0.24547D 03	0.22873D-01
0.99493D 00	0.24572D 03	0.71616D-01
0.99591D 00	0.24596D 03	0.21329D 00
0.99689D 00	0.24620D 03	0.46974D 00
0.99788D 00	0.24644D 03	0.52820D 00
0.99886D 00	0.24669D 03	0.54333D 00
0.99984D 00	0.24693D 03	0.64851D 00

CON= 60 PPM

n = 0.14395D 05

$\overline{\Delta}$ = 0.14412D-01

$\tilde{\delta}_a$ = 0.99994D 00

$\tilde{y}$	$\tilde{\vartheta}$	ε
0.99720D 00	0.30493D 03	0.85134D-03
0.99750D 00	0.30502D 03	0.25926D-02
0.99781D 00	0.30511D 03	0.78561D-02
0.99811D 00	0.30521D 03	0.23612D-01
0.99842D 00	0.30530D 03	0.69791D-01
0.99872D 00	0.30539D 03	0.19460D 00
0.99902D 00	0.30548D 03	0.34364D 00
0.99933D 00	0.30558D 03	0.36205D 00
0.99963D 00	0.30567D 03	0.37309D 00
0.99994D 00	0.30576D 03	0.44574D 00

CON= 100 PPM

n = 0.67428D 05

$\overline{\Delta}$ = 0.15265D-01

$\tilde{\delta}_a$ = 0.99998D 00

$\tilde{y}$	$\tilde{\vartheta}$	ε
0.99940D 00	0.32369D 03	0.55500D-03
0.99946D 00	0.32371D 03	0.16658D-02
0.99953D 00	0.32373D 03	0.50989D-02
0.99959D 00	0.32375D 03	0.15320D-01
0.99966D 00	0.32377D 03	0.45409D-01
0.99972D 00	0.32379D 03	0.12297D 00
0.99979D 00	0.32381D 03	0.17592D 00
0.99985D 00	0.32383D 03	0.18054D 00
0.99992D 00	0.32386D 03	0.18625D 00
0.99998D 00	0.32388D 03	0.22206D 00

TUBE E

CON= 10 PPM

n = 0.48091D 02

$\bar{\Delta}$ = 0.11225D-02

$\tilde{\delta}_a$= 0.98968D 00

$\tilde{y}$	$\overset{o}{y}$	ε
0.50000D 00	0.28682D 01	0.42716D-02
0.55441D 00	0.31803D 01	0.13509D-01
0.60882D 00	0.34924D 01	0.49228D-01
0.66323D 00	0.38045D 01	0.13767D 00
0.71763D 00	0.41166D 01	0.33076D 00
0.77204D 00	0.44287D 01	0.57397D 00
0.82645D 00	0.47408D 01	0.65321D 00
0.88086D 00	0.50529D 01	0.68013D 00
0.93527D 00	0.53650D 01	0.71385D 00
0.98968D 00	0.56771D 01	0.83243D 00

CON= 30 PPM

n = 0.28952D 03

$\bar{\Delta}$ = 0.30361D-02

$\tilde{\delta}_a$= 0.99746D 00

$\tilde{y}$	$\overset{o}{y}$	ε
0.87500D 00	0.13576D 02	0.11097D-02
0.88861D 00	0.13787D 02	0.34641D-02
0.90221D 00	0.13998D 02	0.10571D-01
0.91582D 00	0.14209D 02	0.31429D-01
0.92943D 00	0.14421D 02	0.90170D-01
0.94304D 00	0.14632D 02	0.24124D 00
0.95664D 00	0.14843D 02	0.47072D 00
0.97025D 00	0.15054D 02	0.52600D 00
0.98386D 00	0.15265D 02	0.54549D 00
0.99746D 00	0.15476D 02	0.64999D 00

CON= 60 PPM

n = 0.89737D 03

$\bar{\Delta}$ = 0.37512D-02

$\tilde{\delta}_a$ = 0.99897D 00

$\tilde{y}$	$\overset{o}{y}$	ε
0.95700D 00	0.18346D 02	0.73384D-03
0.96166D 00	0.18435D 02	0.22233D-02
0.96633D 00	0.18524D 02	0.66693D-02
0.97099D 00	0.18614D 02	0.19755D-01
0.97565D 00	0.18703D 02	0.57387D-01
0.98032D 00	0.18793D 02	0.15925D 00
0.98498D 00	0.18882D 02	0.32443D 00
0.98964D 00	0.18971D 02	0.36111D 00
0.99431D 00	0.19061D 02	0.37371D 00
0.99897D 00	0.19150D 02	0.44643D 00

CON= 100 PPM

n = 0.42076D 04

$\bar{\Delta}$ = 0.39641D-02

$\tilde{\delta}_a$ = 0.99974D 00

$\tilde{y}$	$\overset{o}{y}$	ε
0.99120D 00	0.20080D 02	0.88114D-03
0.99215D 00	0.20099D 02	0.24440D-02
0.99310D 00	0.20118D 02	0.67434D-02
0.99405D 00	0.20137D 02	0.18462D-01
0.99500D 00	0.20157D 02	0.49804D-01
0.99594D 00	0.20176D 02	0.12304D 00
0.99689D 00	0.20195D 02	0.17530D 00
0.99784D 00	0.20214D 02	0.18112D 00
0.99879D 00	0.20233D 02	0.18723D 00
0.99974D 00	0.20253D 02	0.22226D 00

Table 5.10-2

Polyox Coagulant in 0.3M K_2SO_4

TUBE A

CON= 10 PPM

n = 0.53184D 03

$\bar{\Delta}$ = 0.30847D-02

$\tilde{\delta}_a$ = 0.99923D 00

$\tilde{y}$	$\overset{o}{y}$	ε
0.92500D 00	0.75573D 02	0.11335D-02
0.93325D 00	0.76247D 02	0.37713D-02
0.94150D 00	0.76921D 02	0.12345D-01
0.94974D 00	0.77594D 02	0.39561D-01
0.95799D 00	0.78268D 02	0.12228D 00
0.96624D 00	0.78942D 02	0.34630D 00
0.97449D 00	0.79616D 02	0.68296D 00
0.98273D 00	0.80290D 02	0.74969D 00
0.99098D 00	0.80964D 02	0.76773D 00
0.99923D 00	0.81637D 02	0.88847D 00

CON= 30 PPM

n = 0.25113D 04

$\bar{\Delta}$ = 0.83836D-02

$\tilde{\delta}_a$= 0.99976D 00

$\tilde{y}$	$\overset{o}{y}$	ε
0.98250D 00	0.21816D 03	0.48126D-03
0.98442D 00	0.21859D 03	0.16745D-02
0.98634D 00	0.21901D 03	0.57859D-02
0.98825D 00	0.21944D 03	0.19788D-01
0.99017D 00	0.21986D 03	0.66374D-01
0.99209D 00	0.22029D 03	0.21170D 00
0.99401D 00	0.22072D 03	0.52858D 00
0.99593D 00	0.22114D 03	0.63420D 00
0.99785D 00	0.22157D 03	0.65115D 00
0.99976D 00	0.22199D 03	0.77218D 00

CON= 60 PPM

n = 0.52833D 04

$\bar{\Delta}$ = 0.10283D-01

$\tilde{\delta}_a$ = 0.99986D 00

$\tilde{y}$	$\overset{o}{y}$	ε
0.99220D 00	0.27023D 03	0.88764D-03
0.99305D 00	0.27046D 03	0.28049D-02
0.99390D 00	0.27069D 03	0.88117D-02
0.99475D 00	0.27092D 03	0.27419D-01
0.99560D 00	0.27115D 03	0.83641D-01
0.99645D 00	0.27139D 03	0.24084D 00
0.99731D 00	0.27162D 03	0.48187D 00
0.99816D 00	0.27185D 03	0.52346D 00
0.99901D 00	0.27208D 03	0.53828D 00
0.99986D 00	0.27231D 03	0.64206D 00

CON= 100 PPM

n = 0.10435D 05

$\bar{\Delta}$ = 0.10880D-01

$\tilde{\delta}_a$ = 0.99992D 00

$\tilde{y}$	$\overset{o}{y}$	ε
0.99600D 00	0.28701D 03	0.66837D-03
0.99644D 00	0.28714D 03	0.21275D-02
0.99687D 00	0.28726D 03	0.67383D-02
0.99731D 00	0.28739D 03	0.21168D-01
0.99774D 00	0.28751D 03	0.65409D-01
0.99818D 00	0.28764D 03	0.19207D 00
0.99861D 00	0.28776D 03	0.37801D 00
0.99905D 00	0.28789D 03	0.40534D 00
0.99948D 00	0.28801D 03	0.41735D 00
0.99992D 00	0.28814D 03	0.49944D 00

TUBE E

CON= 10 PPM

n = 0.32084D 02

$\bar{\Delta}$ = 0.82752D-03

$\tilde{\delta}_a$ = 0.98780D 00

$\tilde{y}$	$\overset{o}{y}$	ε
0.50000D 00	0.26395D 01	0.78246D-01
0.55420D 00	0.29256D 01	0.17830D 00
0.60840D 00	0.32117D 01	0.35458D 00
0.66260D 00	0.34978D 01	0.56643D 00
0.71680D 00	0.37840D 01	0.67416D 00
0.77100D 00	0.40701D 01	0.70862D 00
0.82520D 00	0.43562D 01	0.73134D 00
0.87940D 00	0.46423D 01	0.75588D 00
0.93360D 00	0.49284D 01	0.79145D 00
0.98780D 00	0.52146D 01	0.89276D 00

CON= 30 PPM

n = 0.15793D 03

$\bar{\Delta}$ = 0.22285D-02

$\tilde{\delta}_a$ = 0.99629D 00

$\tilde{y}$	$\overset{o}{y}$	ε
0.79500D 00	0.11302D 02	0.24125D-02
0.81737D 00	0.11620D 02	0.73827D-02
0.83973D 00	0.11938D 02	0.21762D-01
0.86210D 00	0.12256D 02	0.61500D-01
0.88446D 00	0.12574D 02	0.16408D 00
0.90683D 00	0.12892D 02	0.38765D 00
0.92919D 00	0.13210D 02	0.59713D 00
0.95156D 00	0.13528D 02	0.63315D 00
0.97392D 00	0.13845D 02	0.65658D 00
0.99629D 00	0.14163D 02	0.77403D 00

CON= 60 PPM

n = 0.33576D 03

$\overline{\Delta}$ = 0.27417D-02

$\tilde{\delta}_a$ = 0.99779D 00

$\tilde{y}$	$\overset{o}{y}$	ε
0.89500D 00	0.15654D 02	0.16851D-02
0.90642D 00	0.15853D 02	0.49756D-02
0.91784D 00	0.16053D 02	0.14411D-01
0.92926D 00	0.16253D 02	0.40767D-01
0.94069D 00	0.16453D 02	0.11137D 00
0.95211D 00	0.16652D 02	0.28091D 00
0.96353D 00	0.16852D 02	0.48489D 00
0.97495D 00	0.17052D 02	0.52238D 00
0.98637D 00	0.17252D 02	0.54098D 00
0.99779D 00	0.17451D 02	0.64336D 00

CON= 100 PPM

n = 0.66615D 03

$\overline{\Delta}$ = 0.29038D-02

$\tilde{\delta}_a$ = 0.99868D 00

$\tilde{y}$	$\overset{o}{y}$	ε
0.94500D 00	0.17505D 02	0.12986D-02
0.95096D 00	0.17616D 02	0.37638D-02
0.95693D 00	0.17726D 02	0.10781D-01
0.96289D 00	0.17837D 02	0.30416D-01
0.96886D 00	0.17947D 02	0.83749D-01
0.97482D 00	0.18058D 02	0.21625D 00
0.98079D 00	0.18168D 02	0.37831D 00
0.98675D 00	0.18279D 02	0.40564D 00
0.99272D 00	0.18389D 02	0.41976D 00
0.99868D 00	0.18500D 02	0.50034D 00

Table 5.11

Limiting anomalous zone thickness, $\bar{\Delta}_\infty$, with constants α and n'

Polyox Coagulant in distilled water

Tube	$\bar{\Delta}_\infty \times 10^2$	α	n'
A	1.58686	183.89	1.834
B	1.19874	179.52	1.815
C	0.81636	183.32	1.837
D	0.58762	184.64	1.838
E	0.41175	184.94	1.841
Average		183.25	1.833

Polyox WSR 301 in distilled water

Tube	$\bar{\Delta}_\infty \times 10^2$	α	n'
A	1.25450	128.57	1.410
B	0.94666	132.60	1.421
C	0.63780	133.55	1.424
D	0.45592	124.63	1.394
E	0.32164	127.03	1.404
Average		129.23	1.411

Polyox Coagulant in 0.3M K_2SO_4

Tube	$\bar{\Delta}_\infty$ x10^2	α	n'
A	1.12830	189.53	1.853
B	0.85566	178.76	1.829
C	0.57975	181.31	1.828
D	0.41243	179.20	1.819
E	0.30154	180.93	1.834
Average		181.90	1.833

Polyox WSR 301 in 0.3M K_2SO_4

Tube	$\bar{\Delta}_\infty$ x10^2	α	n'
A	0.90132	120.71	1.384
B	0.67491	131.30	1.410
C	0.45982	114.70	1.376
D	0.32838	128.68	1.408
E	0.23184	129.97	1.407
Average		124.91	1.397

* Average values were evaluated by least squares fitting from the data of all tubes.

Table 5.12

Drag reduction data by Arunachalam Polyox Coagulant in distilled water

Tube B

Re $x10^{-4}$	10 ppm	20 ppm	30 ppm	40 ppm
0.78	0.184	0.260	0.301	0.332
1	0.275	0.350	0.386	0.408
1.5	0.401	0.459	0.491	0.509
2	0.475	0.524	0.551	0.562
3	0.523	0.588	0.621	0.637
4	0.560	0.622	0.648	0.662

Tube D

Re $x10^{-4}$	10 ppm	20 ppm	30 ppm	40 ppm
0.78	0.328	0.475	0.562	0.618
1	0.431	0.562	0.633	0.667
1.5	0.541	0.624	0.671	0.692
2	0.598	0.662	0.689	0.708
3	0.629	0.694	0.723	0.738
4	0.638	0.700	0.728	0.744

Polyox WSR 301 in distilled water

Tube B

Re x10^{-4}	10 ppm	20 ppm	30 ppm	40 ppm
0.78	0.072	0.120	0.151	0.164
1	0.149	0.203	0.231	0.246
1.5	0.271	0.331	0.358	0.371
2	0.372	0.405	0.432	0.439
3	0.421	0.475	0.511	0.528
4	0.460	0.521	0.545	0.559

Tube D

Re x10^{-4}	10 ppm	20 ppm	30 ppm	40 ppm
0.78	0.154	0.226	0.261	0.278
1	0.246	0.321	0.359	0.384
1.5	0.391	0.452	0.476	0.488
2	0.472	0.521	0.543	0.557
3	0.516	0.561	0.582	0.594
4	0.529	0.586	0.612	0.624